2022

The Injury-Induced Neurogenic Response and the Role of Notch1 in Regulating This Process

Nicole M. Weston
Virginia Commonwealth University

THE INJURY-INDUCED NEUROGENIC RESPONSE AND THE ROLE OF NOTCH1 IN REGULATING THIS PROCESS

A dissertation submitted in partial fulfillment of the requirements for the degree of Doctor of Philosophy at Virginia Commonwealth University

by

Nicole M. Weston

Bachelor of Arts, Western Washington University, 2013

Advisor: Dong Sun, MD, PhD

Professor, Department of Anatomy and Neurobiology

Virginia Commonwealth University

Virginia Commonwealth University

Richmond, VA

June 10, 2022

Acknowledgements

First and foremost, I would like to thank my advisor, Dr. Dong Sun, for her incredible guidance and wisdom along this journey. Under her advisement, I have learned to always be inspired no matter the challenge. She has encouraged my creative side and independence through the years while leading me down a path of professional and personal growth. I am exceedingly thankful for the experiences this training has brought me the past 5+ years.

I thank my committee members, Dr. Kirsty Dixon, Dr. Aron Lichtman, Dr. Linda Phillips, and Dr. Thomas Reeves. They have provided me with invaluable perspectives and critique in the shaping of this dissertation research over the years and have been constant positive influences. I especially want to thank Dr. Reeves for our collaboration during the beginning of my PhD and giving excellent advice through the early stages of my training. I also thank my program director, Dr. John Bigbee, for his enthusiasm and constant support, always wanting to be at every major event for any of us neuroscience students.

I thank my husband, Rory Weston, who I have been most fortunate to share this experience with as a fellow graduate student. We have supported each other through the most difficult times of our training, and the fun times when we could just nerd out on neuroscience at home and actually know what the other person was talking about. Thank you to my parents, Gina and Joe, for encouraging me to

always follow my dreams and believe in myself. Thank you to my siblings and in-laws, I will always appreciate having so many wonderful people support me. Also, thank you to all my close friends who have made my time in Richmond and at VCU a most memorable experience.

To my lab mates over the years, you were all there in the trenches with me when a day would suddenly turn into an unpredictable nightmare, having to solve why the FPI device suddenly stopped working in the middle of a surgery or that time when the ceiling collapsed on my desk. I especially want to thank Tim Keoprasert, who has worked closely with me for the past few years and has always been there when I needed a helping hand.

I also thank my previous mentors, Dr. Jaqueline Rose for being my first advisor and encouraging my independence as a scientist at an early age, Dr. Mike Mana for making my upper-level undergraduate neuroscience courses some of the most vibrant and energetic moments of my career, Dr. Jeff Dupree for his support and motivation, and Dr. Kimberle Jacobs who has been an excellent mentor during my first few years in Richmond and an all-around great person that I have had the pleasure of getting to know.

Lastly, I thank VCU School of Medicine and the VCU SOM Office of Graduate Education, and Dr. Grotewiel for his dedication and advocacy to improve the graduate student experience on MCV campus.

Table of Contents

List of Tables

List of Figures

List of Abbreviations

BrdU	Bromodeoxyuridine
CA	*Cornu Ammonis*
CDC	Center for Disease Control and Prevention
cKO	conditional Knock Out
DAB	3,3′-Diaminobenzidine
DCX	Doublecortin
DG	Dentate gyrus
DPI	Days post-injury
EC	Entorhinal cortex
GC	Granule cell
GCL	Granule cell layer
GFP	Green fluorescent protein
HICAP	Hilar commissural-associated pathway related cells
HIPP	Hilar perforant pathway-related cells
i.p.	Intraperitoneal injection
IML	Inner Molecular Layer
LEC	Lateral entorhinal cortex

LFPI	Lateral fluid percussion injury
LTP	Long-term potentiation
MEC	Medial entorhinal cortex
MLs	Molecular layers
MML	Middle molecular layer
MOPP	Molecular layer perforant path-associated cell
MWM	Morris water maze
NeuN	Neuronal nuclear protein
NICD	Notch intracellular domain
NOR	Novel object recognition
NS/NPCs	Neural stem and progenitor cells
OML	Outer molecular layer
PBS	Phosphate buffer saline
PP	Perforant pathway
SGC	Semilunar granule cells
SGZ	Subgranular Zone
SVZ	Subventricular Zone
TAM	Tamoxifen
TBI	Traumatic brain injury
WPI	Weeks post-injury

Clarification of Contributions

Integral assistance and support were provided for the studies listed below. All other work described in this dissertation was performed exclusively by the author.

Tim Keoprasert was instrumental in processing, staining, and analyzing the samples for the 2 DPI and 7 DPI studies in Chapter 2. Tim also provided the behavioral work in Chapter 3. Jakob Green helped with the protein isolation and conducted the Western Blot experiments and analysis in Chapter 3.

Microscopy was performed at the VCU Microscopy Facility, supported, in part, by funding from NIH-NCI Cancer Center Support Grant P30 CA016059. Dr. Tytus Bernas and Frances White contributed substantially with advising and troubleshooting on the Zeiss LSM 710 confocal microscope.

Services in support of the research project were provided by the VCU Massey Cancer Center Transgenic/Knockout Mouse Core, supported, in part, with

funding from NIH-NCI Cancer Center Support Grant P30 CA016059. Dr. Jolene Windle provided her expertise in developing the necessary transgenic mouse lines for these studies. Pam Watters provided essential support in maintaining the transgenic mouse lines used in this dissertation.

Abstract

Traumatic Brain Injury (TBI) is a prevalent problem with an estimated 5 million people suffering from chronic cognitive impairments long after the injury. Following TBI there is a series of pathophysiological changes in the brain including neurogenesis, an important response linking endogenous repair and regeneration. The dentate gyrus (DG) of the hippocampus is a primary neurogenic region within the adult brain where neural stem and progenitor cells (NS/NPCs) reside. Studies using rodent models have shown that cognitive recovery after TBI is associated with new neurons generated from the DG. Thus far, in studies examining post-injury neurogenesis, the regulatory mechanisms, functional integration, and morphological development of NS/NPCs are among the key aspects that are poorly understood. A critical regulatory mechanism that may play a role in injury-induced neurogenesis is Notch1 signaling. Studies have shown that the Notch1 pathway is a key mediator for neurogenesis in developing and adult brains, as it has essential roles in regulating stem cell proliferation and fate determination. The formation of neuronal dendritic processes post-mitotically is

another critical role of Notch1, as it facilitates complexity in branching patterns of cells that are in direct association with memory performance. Notch1 has a strong association with CREB signaling and synaptic plasticity, specifically in regions critical for cognitive functions and learning such as the hippocampus. As the hippocampus is the most vulnerable region to TBI, the morphological development and synaptic plasticity of new neurons generated in the DG of the hippocampus following TBI may serve an important role in the cognitive recovery process. In this series of studies, we have characterized the role of Notch1 in injury-induced new neuron population dynamics. Additionally, we have discovered that Notch1 does play an essential role for proper dendritic arbor morphology development after TBI, and this is directly associated with an inability to recover learning and memory capabilities at the time of innate cognitive recovery after injury. This series of studies provides fundamental support that injury-induced populations of new neurons contribute to recovery after injury, and Notch1 signaling is crucial for this process to occur in these new neurons.

Chapter 1

Introduction and Background

Neurotrauma and other neurologic insults and diseases are a considerable affliction on individuals, their loved ones, and society. As research advancements are made the potential treatment for targeting these conditions increases. There are a number of strategies from medications, therapeutics, and even stem cell research. A sector of stem cell research concentrates on endogenous stem cell strategies and one specific area is adult neurogenesis. Understanding and harnessing the adult neurogenic process and potential cell signaling processes may provide insight on different strategies for helping neurologic patients, especially those who have had a traumatic brain injury (TBI).

1.1 Traumatic Brain Injury

The Center for Disease Control and Prevention (CDC) defines traumatic brain injuries (TBIs) as a disruption in the normal function of the brain that can be caused

by a bump, blow, or jolt to the head, or penetrating head injury (CDC, 2017). The most prevalent causes of TBI are a broad array which includes falls, car crashes, sports related injuries, and war related injuries. According to the United States Department of Defense, between the years 2000 – 2011 roughly 5.6 million United States military members were diagnosed with a TBI. The impact of TBIs on the United States economy reached $76.5 billion in 2010, and this did not include TBIs that were managed in non-hospital locations and at federal institutions (Finkelstein et al., 2006). TBI is the leading cause of death and disability for those under the age of 45 in the United States, and the 4th leading cause of death for all ages. The CDC has reported that in one year alone in the United States, TBIs accounted for 2.2 million emergency department visits, 280,000 hospitalizations, and 50,000 deaths. These numbers are likely an underestimation considering the frequency of mild head trauma and concussions that are not reported.

Considerably, an estimated 1.1% of the United States population is living with a long-term disability resulting from a moderate to severe TBI (Zaloshnja et al., 2005). Within the past 10 years there have been significant improvements in reducing the mortality caused by TBI, however annually an approximate 80,000 individuals within the USA sustain a TBI that results in significant long-term deficits (Thurman et al., 1999). Due to the heterogeneity of TBI it is difficult to follow predictable patterns of recovery outcomes. The CDC has reported five-year

outcome estimates from the United States population TBIMS National Database (**Figure 1.1**). This data refers to individuals 16 years of age and older with the required criteria of a primary diagnosis of TBI while receiving rehabilitation in an inpatient setting. The findings stated that at five years after injury 22% had died, 30% became worse, 22% stayed the same, and only 26% improved. Generally, the acute and chronic consequences that may arise after injury include memory loss, epilepsy, dementia, and many lifelong disabilities, with limited treatment options available. In the United States alone, there is an estimated 3.2 – 5.3 million individuals living with a long-term cognitive impairment as a result of a TBI (Coronado et al., 2012). Cognitive difficulties are still prevalent up to a reported 10 years after injury, with 60% of individuals reporting memory problems, difficulty concentrating and planning, cognitive fatigue and many other relevant changes in cognition and behavior (Ponsford et al., 2014).

To address recovery from cognitive dysfunction after injury physicians and scientists can assess changes that may have occurred in the brain tissue of patients. On examination of patients with severe TBI, they found significant decreases within the gray matter of the temporal lobe and hippocampus (Christidi et al., 2011). The perforant pathway, a region heavily involved with learning and memory capabilities, had less axons consistent with lower performance on memory tasks. In a study looking at brain tissue samples from TBI patients, there

Figure 1.1. General Outcomes 5 Years Post-TBI. Data are United States population estimates based on the TBIMS National Database. Data refer to people 16 years of age and older who received inpatient rehabilitation services for a primary diagnosis of TBI. Modified from CDC 2017.

was a collection of cells expressing neural stem cell and progenitor cell markers in the perilesional cortex (Zheng et al., 2013). When translating this finding back to bench side, studies on ischemic stroke have been more informative showing that new neuronal populations migrate to the site of injury, possibly from adult neurogenic regions (Arvidsson et al., 2002; Jin et al., 2003; Teramoto et al., 2003). This increased neurogenesis post-ischemic insult has been associated with behavioral recovery and synaptic plasticity (Wi et al., 2016). Although most of these findings have come from ischemic stroke studies, there is some evidence of new neuronal populations occurring at the site of cortical injury in an animal model of TBI (Urrea et al., 2007). This appears to be an endogenous process of recovery.

The connection to endogenous recovery after TBI actually goes back to the beginning of adult neurogenesis research, when Dr. Joseph Altman conducted an

experiment injuring a brain and noticed a response of proliferating cells in regions we now recognize as adult neurogenic niches (Joseph Altman, 1962). In terms of more recent studies, cognitive recovery has been associated with injury-induced neuronal populations generated from the hippocampal dentate gyrus NSCs/NPCs that integrate into the hippocampal circuitry (Chirumamilla et al., 2002; Sun et al., 2007). Anatomical integration long after injury shows neurogenesis correlates with cognitive recovery, especially with evidence that this cellular population integrates into the designated circuitries. Using Ara-C, an antimitotic agent, the cognitive recovery after injury was not observed suggesting this is a function directly related to neurogenesis induced after injury (Sun et al., 2015). Another study has supported this through genetic ablation, providing evidence that these neurogenic populations induced through injury contribute to hippocampal-specific behavioral tasks (Blaiss et al., 2011). Manipulations to directly target newborn cells after injury using optogenetics has been successful for exciting newborn cells, and has shown an increase in cognitive recovery after injury (Zhao et al., 2018). These are some of the many studies demonstrating functional recovery after brain injury is involved with neurogenesis in the hippocampus. An important issue to recognize is that even though significant improvements with cognitive recovery can occur shortly after injury, this response can plateau even when further recovery is needed (Christensen et al., 2008; Schretlen & Shapiro,

2003). A year out from injury there is typically cell loss in the hippocampal neurogenic region, possibly explaining a halt in recovery (Smith et al., 1997). The field of TBI recovery research needs to address the possible resulting complications of the neurogenic population responses to effectively aid in recovery longevity.

1.2 Adult Neurogenesis in the Dentate Gyrus

The dentate gyrus (DG) is an arch shaped anatomical structure included as part of the hippocampal formation (**Figure 1.2**). The hippocampus, located deep within the temporal lobe, is well recognized for its role in learning and memory. The DG is important in contributing to this function, but what makes it unique is that it is considered one of the few neurogenic regions in the adult mammalian brain. The subgranular zone (SGZ) of the DG contains neural stem and progenitor cell populations which have the potential for proliferation, differentiation, and migration to become mature neurons and integrate fully into the pre-existing circuitries (Altman, 1962; Eriksson et al., 1998). The granule cells (GC) located in the DG are the main product of hippocampal neurogenesis and thought to be the major contributor for memory formation (Clelland et al., 2009; Kempermann et al., 1997; Sahay et al., 2011; van Praag et al., 1999). Studies of endogenous neurogenic

mechanisms such as the DG provide an avenue towards recovery from neurological diseases or neurotrauma.

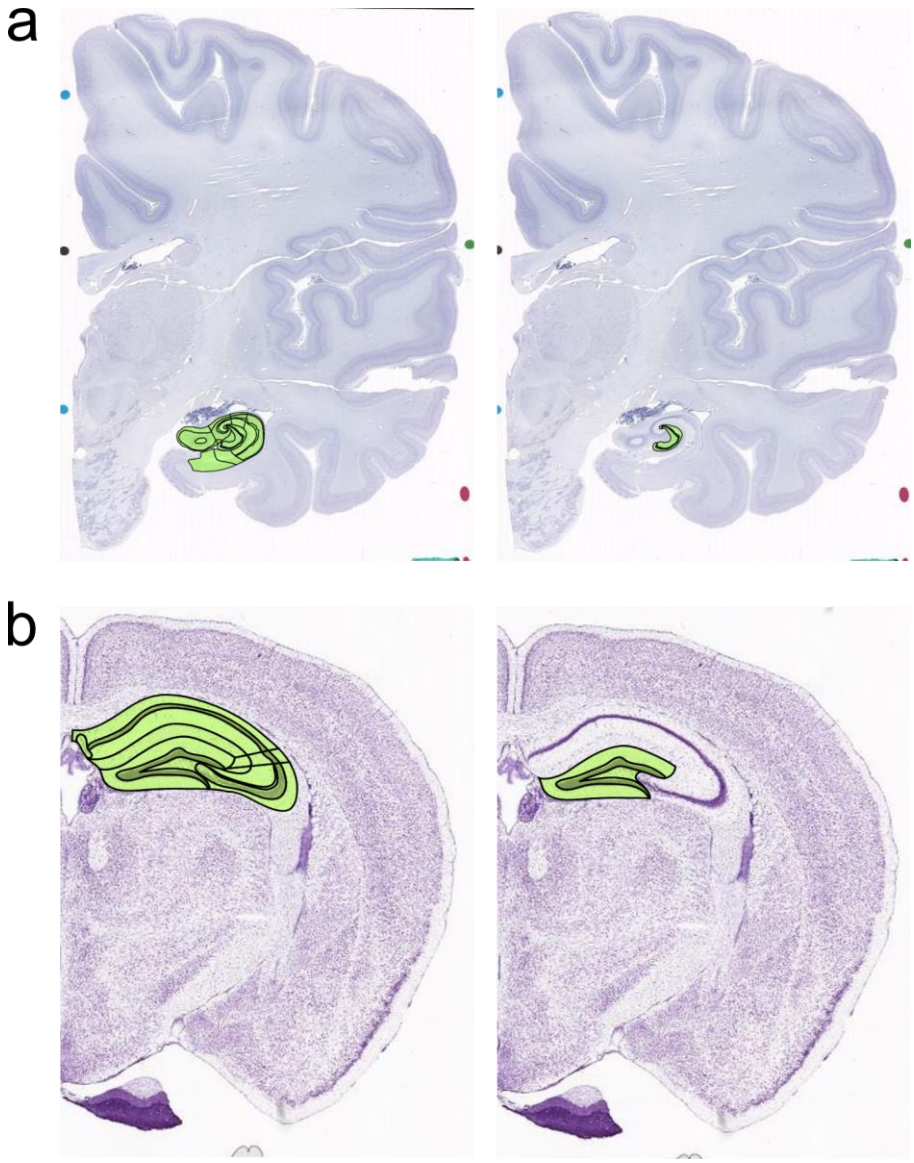

Figure 1.2. Brain Map of the Dentate Gyrus and Hippocampus. Nissl-stained coronal samples from the Allen Brain Atlas showing the hippocampus (left) and dentate gyrus (right) in (**a**) human tissue and (**b**) mouse tissue. Regions are highlighted.

1.2.1 Historical Significance

For centuries the adult human brain was considered unchangeable. Our understanding began to transform with the recognition of both neuroplasticity and neurogenesis transpiring in the adult brain. In the 1960s, Dr. Joseph Altman made a fundamental discovery paving the way for postnatal neurogenesis research (Altman, 1962). Dr. Altman administered thymidine-H^3 to rats due to its known capability to label proliferating cells (Altman & Das, 1965; Altman & Das, 1966). Thymidine is a precursor to chromosomal DNA and integrates solely into dividing cells. The original intended purpose for this was to observe a general cellular response to brain trauma. The findings from this preliminary work showed labeled cells in regions seemingly irrelevant to the lesion location (Altman, 1962). Dr. Altman conducted experiments to see if this proliferative activity in these specific regions continued independent of brain injury. The autoradiograms used to detect thymidine-H^3 showed a significant number of granule cells labeled within the dentate gyrus of the hippocampus. Due to not enough support from the scientific community, the field was put on pause for nearly 30 years (Gould & Gross, 2002; Kuhn et al., 2018).

It wasn't until the 1990's that postnatal neurogenesis research began receiving support, largely lending to the advancements in scientific techniques at that time. Dr. Fred Gage's group was among the first to revive interest and

findings in this topic. Not only was it reassured adult neurogenesis occurs in animal models, but in 1998 Dr. Gage and colleagues demonstrated neurogenesis in the adult human hippocampus (Eriksson et al., 1998). This was monumental as it opened many doors to understand the capabilities of the adult human brain and allowed for direct translatability from animal models that also exhibit postnatal neurogenesis.

1.2.2 Anatomy of the Dentate Gyrus

The dentate gyrus (DG) is a well-organized structure containing few subregions and a number of different cell types. It is considered part of the hippocampal formation and therefore is involved with the hippocampal trisynaptic circuit. The basic anatomy and circuitry of the hippocampus can be described in a simplistic manner. The hippocampal formation contains the subiculum, the dentate gyrus, and the *Cornu Ammonis* (CA) regions. Generally, information from the rest of the brain arrives to the hippocampus and is processed in a specific sequence of these hippocampal formation subregions beginning with the DG and ending with the subiculum as the major output (**Figure 1.3**). The DG itself contains cell layers and axonal pathway layers. In brief, the DG begins with input from the entorhinal cortex along the perforant pathway (PP) to the molecular layers (MLs). Granule cell (GC) dendritic arbors extend through the molecular

layers receiving this synaptic input. The granule cell somas reside in the granule cell layers (GCL) and extend their axons through the hilus and to region CA3 creating the mossy fiber pathway. These separate regions contain many cell types in addition to their associated pathways.

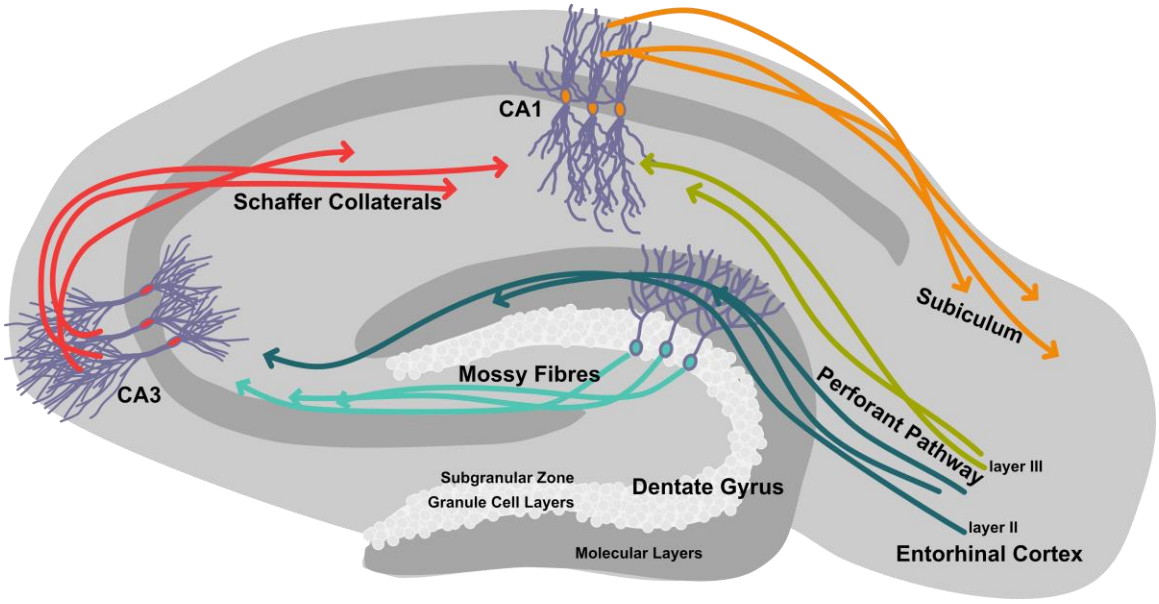

Figure 1.3. Hippocampus Trisynaptic Circuit. Sagittal view of the three main regions of the hippocampal trisynaptic circuit and the corresponding synaptic transmission pathways.

Perforant Pathway

The entorhinal cortex (EC) is located in the medial temporal lobe and is the main source of cortical input to the hippocampus (Witter, 2007). The pyramidal neurons located in layer II of the EC project their axons into the DG giving rise to the perforant pathway (PP). This is the first step of the trisynaptic circuit lending the nickname 'gatekeepter' to the DG. Cells located in layer III of the EC also project to the hippocampus, however the target is CA1 and the subiculum. The perforant pathway locates to the molecular layers (MLs) of the DG where GC dendritic protrusions receive the synaptic input in the middle molecular layer (MML) and outer molecular layer (OML). Generally, the medial EC terminates to the MML and the lateral EC to the OML. This is believed to serve a functional purpose with the type of information being processed. For example, the medial EC cells are more involved with spatial modulation compared to the lateral EC (Hafting et al., 2005).

Cells of the Dentate Gyrus: Perforant Pathway and Molecular Layers

The MLs are predominately composed of axons and dendrites, however there are a few cell types that reside here. The majority of the cells found in the MLs are interneurons. Most recently, a subtype of GC has also been recognized as being located in the MLs.

Semilunar Granule Cells

The semilunar granule cells (SGCs) (**Figure 1.4-1)** are a subtype of GC that reside in the inner molecular layer (IML). They are thought to play a role in regulating GC feedback inhibition, pattern separation, and sparse coding (Gupta et al., 2020; Williams et al., 2007). SGCs were originally identified by Ramón y Cajal, but haven't received a lot of attention until relatively recently. They have been historically difficult to study due to there being no specific neurochemical marker to differentiate them. Instead, research can only go off of morphological characteristics or electrophysiological firing patterns.

The SGCs are estimated to make up 3% of the new neurons produced from DG adult neurogenesis (Save et al., 2019). The defining features are that they have a more expansive dendritic arbor and higher sustained firing activity. The number of primary dendrites, dendrite angles, and soma width are all higher in comparison to GCs. The general overall complexity is lower; however, they have the same number of terminal nodes and their dendrites still extend to the MLs and axons to CA3. SGCs are under stronger inhibitory regulation than GCs (Gupta et al., 2012). They sometimes extend axon collaterals into the GCLs and have a strong connectivity with mossy cells (Rovira-Esteban et al., 2020; Williams et al., 2007).

MOPP Cells

One type of inhibitory interneuron located in the MLs is the molecular layer perforant path-associated cell (MOPP) (**Figure 1.4-2**). The MOPP dendrites and axons are restricted to the MLs and PP, however can have large extensions that cover a significant area. When the PP is stimulated, the MOPP cells are activated prior to GCs being activated. They have a strong inhibitory connection with the newly born GCs and act on these cells through feed-forward inhibition (Li et al., 2013).

Additional Molecular Layer Interneurons

Parvalbumin+ interneurons reside throughout most of the dentate gyrus and this includes the molecular layers. They are typically chandelier/axo-axonic cells (**Figure 1.4-3**) with their soma residing in the IML. Another type of interneuron that can be seen throughout the dentate gyrus are the hilar perforant pathway-related cells (HIPPs). Some work suggests they are primarily located in the hilus, however there is substantial evidence that their somas can reside in the GCLs or MLs, as well (Hosp et al., 2014; Myers & Scharfman, 2009). The most distinguishing feature of the HIPP cells in their axonal protrusions extend to the OML.

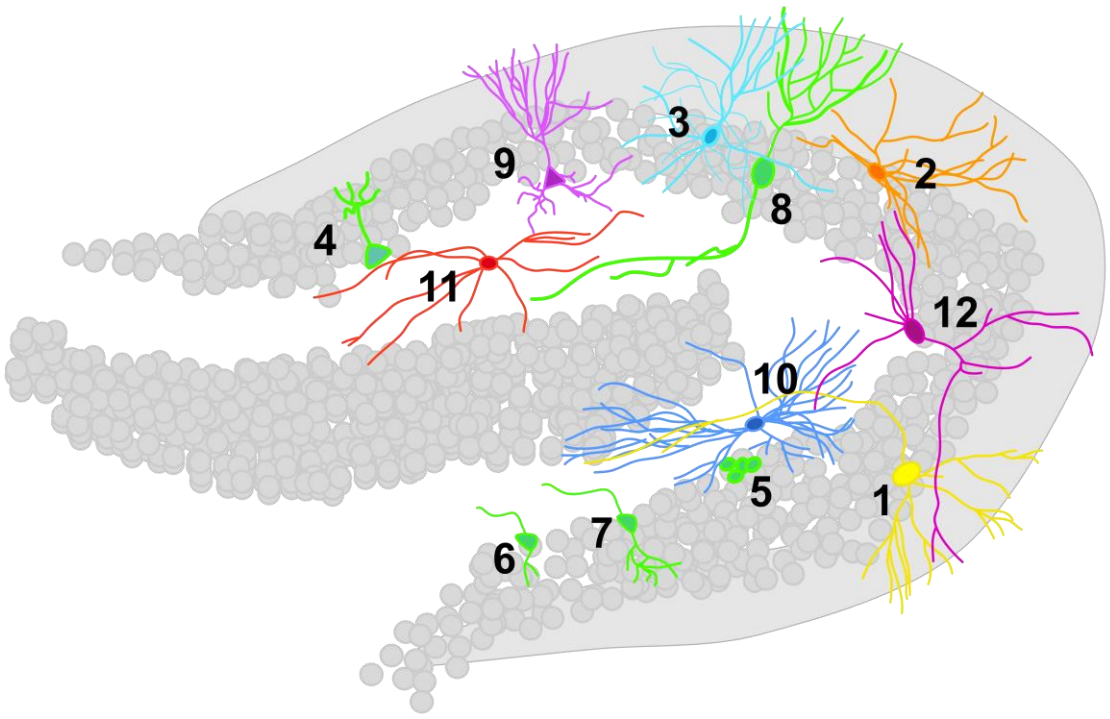

Molecular Layers		Subgranular Zone		Granule Cell Layers		Polymorphic Layer	
1 Semilunar Granular Cells (SGCs)		4 Radial Glial-Like Neural Stem Cells		7 Immature Granular Cells		10 Mossy Cells	
2 Molecular Layer Perforant Path Associated Cells (MOPP)		5 Neural Progenitor Cells		8 Mature Granular Cells		11 Hilar Perforant Pathway-Related Cells (HIPP)	
3 Chandelier/Axo-axonic PV+ Interneurons		6 Immature Granule Cells (Type 3)		9 Dentate Pyramidal Basket Cells		12 Hilar Commissural-Associated Pathway Related Cells (HICAP)	

Figure 1.4. Cells of the Dentate Gyrus. The different cell types located in the molecular layers, subgranular zone, granule cell layers, and polymorphic layers. Each cell type is listed in the table underneath with a number and color reciprocated in the drawing.

Cells of the Dentate Gyrus:
Granule Cell Layers

The only cell type generated from adult hippocampal neurogenesis are the excitatory principal neurons termed granule cells (**Figure 1.4-8**) (Kembermann et al., 2015). Their cell bodies are densely packed making the GCLs a total of roughly 6 to 8 cells deep (Ribak & Shapiro, 2007). A mature GC has dendrites fully extended to the MML and OML and ending towards the hippocampal fissure (**Figure 1.5**). They receive synaptic transmission along the perforant pathway from the entorhinal cortex. The axons of mature GCs extend into the hilus and CA3 forming the mossy fibre pathway. The GCLs can be divided into thirds with the two outer layers consisting of primarily mature or maturing GCs, and the first layer which contains the subgranular zone (SGZ). The SGZ borders the hilus and contains the neurogenic pool of neural stem and progenitor cell populations. The maturation process of these cells has a critical period that is directly related to their involvement in memory formation (Aasebø et al., 2011; Sahay et al., 2011). The main functional purpose for these cells is to create separation patterns of information which is performed through competitive learning between the GCs, essentially replicating sparse code (Ikrar et al., 2013; Rolls, 2013).

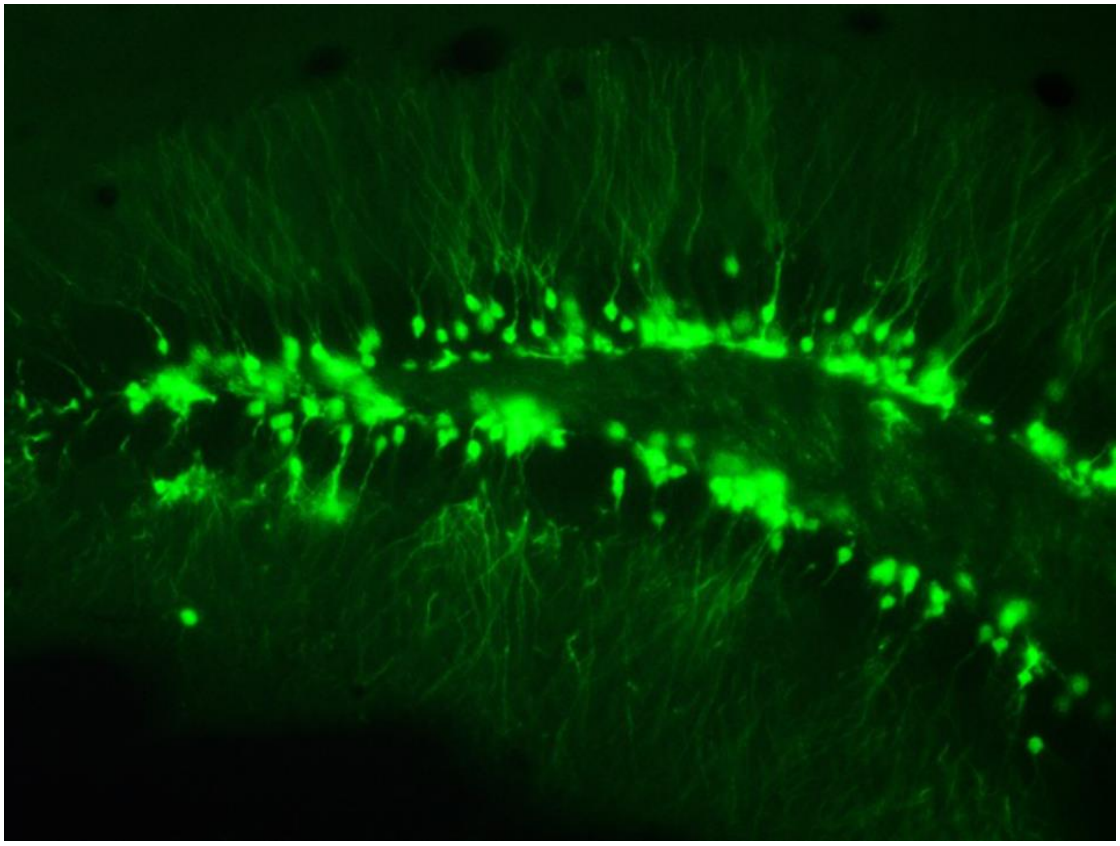

Figure 1.5. Fluorescently Labeled Granule Cells. Green Fluorescent Protein (GFP+) granule cells located in the dentate gyrus. Their somas are visible within the GCLs and dendritic extensions protruding outwards through the MLs.

Granule Cells and the Neurogenic Process

New granule cells are produced from the NSC/NPC populations with a series of stages throughout the cell maturation process (Kempermann et al., 2004; Lledo et al., 2006; Zhao et al., 2006). In embryonic development, neurogenesis and precursor cell proliferation are one and the same, but in adult neurogenesis, precursor cell proliferation is independent as neurogenesis relies on survival and

functional integration (Paterno et al., 2017). To distinguish between neural stem cells and neural progenitor cells, the NSCs have unlimited self-renewing and are multipotent and capable of generating astrocytes, oligodendrocytes, and neurons. In comparison, the NPCs have a limited capacity for self-renewal and have restricted potential for differentiation. NSCs phenotypically and morphologically appear as radial glial like precursors with extensions up through the GCLs (**Figure 1.4-4**) (Seri et al., 2001). In the DG these are vertical radial-glia astrocyte-like stem cells, however there are non-proliferative astrocytes that reside in the DG as well. These horizontal or non-precursor astrocytes are found all over the DG, most frequently in the hilus, a large number in the MLs, and less often in the SGZ and GCLs.

In reference to the adult neurogenic process, the radial granule NSCs are also termed Type 1. These NSCs transition into intermediate progenitors (**Figure 1.4-5)**, termed Type 2a and Type 2b (Kempermann et al., 2015; Redell et al., 2020). The different stages can be identified through markers that recognize different phenotypic expressions. Type 2a express GFAP, Sox2, BLBP, and nestin, and occurs within the proliferation days briefly before differentiation stages begin. Type 2b, another progenitor type, and Type 3, an immature GC type, express similar markers including NeuroD, Prox1, and Doublecortin. The period of these two cell types extends from week 1 at the beginning of differentiation, out to week

4 when immature GCs transition to having a mature phenotype. The distinction between these two types is obvious from Type 3 developing neurite extensions (**Figure 1.4-6**).

Around week 2 after cell division, the new GCs project their axons into the hilus and dendrites into the molecular layers, with the dendritic protrusions appearing towards week 3 (**Figure 1.4-7**) (Hastings & Gould, 1999; Sun et al., 2013; Zhao et al., 2006). Synapses form with hilar interneurons and CA3 around this same time (Toni et al., 2008). Between weeks 4 – 8 the GCs are considered mature and can be identified with NeuN or Calbindin (**Figure 1.4-8**). Even though they are considered mature GCs, they still have a significant amount of plasticity and rearranging occurring with regards to their branching and spines, in addition to enhanced excitability (Ge et al., 2007; Schmidt-Hieber et al., 2004; Toni et al., 2008; Tronel et al., 2010). By 8 weeks this dynamic growth reaches a plateau and the morphology is indistinguishable from older mature GCs.

There are a number of factors that contribute to the differentiation and maturation process of new GCs. Throughout maturation these cells receive afferents from mature GCs, mossy cells, interneurons, CA3 pyramidal cells, the septum, and lateral entorhinal cortex (Vivar et al., 2012). Most recently, evidence supports newly born cells having preferential input from the lateral entorhinal cortex (LEC), while mature neurons receive a balanced input from both the LEC

and medial entorhinal cortex (MEC) (Woods et al., 2018). Astrocytic processes are also involved as they ensheath the newborn neuron synapses, regardless of which stage they are at (Krzisch et al., 2015). The newborn GCs still located in the SGZ are wrapped or 'cradled' by an astrocyte and part of this aids in outgrowth for the new GC (Shapiro et al., 2005). Additionally, the CA3 axons terminate in the IML, providing evidence for back projections from CA3 to both mature and new GCs (Abbott & Nigussie, 2020). Another important aspect is GABAergic signaling controls multiple stages of adult neurogenesis (Markwardt et al., 2009). During the first 2 to 3 weeks the new cells are excitable to GABAergic inputs. A regulated balance between GABA and glutamate signaling occurs as the new GCs mature (Ge et al., 2008).

Interneurons of the Granule Cell Layers

There are two types of Parvalbumin+ interneurons, axo-somatic (basket) and axo-axonic (chandelier) (Kosaka et al., 1987; Nitsch et al., 1990; Soriano & Frotscher, 1989). There is a significantly lower abundance of the axo-axonic/chandelier cells within the GCLs (Hosp et al., 2014). The dentate pyramidal basket cells are in a higher abundance and are typically more recognized when describing the DG circuit (**Figure 1.4-9**). They have a signature pyramidal shaped body with dendritic protrusions through the MLs and axons near the hilus-GCL

border. Their soma specifically lies on the intersection of the GCLs and hilus, receiving input from both mossy fibers through IML and the PP through MML and OML (Seress & Ribak, 1984; Zipp et al., 1989). The majority of their perisomatic excitatory drive is from the semilunar GCs (Rovira-Esteban et al., 2020).

Mossy Fiber Pathway

The mossy fibers were discovered and named by Golgi in the 1880's due to their moss-like varicosities. The fibers originate from the granule cells and are thin and unmyelinated (Blaabjerg & Zimmer, 2007). These fibers pass into the hilus and have several collateral branches contacting different hilar and subgranular neurons. Once the fibers reach the pyramidal cell layer of CA3 they no longer have collaterals, and instead lay along the pyramidal cells following the transverse axis of the hippocampus.

Cells of the Dentate Gyrus: Hilus Region

Mossy Cells

The mossy cells are the secondary excitatory cell of the DG. They have large extensions and their axons project to the IML, with their dendrites covered in distinguishable large spines (**Figure 1.4-10**). They are believed to be important in

regulating Parvalbumin+ basket cells and project back to GCs (Rovira-Esteban et al., 2020). They are the smallest population of cell types in the hilus, however their specific characteristics of being an excitatory neuron and located spread-out through the hilus suggest a significant role in the DG circuit (Henze & Buzsáki, 2007).

Interneurons of the Hilus

There are a significant number of interneuron types that have been described as residing in the hilar region. Specific GABAergic interneurons include Parvalbumin+, Somatostatin+, and Neuropeptide Y+ cells (Vivar & van Praag, 2013). The Somatostatin+ interneurons typically target the distal dendrites of GCs and other interneurons (Hainmueller & Bartos, 2020). The Somatostatin+ HIPP cells previously mentioned in the MLs also reside in the hilus, with their axons extending into the MML and OML (**Figure 1.4-11**) (Myers & Scharfman, 2009). Another notable interneuron is the CCK+ expressing hilar commissural-associated pathway related cells (HICAP) that extend their axons into the IML (**Figure 1.4-12**) (Hosp et al., 2014).

CA3 Onward

The mossy fibre pathway extends to the hilus and CA3 regions. The Schaffer commissural pathway continues this circuit through CA3 pyramidal cells synapsing on CA1 pyramidal cells. Finally, axons from CA1 are sent back to the subiculum and entorhinal cortex completing the trisynaptic circuit. The pathways are more complex than described, with specific regions and cell types interacting in very intricate and involved ways. Behavior and functional characteristics can also be narrowed down to very specific aspects of the hippocampus, or even just pertaining to the dentate gyrus.

Dentate Gyrus Function

An estimated 700 new neurons in the adult human DG are generated each day, equating to nearly 2% of the DG population each year (Spalding et al., 2013). This highlights the significance of this process and has led to a large number of works determining their functional roles. The cells of the DG are thought to be involved in hippocampal dependent learning and memory, because formation of learning and memory results in plasticity of the newborn cells and an acceleration of spine formation (Petsophonsakul et al., 2017). Once matured, the granular cells of the DG fire in a sparseness of coding that some call 'engrams' and this sparseness is controlled by multiple inputs from inhibitory neurons in the DG and

hilus. The cells involved with this are chandelier cells, MOPP cells, basket cells in the subgranular layer, HIPP, and HICAP cells (Li et al., 2013). The further along new granule cells succeed in maturation, the more likely they are to incorporate into circuits enhancing memory (Kee et al., 2007).

There are multiple types of memory the DG is believed to be involved with. When neurogenesis is ablated, long-term spatial and context-dependent memory is affected (Kopan et al., 2009; Saxe et al., 2006; Tronel et al., 2012). Elimination of NSC/NPCs (nestin+) results in a lost ability to learn spatial memory tasks such as the Morris Water Maze (MWM) (Goodman et al., 2010). Erythropoietin is a neuroprotective agent that results in a significant increase in new neurons and improvement on spatial memory with MWM (Dmytriyeva et al., 2019). Another interesting study involved rats exploring their environment while recordings were simultaneously exhibiting firing patterns in the DG. In addition to spatial memory networks and function the DG is believed to be involved with experience-dependent remodeling of connections, especially considering the observed high excitability and enhanced synaptic plasticity (Bergami et al., 2015; Ge et al., 2007; Gupta et al., 2012; Kee et al., 2007; Mongiat et al., 2009; Restivo et al., 2015). When DG cell firing activity was prevented during memory encoding, the ability to recall the memory was prevented (Deng et al., 2013; Denny et al., 2015). Computational modeling has been beneficial to the field by providing supporting evidence that

the DG plays a role in cognitive flexibility, memory interference avoidance, temporal information memory formation, and pattern separation (Aimone et al., 2006, 2009; Becker & Wojtowicz, 2006; Chambers et al., 2004; Rangel et al., 2014).

The DG is involved with both pattern separation and pattern completion. Pattern separation is considered a form of recall and the formation of generalizations from inputs that are not complete, while pattern completion involves creating distinctions between two very similar inputs. Studies have substantially focused more on pattern separation and how the constantly changing new synapses with new granule cells being added are a requirement (Brunner et al., 2014; Clelland et al., 2009; Danielson et al., 2016; Fenton & Dranovsky, 2011; Nakashiba et al., 2012). The DG's role in pattern separation has even been successfully observed in human studies that used BOLD signals in an MRI study while patients were performing relevant tasks (Ca et al., 2008). How the DG creates pattern separation, especially with implementing the new granular cells, is still up to debate (GoodSmith et al., 2017). Pattern separation may be developed four to six weeks after mitosis, when immature adult born GCs exhibit distinct functional properties compared to mature adult born GCs or previously born older GCs, such as less inhibitory input (Krzisch et al., 2014; Marin-Burgin et al., 2012). There is strong evidence in support of the classical models for the granule cells' sparse selectivity, and it helps resolve the conflicting literature by identifying

the firing patterns of the multi-field being a function corresponding to the mossy cells instead of the granule cells. Granule cells use more independent ensembles of cells to represent environments, whereas mossy cells use large overlapping groupings or ensembles of cells, with each cell displaying a different spatial firing pattern to each environment (Almeida-Suhett et al., 2014; GoodSmith et al., 2017). One supporting theory behind these granular cells is that they do pattern separation as a sort of "sparse code" and the mossy cells in the hilus that receive input from them exhibit changes in firing field locations.

Summary

The dentate gyrus contains a variety of cells involved with the various pathways that ultimately contribute to learning and memory function. The subgranular zone in the DG contains the NSC/NPC populations that continuously produce new granule cells that are thought to play a significant role in function. Th acceptance of adult neurogenesis is substantially important as it provides new avenues to explore ways of addressing neurologic diseases and injuries.

1.3 Notch Signaling

Notch is a single pass transmembrane cell surface receptor known for its contribution to development (Sibbe et al., 2009). The Notch signaling pathway is unidirectional involving a series of proteolytic cleavages ultimately resulting in the transcription of downstream targets. A neighboring cell containing the ligand Delta-like or Jagged bind to the Notch receptor and this causes tension to reveal a cleavage site at the inner edge of the plasma membrane (**Figure 1.6**). Gamma secretase cleaves Notch at this site releasing an intracellular domain (NICD) that translocates to the nucleus. Once in the nucleus, NICD forms a transcriptional regulatory complex with CSL/RBPJ, Mastermind, and p300 (Kopan & Ilagan, 2009). Upregulation in the expression of hairy and enhancer of split (HES) and other related genes are the result of these events.

In embryonic development the canonical Notch pathway results in various developmental commitments in the nervous system. These encompass maintenance and proliferation of neural stem cells, cell fate specification, differentiation, migration, morphology, and cell death (Aguirre et al., 2010; Gaiano & Fishell, 2002; Imayoshi et al., 2010). In adult neurogenesis Notch receives significant attention due to its role in maintaining the NSC and NPC pools (Androutsellis-Theotokis et al., 2006; Imayoshi et al., 2010). Notch regulates the number of cells that exit the pool while simultaneously ensuring the cell pool is

not depleted (Ables et al., 2010). When Notch activity is low, pro-neural basic helix-loop-helix genes including Ascl1 and NGN2 are activated for cell cycle exit and preparation for migration (Kageyama et al., 2009). Notch signaling controls the specification of neural identity through lateral inhibition, with the cell containing the Notch receptor undergoing the inhibition (Šestan et al., 1999).

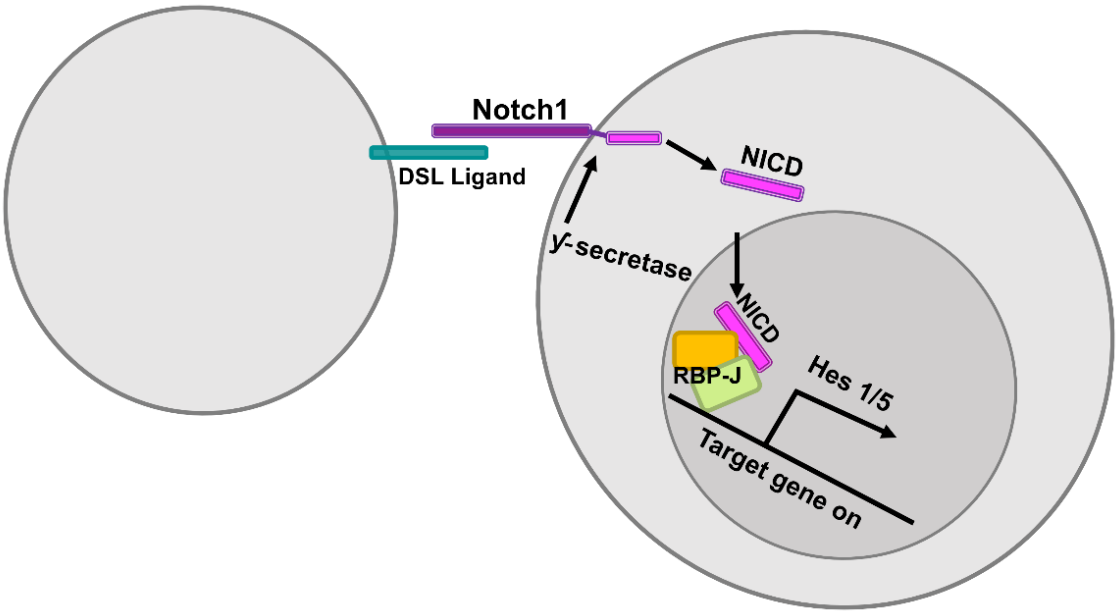

Figure 1.6. Overview of Canonical Notch1 Signaling. A cell communicates with an adjacent cell through a Notch1 receptor resulting in a cleaved intracellular portion of Notch1 (NICD) that interacts with a transcriptional activation complex and ultimately induces the expression of target genes.

The primary form of Notch that is involved with adult hippocampal neurogenesis is Notch1. There are 3 other forms of Notch with various functions and locations (Hallaq et al., 2015). Notch3 is located in vascular smooth muscle, thymocytes, and t-cells and is overexpressed in several types of cancers, and it is involved in the hypothalamic-neurohypophysial system (Salazar et al., 2020). Notch4 is primarily expressed in vasculature, but may play a minor role in inhibition of Notch1 signaling (Ables et al., 2011). Notch1 and Notch2 are the only forms that lead to embryonic lethality, highlighting their importance in embryonic development (Miele, 2006). Additionally, Notch has also been found in intestinal crypt cells and can determine their fate (VanDussen et al., 2012). In mammals, all four Notch proteins bind to Jagged 1/2 or Delta 1/4 and the intracellular portions all bind to RBPJ and the coactivator Mastermind.

As Notch influences differentiation of NSCs, it is also involved in morphology and neurite outgrowth (Ables et al., 2011; Muroyama et al., 2016; Salama-Cohen et al., 2006). Notch1 is engaged in the stabilization of microtubules, turnover of varicosities, filopodia of neurites, and changes in expression of the cytoskeleton and signaling proteins that modulate growth (Ferrari-Toninelli et al., 2008; Giniger, 2012). The expression levels of Notch alternate with the new developing cells in the DG, from high levels very early on followed by a significant decrease during the initial expression of doublecortin (DCX), and back to higher

levels when a cell differentiates into an immature neuron with DCX still present (Giniger, 2012). The latter half of this Notch expression pattern is during neurite development of the new neurons. Notch reduces the length of dendritic branches while increasing the branch number, and it acts through lateral inhibition so dendrites do not overlap with one another (Berezovska et al., 1999; Redmond et al., 2000). Overexpression of NICD (activated/cleaved Notch) increases dendritic complexity, while conditional Notch1 knockouts (cKOs) result in a decrease of dendritic complexity (Breunig et al., 2007). Dendritic complexity is associated with synaptic plasticity, and Notch1 participates in this function (Alberi et al., 2011; Liu et al., 2015; Wang et al., 2004). Notch1 is present at the synapse and neuronal activity induces both its expression and signaling (Alberi 2011). It is located post-synaptically, it regulates both NMDAR expression and composition, it interacts with the Reelin cascade, and it influences a cascade of cellular events culminating in CREB activation (Brai et al., 2015). On a broader functional level, Notch1 is believed to be a major component in cognitive function and memory (Alberi et al., 2013; Ding et al., 2016; Feng et al., 2017; Hallaq et al., 2015). Investigating Notch1 on the injury-induced neurogenic population and the possible relevance to cognitive function may prove to be a useful target in addressing cognitive impairments after brain injury.

1.4 Dissertation Objectives

The purpose of the work in this dissertation attends to the process of recovery after TBI. TBI causes severe and lifelong deficits in various neurological functions including learning and memory (Coronado et al., 2012). The discovery of adult neural stem cells has allowed for more promising recovery opportunities (Thurman et al., 1999). In particular, cognitive recovery is associated with the injury-induced neuronal populations generated from neural stem and progenitor cells (NSCs/NPCs) residing in the DG of the hippocampus (Altman & Das, 1965; Blaiss et al., 2011; Eriksson et al., 1998; Imayoshi et al., 2010; Sun, 2005; Sun et al., 2007, 2015).

Our lab has made significant contributions to the field over the past several years. To address the survival of injury-induced new cells, rats received bromodeoxyuridine (BrdU) during 2 – 5 days post-injury (Sun et al., 2007). The majority of BrdU+ cells that survived out to 10 weeks post-injury had differentiated into dentate granule neurons. These BrdU+/NeuN+ cells also labeled for synaptophysin, suggesting that these cells receive synaptic input. This study also addressed cognitive deficits after injury by using Morris Water Maze at different intervals of days post-injury. The deficits were apparent until the 56-60 days post-TBI test interval. This suggests an innate recovery is occurring in the

hippocampus around 56-60 days post-injury and it aligns with the injury-induced population that survived to become neurons.

Based on these results, our lab wanted to investigate the direct association of injury-induced neurogenesis and cognitive recovery, and to see if this cognitive recovery was still apparent if the injury-induce cell proliferation was inhibited (Sun et al., 2015). We administered an antimitotic agent called arabinofuranosyl cytidine (Ara-C), for 7 days following TBI. The animals received BrdU to label proliferating cells and were sacrificed 7 days after the injury. The total number of BrdU+ cells and new immature neurons in the DG were significantly reduced in animals that received Ara-C compared to vehicle. Another cohort of animals received Ara-C for 7 days after injury and were tested on the same MWM paradigm 56-60 days after injury. The inhibition of proliferation resulted in a completely eliminated innate cognitive recovery on the MWM task. These results support the hippocampal DG neurogenesis and cognitive recovery theory and emphasize this topics importance.

Most recently, our lab explored a more direct route of studying learning and memory recovery from injury-induced neurogenic populations. Physiological recordings were conducted to target the hippocampal function after injury. The capacity for long-term potentiation (LTP) was assessed in rats 30 or 60 days after they received sham surgery or lateral fluid percussion injury (LFPI)

(Weston et al., 2021). These time points were chosen to coincide with the behavioral assays accomplished by our lab, with 60 days matching the innate cognitive recovery time, and 30 days matching cognitive deficits. We assessed LTP in the medial perforant pathway as this pathway provides input from entorhinal cortex to the DG containing the new granular cells (Ibrahim et al., 2016; Villasana et al., 2015). We found recordings predominantly reflecting LTP elicited in newly born granule cells (GCs) showed a time-dependent cycle of functional impairment at 30 days post-injury (DPI) followed by recovery at 60 DPI (**Figure 1.7**), and we did not see this recovery response from recordings that reflected the larger population of mature GCs either. This work signifies the physiological contribution of newly born GCs to recovery by capacity for LTP and directly ties to the 60 DPI recovery on the MWM task. The hippocampus plays an integral role in cognitive functions, and the new neurons directly participate in this function under a physiological capacity.

Following these studies, there is still a gap in the knowledge of how these new neuronal populations contribute to recovery post-TBI. The morphological development of these post-injury new neurons, the regulatory mechanisms driving their maturation, and their functional integration in the hippocampal circuitry are poorly understood. Recent studies have reported that post-injury newly generated neurons in the DG have altered dendritic complexity, but the

findings are limited and the implications are unknown (Ding et al., 2016; Redmond et al., 2000). To increase the understanding of the contribution of injury-induced new neurons to cognitive recovery following TBI, it is paramount to elucidate their underlying cellular mechanisms in regards to their dendritic development and functional plasticity.

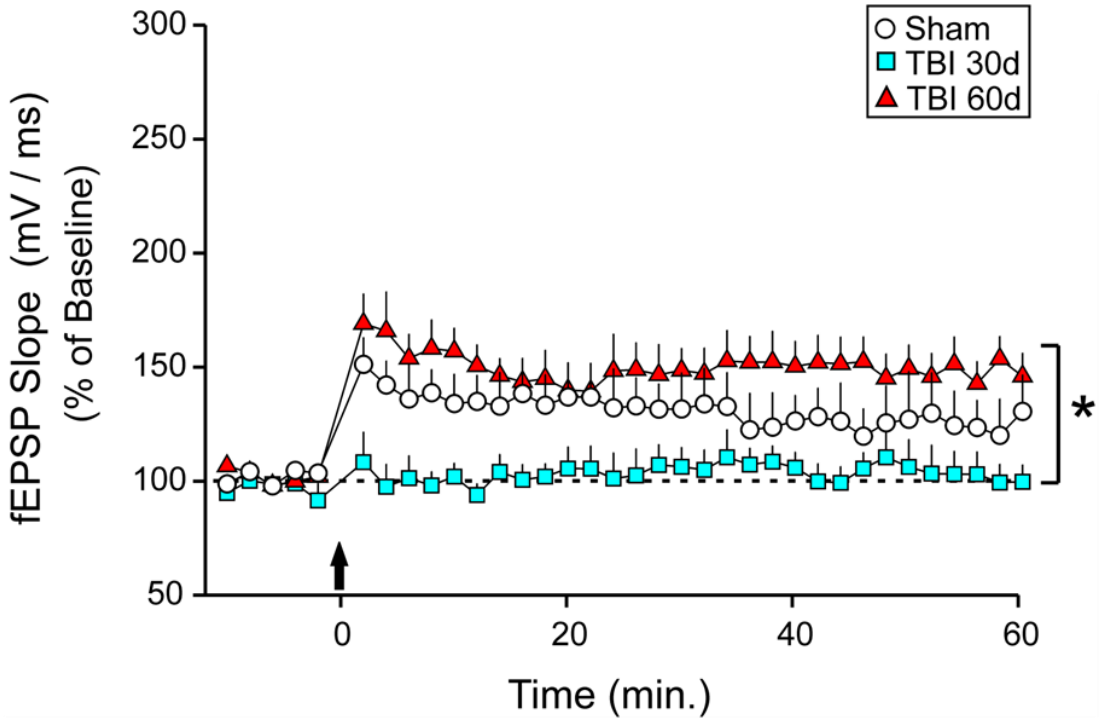

Figure 1.7. Capacity for Long-Term Potentiation in the Perforant Pathway after Traumatic Brain Injury. Mean fEPSP slopes (+SEM), expressed as percent of baseline level, are plotted for sham-injury, TBI 30 dpi, and TBI 60 dpi, showing the final 10 min. of baseline recording and 60 min. of post-high frequency stimulation recording. Responses were evoked and collected at a rate of 1/30 s, but for statistical and graphical analyses were aggregated into 2 min. epochs. The magnitude of LTP in the TBI 60 dpi group, averaged over the 60 min. of post-HFP recording, was significantly larger than in the TBI 30 dpi group (*$p < 0.05$). (Weston et al., 2021)

A critical aspect guiding the focus of this proposal is to explore mechanisms that regulate neurogenic development following TBI, with this focus being Notch1 signaling, as Notch1 signaling is a key regulator of neurogenesis during developmental stage and adult in physiological condition (Alberi et al., 2011; Feng et al., 2017; Fraser et al., 2019; Hallaq et al., 2015). In the setting of TBI, preliminary studies from our group suggest important implications of Notch1 signaling under neuropathological conditions. We found an increase in protein expression levels of Notch1 signaling elements in the neurogenic regions coincide with the injury-enhanced proliferation of NSC/NPCs and new neuron maturation (unpublished data). Work from other groups also show that Notch1 signaling is a strong contender for a role in recovery after TBI. NICD upregulation in rats that received a TBI had an increase in the injury-induced neurogenic population (Wang, 2017). Manipulating the downstream target, Hes-1, resulted in a large increase in the neurogenic response after TBI and a vast maturation period of neurogenic cells. Increasing Hes-1 results in a decrease of memory, and on MWM tasks animals show an increase in memory after knocking down Hes-1 (Zhang et al., 2014). These results are evidence of the importance of Notch1 as Hes-1 is directly downstream from it, and how Hes-1 acts as a feedback regulator for the functions of this signaling pathway. Since Notch1 has been implicated for neurogenic proliferation, it would be a useful signaling pathway to target for TBI recovery

especially because it has been shown that Notch1 deficiency leads to cognitive impairments and emotional impairment, providing prospective recovery in these two deficits after TBI in relevance to the neurogenic population of the DG (Feng et al., 2017; Wang, 2017). Taken together, these studies suggest Notch1 signaling may be an essential player for regulation of TBI-induced new neurons and their functional participation in the hippocampus following TBI.

This dissertation addresses the cognitive deficits after TBI and lack of fully understanding the mechanisms contributing to cognitive dysfunction. Recent studies have shown that endogenous repair through neurogenesis plays an important role in cognitive recovery following TBI and Notch1 may play a substantial part in this, and so this work was intended to dissect the mechanisms driving this endogenous response. This dissertation examines the cell population, morphology, and behavioral function of TBI-induced new neurons and the importance of Notch1 in the setting of post-TBI recovery stage. Based on this premise, it's hypothesized that the maturation, survival, and dendritic development of newly generated cells after injury are an essential component for contribution to functional recovery and Notch1 serves a role in this response. The results from these studies may help the population of individuals suffering from long-term cognitive dysfunction as a result of TBI.

Chapter 2

Notch1 and Injury-Induced Neurogenic Cell Response in the Dentate Gyrus

2.1 Introduction

Traumatic brain injury can cause a host of physiologic responses including new populations of neurons from neural stem cell niches (Dash et al., 2001). The fate and purpose of these injury-induced new cells we have only recently begun to understand. Under normal homeostatic conditions these neurogenic regions continuously supply new cells that mature and contribute to the overall function. Restricted to the subventricular zone (SVZ) and dentate gyrus, new neurons become either involved in olfactory capabilities and behavior or in hippocampal-dependent learning and memory. It's possible that injury-induced populations may contribute to these same functions in a similar capacity.

Varying models of TBI consistently show a strong proliferative response in neurogenic regions of adult brain (Bye et al., 2011; Chirumamilla et al., 2002;

Villasana et al., 2014). The first week after injury there is a heightened proliferative period with 2 days post-injury being the peak (Dash et al., 2001; Rice et al., 2003; Sun, 2005). The injury-induced response is believed to be a regenerative mechanism, however most original studies only focused on this first week of proliferation (Chirumamilla et al., 2002). Immature neuronal amounts were shown to increase 7 days after diffuse injury (Shapiro, 2017). The fate of these injury-induced proliferative populations was examined from the first week post-injury to 10 weeks post-injury, with findings that the majority of these cells matured into neurons and also positively labeled for synaptophysin (Sun et al., 2007). These findings established the possibility for injury-induced new cells to mature into functioning neurons that could help recover the injured brain.

The capability to harness this response may push the field of TBI recovery further. This would require an understanding of the mechanisms that tightly control the injury-induced proliferative response. Notch1 is a strong contender due to its widely essential roles in NSC maintenance, proliferation, and survival in both development and adult neurogenic processes (Androutsellis-Theotokis et al., 2006; Hitoshi et al., 2002). Notch1 signaling manages the necessary amounts of cells to remain in the NSC pool or leave by communicating with neighboring cells (Ables et al., 2010; Aguirre et al., 2010; Imayoshi et al., 2010). Due to this essential role, it is likely Notch1 signaling is involved in the robust injury-induced

proliferation, especially because after injury large amounts of changes are made to the number of cells that leave the NSC pool.

Transgenic mouse lines allow for creative designs to pinpoint the importance and roles of different genes. These experiments used a conditional Notch1 knockout that is specific to neural stem and progenitor cells. This allows to directly investigate the importance of Notch1 in the injury-induced neurogenic response. To complement the Notch1 knockout, a control mouse line was used and both knockout and control had a fluorescent reporter. Both mouse lines had the Cre-lox system design and induction was only specified to NSCs. Additionally, use of the synthetic thymidine analog BrdU provides the ability to tag proliferating cells. The setup of these parameters should help us understand the consequences to the injury-induced neurogenic process of knocking out Notch1 in NSC/NPCs. Not only can we investigate the acute response, but we can also investigate more chronic consequences several weeks after injury. In these experiments it is hypothesized that there will be a significantly higher number of neurogenic cells produced from injury, and knockout of Notch1 will diminish this result.

2.2 Methods

Experimental Animals

A combination of female and male adult mice equating to 94 total were used in these studies (**Table 2.1; Appendix A**). Animals received either surgery or a moderate lateral fluid percussion injury (**Appendix B**) and were sacrificed at 2 DPI, 7 DPI, 4 WPI, or 8 WPI. The 2 DPI and 7 DPI animals only received one i.p. injection of BrdU at the concentration of 100mg/kg at 2 hours before perfusion (**Appendix D**) to study injury induced cell proliferation at 2- and 7-days post-injury, whereas in the 4 and 8 WPI groups, animals received i.p. BrdU injection single daily (50mg/kg) at 1-7 DPI to study the survival of BrdU-labeled new cells at these two time points.

Group	2 DPI	7 DPI	4 WPI	8 WPI
NC-Y Sham	6	6	6	8
NC-Y LFPI	5	6	5	7
NC-NKO-Y Sham	5	6	5	7
NC-NKO-Y LFPI	5	5	6	7

Table 2.1. Total Animals Used for Each Cell Response Experiment. Columns represent the number of days or weeks post-injury in which animals were sacrificed and used for experiments. Rows represent the separate group conditions.

Immunohistochemistry

The standard protocol for staining (**Appendix C**) was followed. In brief, mice were sacrificed at designated experiment post-injury days or weeks. Tissue was fixed with paraformaldehyde and sections were prepared. For the first set of experiments focusing on injury-induced cell proliferation (2 DPI and 7 DPI), five 50μm thick free floating coronal sections containing the dentate gyrus each 400μm apart were collected for BrdU chromogenic labeling. Sections for the cell survival experiments (4 WPI and 8 WPI) were collected in sequence within a span of 800μm of the dentate gyrus, every 5th free floating section was collected for a total of 4 sections per animal.

Sections were washed with PBS followed by application of a blocking solution and sequentially the primary antibody solution. For the 2 DPI and 7 DPI studies the primary antibody used was rat monoclonal anti-BrdU (1:2000; Abcam AB6236) and secondary antibody was biotinylated anti-rat IgG (1:200; Vector Laboratories BA-9401). For the 4 WPI and 8 WPI studies the primary antibodies used were anti-GFP (1:2000; Invitrogen A11122), anti-NeuN (1:100; Millipore MAB377), and anti-BrdU (1:1500; Abcam AB6326). Secondary antibodies used were biotinylated anti-rabbit (1:400; Vector Biolabs BA-1000), AlexaFluor 647 anti-mouse (1:200; Invitrogen A21235), and AlexaFluor 568 anti-rat (1:400; Invitrogen A11077). After ABC Elite kit, TSA™ Fluorescein Tyramide Reagent kit (1:50;

AKOYA Biosciences SAT701001EA) was applied to amplify the GFP signal. Sections were denatured in 2N HCl at 37°C for 30 minutes. The 2 DPI and 7 DPI samples were denatured before beginning the protocol. The 4 WPI and 8 WPI were stained to completion for GFP and NeuN, followed by denaturing and staining for BrdU. For the 2 DPI and 7 DPI study the liquid form of 3,3'-Diaminobenzidine (DAB) (1-part 50x DAB concentrate: 1 part 0.5% H2O2: 50 parts PBS) was applied to use as a chromogenic substrate for peroxidase enzyme to label the cells of interest.

Quantification and Stereology

Stereology was used to calculate total cell estimates for all experiments using $N = \Sigma Q^{-} \cdot t/h \cdot 1/asf \cdot 1/ssf$ where Q^{-} is particles counted, t is measured section thickness, h is counting frame heigh, asf is area sampling fraction, and ssf is section sampling fraction (Zhao & van Praag, 2020).

For the acute proliferation studies an inverted light microscope (1X71 Olympus) was used to view samples and quantify the amount of BrdU+/DAB+ stained cells. The program Visiopharm (Olympus) was used to count cell totals in both the granular cell layers and hilus. Cells located outside of the optical dissector counting frame were not included. For this specific set of experiments the dissector height (h) was set to 25µm, section thickness (t) was taken from five

separate measurements averaged, the average sampling fraction (asf) was set to 1 because the entire region was quantified in these samples, and the sample sampling fraction (ssf) was set to 0.125 due to 5 sections from each brain representing 1/8th of the hippocampus within a span of 2000μm thickness of the dentate gyrus (5x400μm).

For the longevity studies an LSM710 confocal microscope was used to capture images of whole dentate gyrus regions at 20x magnification. The Z-stack and tiling functions in Zeiss Zen microscope software was used to capture a stack made up of 10 images, each spanning a total of 1μm and all adjacent to each other for a total stack size of 10μm. Z-stack files were put into FIJI and merged into a Z-projection. Spectral unmixing was conducted on each image to remove the bleed through of channels that were used to capture Alexa 568 and Alexa 647 fluorescent labeling. The total amount of cells was counted for the three GCLs using the FIJI plugin Cell Counter. For this specific set of experiments the dissector height (h) was set to 10μm, section thickness (t) was taken from four separate averaged measurements, the average sampling fraction (asf) was set to 1 because the entire region was quantified in these samples, and the sample sampling fraction (ssf) was set to 0.2 due to 4 sections from each brain representing 1/5th of the hippocampus within a span of 800μm thickness of the dentate gyrus.

Statistical Analysis

Stereologically calculated cell numbers for all data in these experiments was evaluated using ANOVA (JMP Pro v16) combined with Tukey HSD post hoc tests. The significance level was set to $\alpha = 0.05$ for all analyses performed, and averaged values are expressed as mean ± SEM.

2.3 Results

2.3.1 Cell Proliferative Response is Reduced with Notch1 Deletion

Models assessing neurogenesis after TBI have consistently shown an increase in the proliferative response acutely after injury. In order to measure this response with Notch1 deletion in injury-induced newborn DG cells, the number of BrdU+ cells were measured and calculated using stereological techniques. The regions analyzed were the hippocampal DG granular cell layers (GCLs) and hilus (**Figure 2.1a**) on the hemisphere ipsilateral to the injury. Cell counts were conducted at two and seven days after TBI since the first week post-injury exhibits the highest proliferative cell response (**Table 2.2**).

At two days post-injury, ANOVA analyses showed the GCLs had no significant changes from injury [F(1,18) = 0.588; p = 0.453], genotype [F(1,18) = 2.860; p = 0.108], and no interactions [F(1,18) = 2.160; p = 0.159], (**Figure 2.1b**). However, the hilus at two days post-injury did show a main effect of injury [F(1,18) = 6.586; p = 0.0194*], and Tukey's posthoc revealed the LFPI NC-N-Y group had significantly higher amounts of BrdU+ cells than sham NC-NKO-Y (p = 0.037*). The hilus had no significant changes by genotype [F(1,18) = 2.712; p = 0.117], and no interactions [F(1,18) = 1.405; p = 0.251], (**Figure 2.1c**).

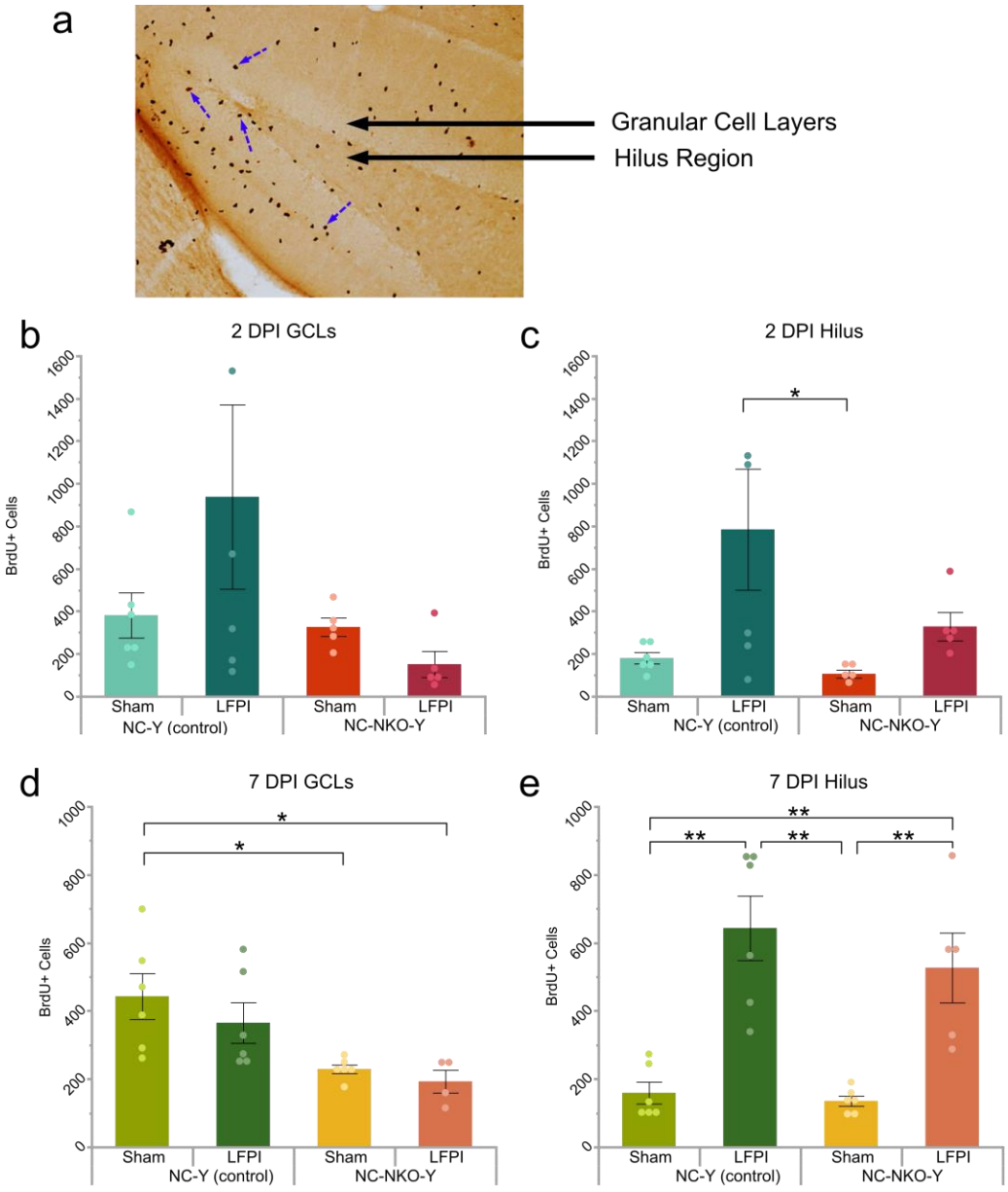

Figure 2.1. Injury-induced Acute Proliferation is Altered by Notch1 Deletion. (**a**) Image taken (4x objective) of a mouse brain showing the two regions analyzed, the GCLs and hilus region in a DG coronal section. The dashed blue arrows indicate example labeled BrdU+ cells. Group means for stereologically calculated BrdU+ cell counts are plotted for (**b**) 2 DPI GCLs, (**c**) 2 DPI hilus, (**d**) 7 DPI GCLs, and (**e**) 7 DPI hilus. Grubbs outlier detected and removed from 7 DPI GCLs for NC-NKO-Y LFPI. Significance levels indicated by $*p < 0.05$, $**p < 0.005$.

ANOVA analyses revealed the GCLs proliferative response at seven days post-injury (**Figure 2.1d**) had no main effect of injury [F(1,19) = 0.0106; $p = 0.919$], however there was a main effect of genotype [F(1,19) = 4.673; $p = 0.044$*]. Tukey's posthoc analysis revealed sham NC-Y had significantly more BrdU+ cells than sham NC-NKO-Y ($p = 0.0304$*) and LFPI NC-NKO-Y ($p = 0.0212$*). There was no interaction for 7 DPI GCLs [F(1,19) = 1.156; $p = 0.296$]. The hilus region seven days post-injury (**Figure 2.1e**) showed a substantially higher number of BrdU+ cells with injury [F(1,19) = 40.224; $p < 0.0001$**], however, there was no effect of genotype [(1,19) = 1.035; $p = 0.322$], and no interaction [F(1,19) = 0.451; $p = 0.510$]. LFPI NC-Y had significantly more cells than sham NC-Y ($p = 0.0001$**) and sham NC-NKO-Y ($p < 0.0001$**). Similarly, LFPI NC-NKO-Y had many more cells than sham NC-NKO-Y ($p = 0.0194$*) and sham NC-Y ($p = 0.0329$*).

Group	Injury	Genotype	Injury*Genotype
2 DPI GCLs	$p = 0.453$	$p = 0.108$	$p = 0.159$
2 DPI Hilus	**$p = 0.0194$***	$p = 0.117$	$p = 0.251$
7 DPI GCLs	$p = 0.919$	**$p = 0.044$***	$p = 0.296$
7 DPI Hilus	**$p < 0.0001$****	$p = 0.322$	$p = 0.510$

Table 2.2. Significance Values for Group Comparisons of BrdU+ 2- and 7- days post-Injury. Separate groups (left column) compared by injury, genotype, or an interaction of injury and genotype with $p < 0.05$ designated in red and $p < 0.005$ designated in orange.

2.3.2 Survival of Injury-Induced Newly Generated Cells

The survival of injury-induced populations of new cells is as important as the production of them. Cells of different phenotypic combinations (**Figure 2.2**) were calculated based on stereology of cell counts in all three granule cell layers (**Tables 2.3 – 2.5**). Any cell labeled with BrdU was a product of the injury-induced response occurring days 1 – 7 post-injury. Positive labeling for NeuN indicates the cell is a mature neuron. The mouse lines used had a fluorescent reporter for nestin+ populations, and in the case of Notch1 successful knockouts within that line also report this fluorescent signal. Any cell with GFP+ labeling is originally from that nestin+ population tagged with the fluorescent reporter.

Four weeks into cell development the expression of NeuN should be evident, and in the case of cells produced as a result of injury the expression of BrdU should also be present. ANOVA analysis revealed a significantly higher amount of both ***BrdU+*** [$F(1,16) = 11.08$; $p = 0.0043$**] and ***BrdU+/NeuN+*** [$F(1,16) = 9.638$; $p = 0.0068$**] as a result of injury (**Figure 2.3a,c**). When the GCLs are divided up into thirds (**Figure 2.3b,d**) this post-injury heightened proliferation remains, with ***BrdU+*** and ***BrdU+/NeuN+*** having significantly more cells in all 3 GCLs (**Table 2.4**). The different genotypes showed no change for ***BrdU+*** [$F(1,16) = 0.133$; $p = 0.721$] (**Figure 2.3a**) nor ***BrdU+/NeuN+*** [$F(1,16) = 0.147$; $p = 0.706$] (**Figure 2.3c**), and there was no interaction between injury and genotype for ***BrdU+*** [$F(1,16) = 0.216$;

$p = 0.648$]. The injury-induced mature neurons (**Figure 2.3c,d**), ***BrdU+/NeuN+***, had no effect by genotype [$F(1,16) = 0.147$; $p = 0.706$], and no interactions [$F(1,16) = 0.195$; $p = 0.665$].

By 8 weeks new neurons in the DG should display characteristics of fully mature cells, including the expression of NeuN. Both ***BrdU+*** [$F(1,24) = 26.358$; $p < 0.0001$**] and ***BrdU+/NeuN+*** [$F(1,23) = 23.759$; $p < 0.0001$*] displayed a robust increase in the number of cells as a result of injury, revealing a significant amount of cells survive to maturity that were originally part of the injury-induced population (**Figure2.4a,c**). For ***BrdU+*** cells, sham NC-Y had a greater number compared to LFPI NC-Y ($p = 0.0421$*) and compared to LFPI NC-NKO-Y ($p = 0.0006$**). The sham NC-NKO-Y had a greater number compared to the LFPI NC-NKO-Y ($p = 0.0011$**). For ***BrdU+/NeuN+*** cells, sham NC-Y had a great number compared to LFPI NC-Y ($p = 0.0396$*) and to LFPI NC-NKO-Y ($p = 0.0021$**). The sham NC-NKO-Y had a greater number compared to the LFPI NC-NKO-Y ($p = 0.0032$**) and to the LFPI NC-Y ($p = 0.0495$*). Similar to 4 weeks after injury, genotype did not alter the amount of surviving ***BrdU+*** [$F(1,24) = 1.289$; $p = 0.268$] or ***BrdU+/NeuN+*** [$F(1,23) = 0.804$; $p = 0.379$] cells, nor were there interactions for ***BrdU+*** [$F(1,24) = 1.605$; $p = 0.217$] or ***BrdU+/NeuN+*** [$F(1,23) = 1.069$; $p = 0.312$].

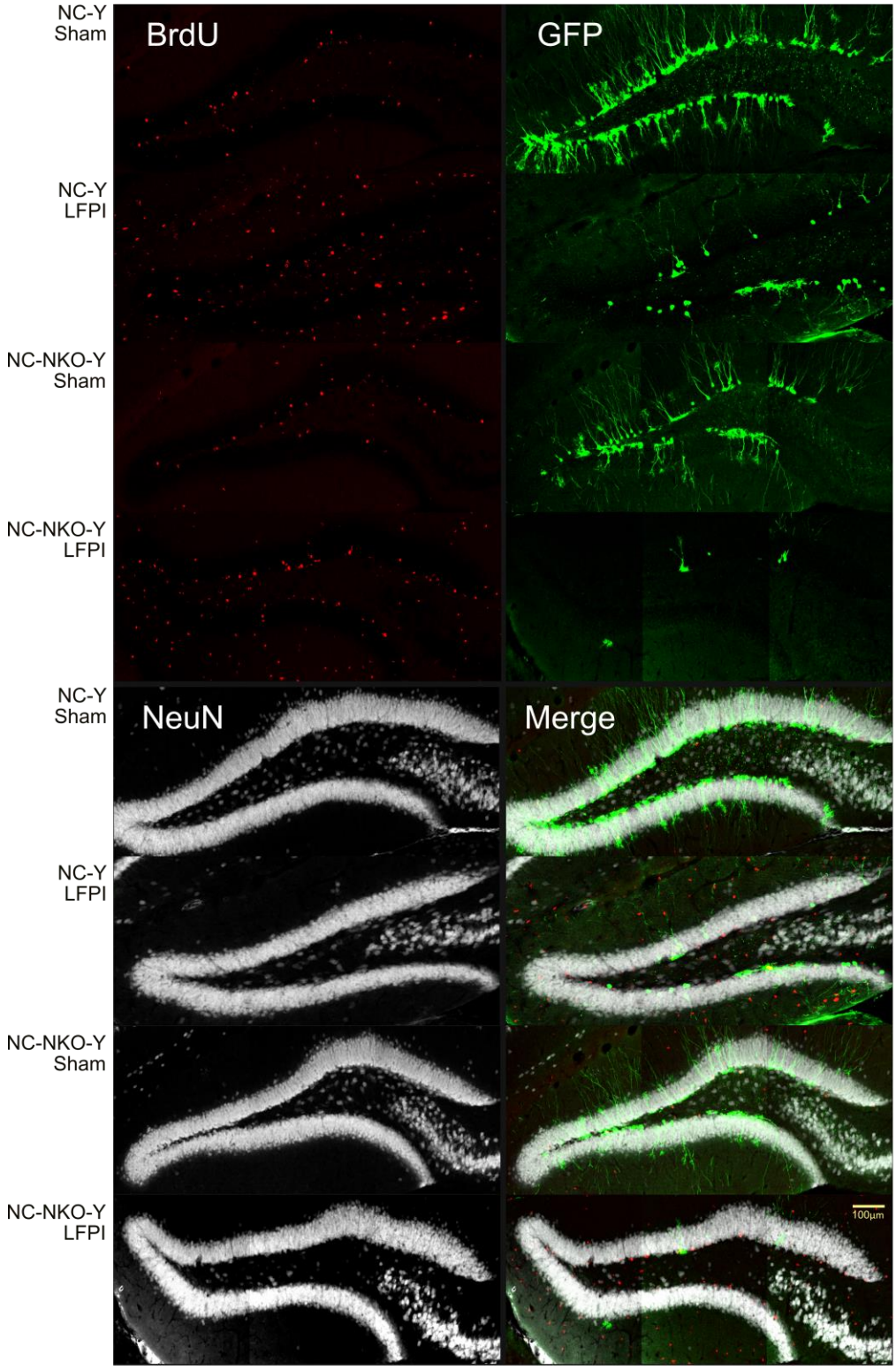

Figure 2.2. Populations of Cells after Injury and Loss of Notch1. Representative images taken on a LSM710 confocal with a 20x objective. All four groups comparing injury and genotype were labeled for BrdU, GFP, and NeuN. Separate groups are listed along the Y-axis.

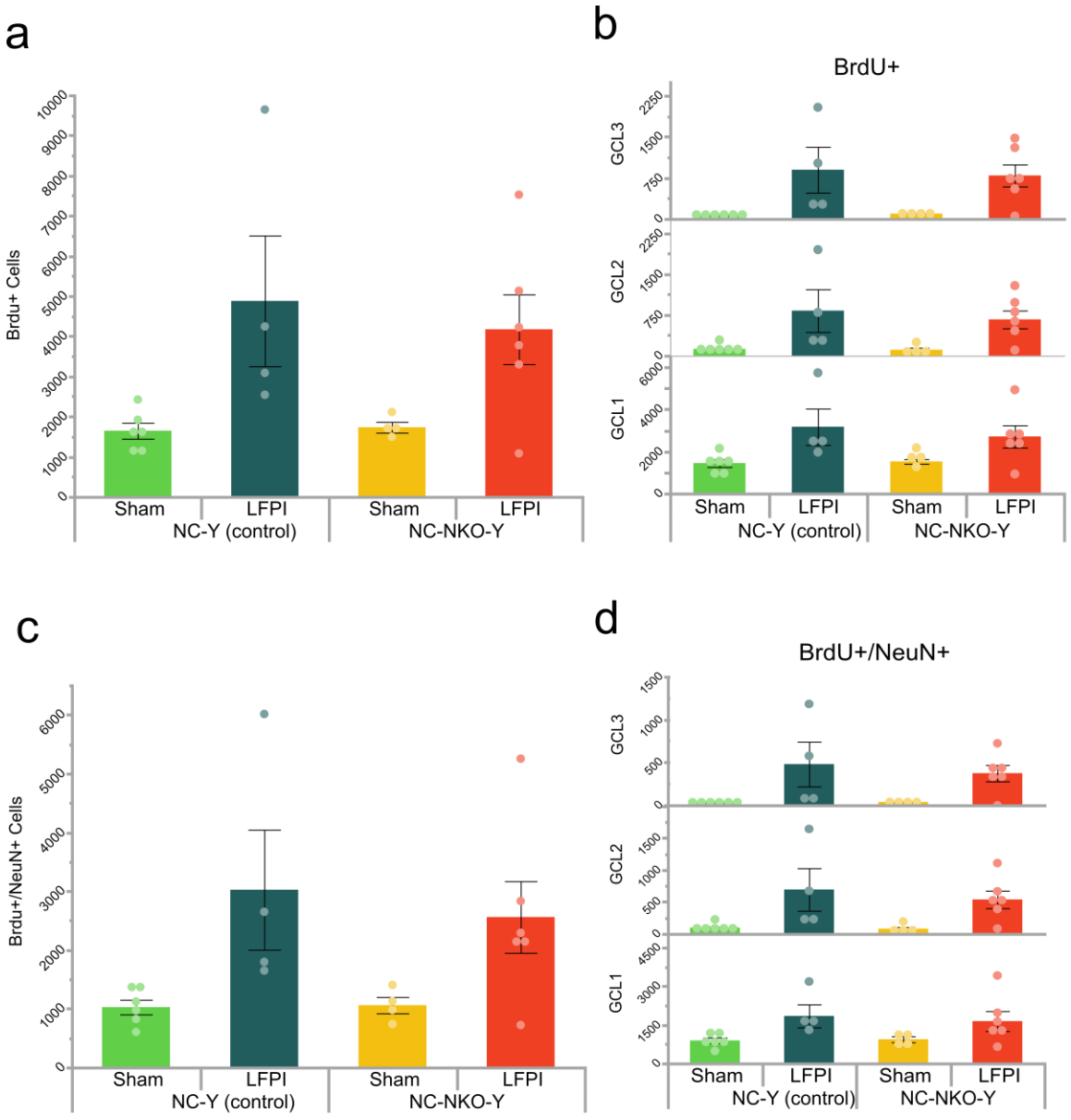

Figure 2.3. Injury-Induced New Cells Survive to 4 WPI. Group means for stereologically calculated cell amounts are plotted for (**a**) BrdU+ cells in all GCLs total, (**b**) BrdU+ cells in the GCLs separated into thirds, (**c**) BrdU+/NeuN+ cells in all GCLs total, and (**d**) BrdU+/NeuN+ cells in the GCLs separated into thirds. Overall, there was significantly more BrdU+ and BrdU+/NeuN+ cells in the injured animals.

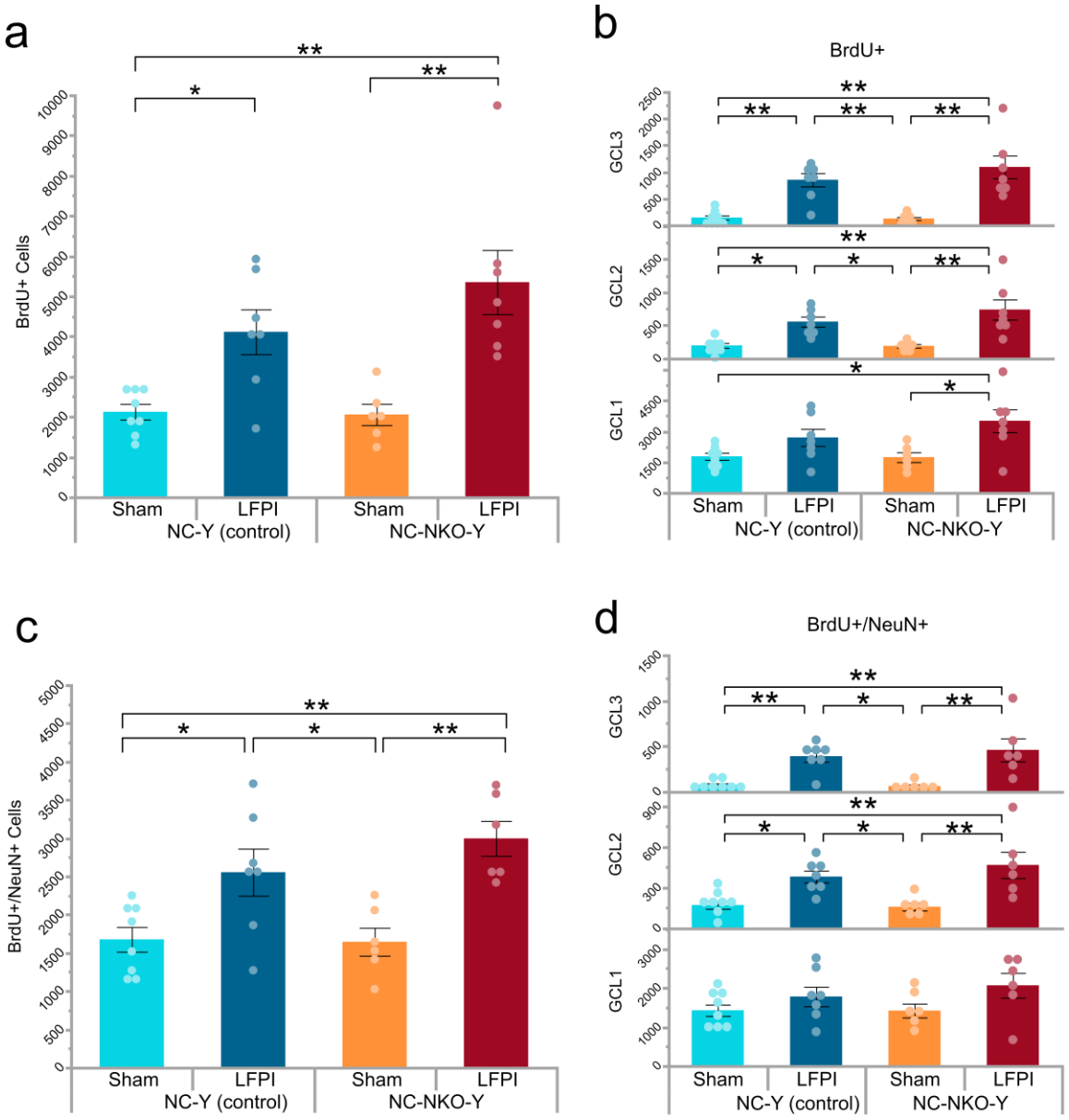

Figure 2.4. Injury-Induced New Cells Survive to 8 WPI. Group means for stereologically calculated cell amounts are plotted for (**a**) BrdU+ cells in all GCLs total, (**b**) BrdU+ cells in the GCLs separated into thirds, (**c**) BrdU+/NeuN+ cells in all GCLs total, and (**d**) BrdU+/NeuN+ cells in the GCLs separated into thirds. Overall, there was significantly more BrdU+ and BrdU+/NeuN+ cells in the injured animals. Grubbs outlier detected and removed from NC-NKO-Y. Significance levels indicated by $*p < 0.05$, $**p < 0.005$.

Cell Phenotype	Injury	Genotype	Injury*Genotype
	4 WPI		
BrdU+	***p* = 00.0043****	*p* = 0.721	*p* = 0.648
GFP+	*p* = 0.848	*p* = 0.538	*p* = 0.571
BrdU+/GFP+	*p* = 0.294	*p* = 0.326	*p* = 0.254
BrdU+/NeuN+	***p* = 0.0068****	*p* = 0.706	*p* = 0.665
GFP+/NeuN+	*p* = 0.317	*p* = 0.947	*p* = 0.799
BrdU+/GFP+/NeuN+	*p* = 0.111	*p* = 0.495	*p* = 0.281
	8 WPI		
BrdU+	***p* < 0.0001****	*p* = 0.268	*p* = 0.217
GFP+	***p* = 0.0054****	*p* = 0.434	*p* = 0.784
BrdU+/GFP+	*p* = 0.982	*p* = 0.729	*p* = 0.129
BrdU+/NeuN+	***p* < 0.0001****	*p* = 0.379	*p* = 0.312
GFP+/NeuN+	*p* = 0.257	*p* = 0.072	*p* = 0.137
BrdU+/GFP+/NeuN+	*p* = 0.283	*p* = 0.087	*p* = 0.085

Table 2.3. Significance Values for Comparisons of 4- and 8-week post-Injury. The cell populations of the different variations in phenotypic expressions (left column) compared by injury, genotype, or an interaction of injury and genotype with $p < 0.005$ designated in orange. Data is separated by 4 WPI (top) and 8 WPI (bottom).

Cell Phenotype	Injury	Genotype	Injury*Genotype
	4 WPI		
	GCL 1		
BrdU+	***p* = 00.0091****	*p* = 0.702	*p* = 0.591
GFP+	*p* = 0.772	*p* = 0.478	*p* = 0.619
BrdU+/GFP+	*p* = 0.320	*p* = 0.325	*p* = 0.257
BrdU+/NeuN+	***p* = 0.0171***	*p* = 0.807	*p* = 0.699
GFP+/NeuN+	*p* = 0.125	*p* = 0.416	*p* = 0.236
BrdU+/GFP+/NeuN+	*p* = 0.125	*p* = 0.416	*p* = 0.236
	GCL 2		
BrdU+	***p* = 0.0038****	*p* = 0.644	*p* = 0.697
GFP+	*p* = 0.351	*p* = 0.925	*p* = 0.416
BrdU+/GFP+	*p* = 0.157	*p* = 0.529	*p* = 0.330
BrdU+/NeuN+	***p* = 0.0041****	*p* = 0.592	*p* = 0.666
GFP+/NeuN+	*p* = 0.091	*p* = 0.663	*p* = 0.529
BrdU+/GFP+/NeuN+	*p* = 0.091	*p* = 0.663	*p* = 0.530
	GCL 3		
BrdU+	***p* = 0.0022****	*p* = 0.844	*p* = 0.764
GFP+	*p* = 0.696	*p* = 0.704	*p* = 0.499
BrdU+/GFP+	*p* = 0.224	*p* = 0.224	*p* = 0.224
BrdU+/NeuN+	***p* = 0.0048****	*p* = 0.674	*p* = 0.653
GFP+/NeuN+	*p* = 0.231	*p* = 0.272	*p* = 0.231
BrdU+/GFP+/NeuN+	*p* = 0.220	*p* = 0.272	*p* = 0.231

Table 2.4. Significance Values for Comparisons of 4 WPI Separated by GCL. The cell populations of the different variations in phenotypic expressions (left column) compared by injury, genotype, or an interaction of injury and genotype with $p < 0.05$ designated in red and $p < 0.005$ designated in orange. Data is separated by GCL 1 (top), GCL 2 (middle), GCL 3 (bottom).

Cell Phenotype	Injury	Genotype	Injury*Genotype
	8 WPI		
	GCL 1		
BrdU+	***p* = 00.0015****	*p* = 0.317	*p* = 0.268
GFP+	***p* = 0.0036****	*p* = 0.394	*p* = 0.757
BrdU+/GFP+	*p* = 0.616	*p* = 0.886	*p* = 0.163
BrdU+/NeuN+	***p* = 0.0365***	*p* = 0.541	*p* = 0.520
GFP+/NeuN+	*p* = 0.595	*p* = 0.081	*p* = 0.166
BrdU+/GFP+/NeuN+	*p* = 0.611	*p* = 0.066	*p* = 0.079
	GCL 2		
BrdU+	***p* < 0.0001****	*p* = 0.332	*p* = 0.299
GFP+	*p* = 0.485	*p* = 0.881	*p* = 0.904
BrdU+/GFP+	*p* = 0.494	*p* = 0.356	*p* = 0.278
BrdU+/NeuN+	***p* < 0.0001****	*p* = 0.497	*p* = 0.364
GFP+/NeuN+	***p* = 0.0051****	*p* = 0.157	*p* = 0.105
BrdU+/GFP+/NeuN+	*p* = 0.135	*p* = 0.559	*p* = 0.413
	GCL 3		
BrdU+	***p* < 0.0001****	*p* = 0.391	*p* = 0.316
GFP+	*p* = 0.951	*p* = 0.591	*p* = 0.983
BrdU+/GFP+	*p* = 0.310	*p* = 0.310	*p* = 0.310
BrdU+/NeuN+	***p* < 0.0001****	*p* = 0.671	*p* = 0.536
GFP+/NeuN+	*p* = 0.0796	*p* = 0.594	*p* = 0.996
BrdU+/GFP+/NeuN+	*p* = 0.115	*p* = 0.899	*p* = 0.826

Table 2.5. Significance Values for Comparisons of 8 WPI Separated by GCL. The cell populations of the different variations in phenotypic expressions (left column) compared by injury, genotype, or an interaction of injury and genotype with $p < 0.05$ designated in red and $p < 0.005$ designated in orange. Data is separated by GCL 1 (top), GCL 2 (middle), GCL 3 (bottom).

2.3.3 GFP+ Cell Populations Shift with Increased Time from Injury

If injury-induced proliferative populations are significantly increased several weeks after the injury, the next question is what is happening in the NSC pools where the neurogenic response is arising from. The transgenic mice used in these studies express GFP in nestin+ cells and their descendants, making it possible to examine the long-term outcome of cells coming from NSC populations.

At 4 weeks post-injury the ***GFP+*** cells (**Figure 2.5a**) did not differ due to injury [$F(1,16) = 0.038$; $p = 0.848$], genotype, [$F(1,16) = 0.397$; $p = 0.538$], or from an interaction [$F(1,16) = 0.335$; $p = 0.571$]. The division of GCLs reflected these results with no differences (**Figure 2.5b**). The 8 weeks post-injury ***GFP+*** cell populations (**Figure 2.6a**) did have a significant reduction as a result of injury [$F(1,25) = 9.275$; $p = 0.0054$**] with sham NC-Y having the highest number of cells compared to LFPI NC-NKO-Y ($p = 0.0489$*). There was no effect of genotype [$F(1,25) = 0.633$; $p = 0.434$] or an interaction [$F(1,25) = 0.077$; $p = 0.784$]. These results show a decrease in GFP+ cells after injury, predominately in GCL1, suggesting depletion of the NSC pool 8 weeks after injury (**Figure 2.6b**).

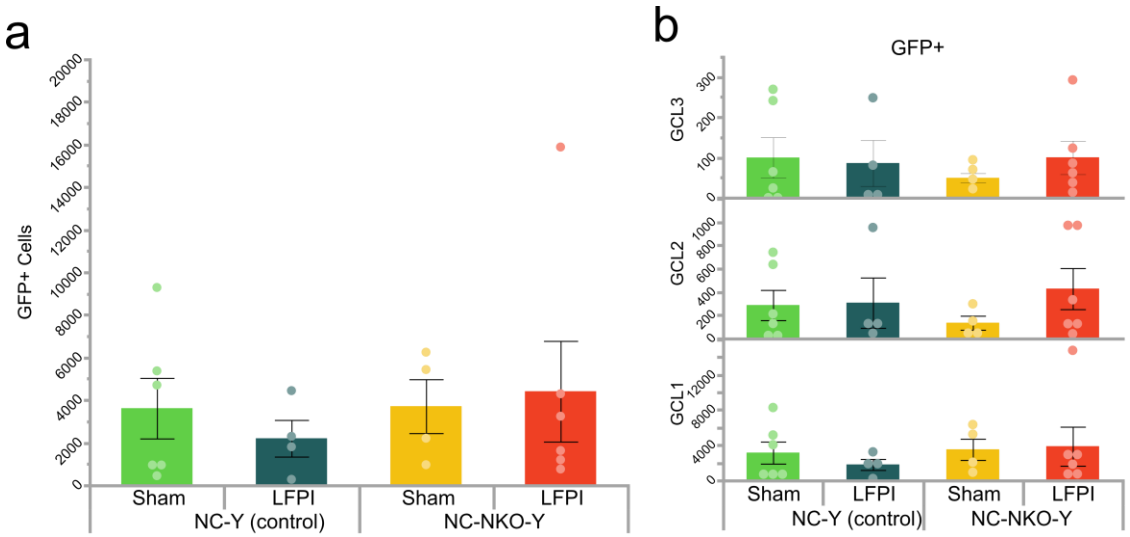

Figure 2.5. GFP+ Populations Remain Unaltered at 4 WPI. Group means for stereologically calculated cell amounts are plotted for (**a**) GFP+ cells in all GCLS and (**b**) GFP+ cells divided by the GCLs. No differences were observed between the separate conditions.

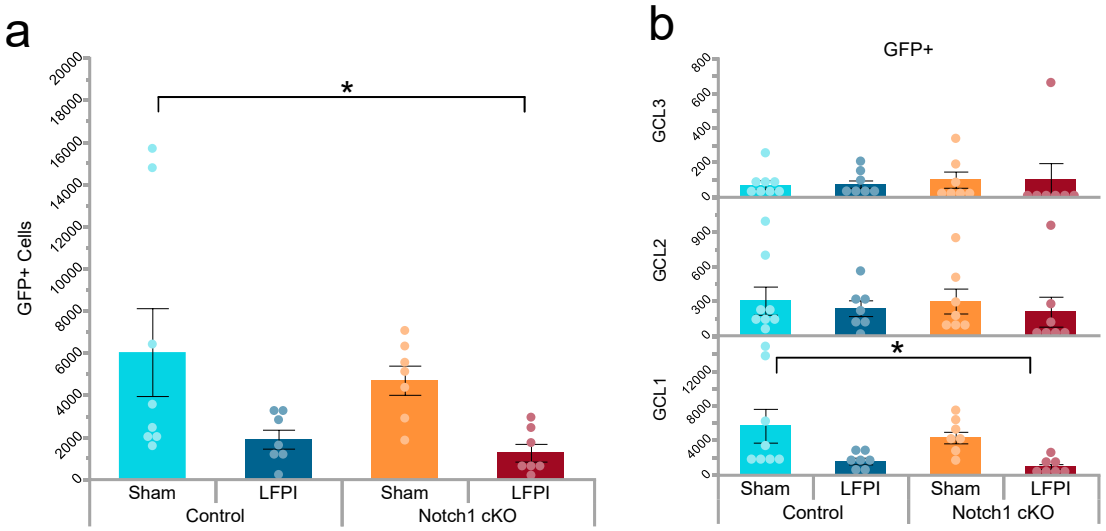

Figure 2.6. GFP+ Populations Show Differences at 8 WPI. Group means for stereologically calculated cell amounts are plotted for (**a**) GFP+ cells in all GCLS and (**b**) GFP+ cells divided by the GCLs. Injured groups had a significant reduction in GFP+ cells compared to animals that received sham surgery. Significance levels indicated by $*p < 0.05$.

2.3.4 Loss of *Notch1* Does Not Play a Significant Role in Injury-Induced Populations of Cells

The Notch1 signaling pathway is known for its role in cell proliferation and this includes the adult neurogenic regions such as the DG. The mice used in this study have either an induced Notch1 conditional knock-out (cKO) in nestin+ cells that occurs before the time of injury (NC-NKO-Y), or are a control with Notch1 still present (NC-Y). This cKO is to determine the role Notch1 plays in these injury-induced cell populations.

At 4 weeks after injury, there were no differences from the injury between ***BrdU+/GFP+*** [$F(1,16) = 1.176$; $p = 0.294$] or ***BrdU+/GFP+/NeuN+*** [$F(1,16) = 2.849$; $p = 0.111$] cell totals (**Figure 2.7a,c**), and no differences from injury when divided by GCL (**Figure 2.7b,d**). There were also no differences by genotype between ***BrdU+/GFP+*** [$F(1,16) = 1.026$; $p = 0.326$] or B***rdU+/GFP+/NeuN+*** [$F(1,16) = 0.489$; $p = 0.495$] cell counts, and no differences from genotype when divided by GCL. Likewise, there were no differences from interactions for cell totals of ***BrdU+/GFP+*** [$F(1,16) = 1.402$; $p = 0.254$], ***BrdU+/GFP+/NeuN+*** [$F(1,16) = 1.246$; $p = 0.281$].

At 8 weeks after injury, there were no differences between the groups from injury for ***BrdU+/GFP+*** [$F(1,25) = 0.0005$; $p = 0.982$] or ***BrdU+/GFP+/NeuN+*** [$F(1,21) = 1.214$; $p = 0.283$] (**Figure 2.8a,c**). There were no differences from genotype for ***BrdU+/GFP+*** [$F(1,25) = 0.123$; $p = 0.729$], and although there appears to be a trend,

there is no statistically significant difference for ***BrdU+/GFP+/NeuN+*** [$F(1,21) = 3.223$; $p = 0.087$], and no differences from an interaction for ***BrdU+/GFP+*** [$F(1,25) = 2.472$; $p = 0.129$] or ***BrdU+/GFP+/NeuN+*** [$F(1,21) = 3.27$; $p = 0.085$]. The GCLs followed the same results (**Figure 2.8b,d**) with no differences from injury, genotype, or an interaction, however there appeared to be a trend for ***BrdU+/GFP+/NeuN+*** GCL1 similar to the results of all the GCLs combined (**Figure 2.8c,d**).

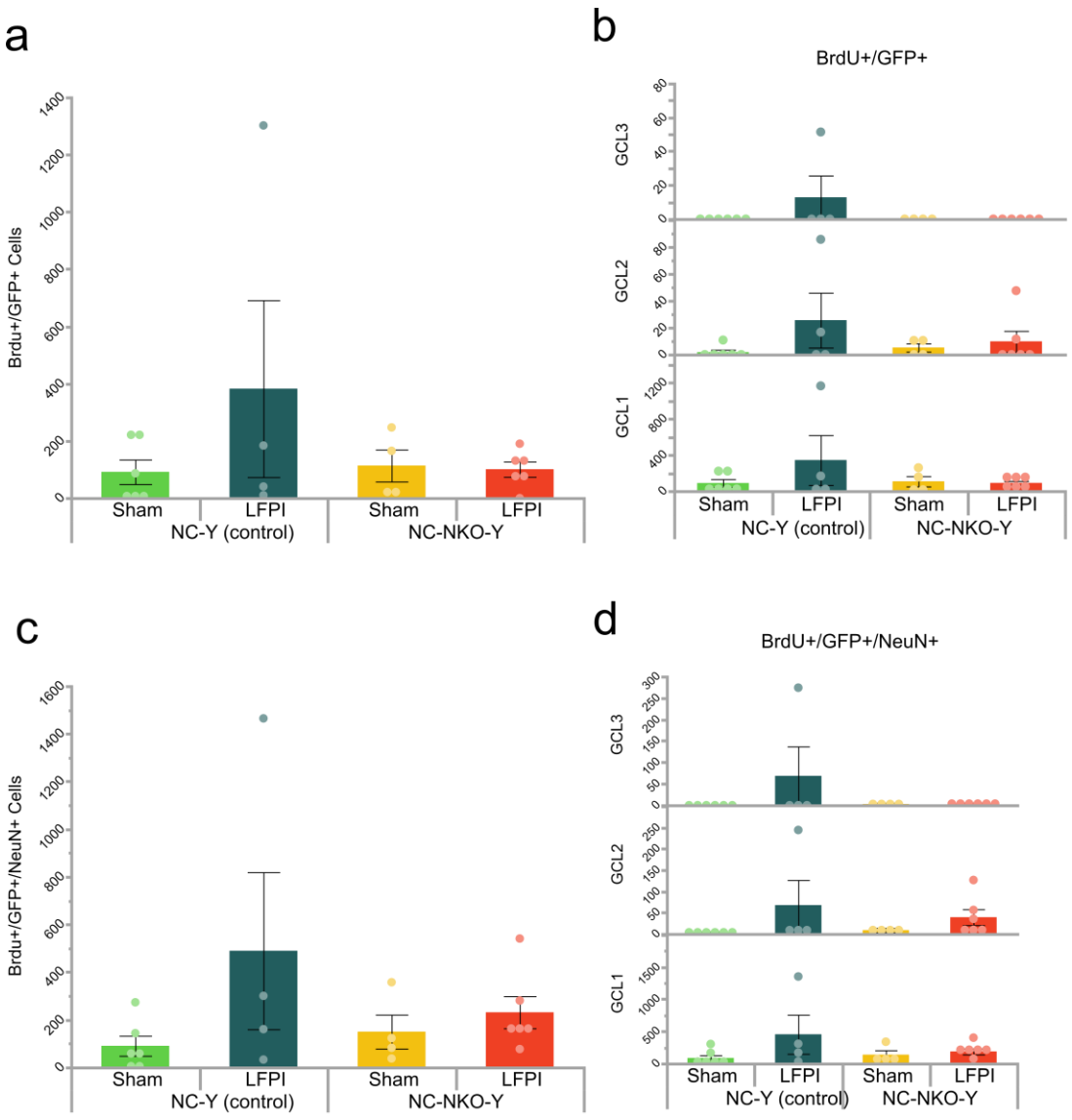

Figure 2.7. Loss of Notch1 Does Not Alter Injury-Induced Populations 4 WPI. Group means for stereologically calculated cell amounts are plotted for (**a**) BrdU+/GFP+ in all GCLS, (**b**) BrdU+/GFP+ separated by GCL, (**c**) BrdU+/GFP+/NeuN+ in all GCLs, and (**d**) BrdU+/GFP+/NeuN+ separated by GCL. No differences were observed between the different conditions.

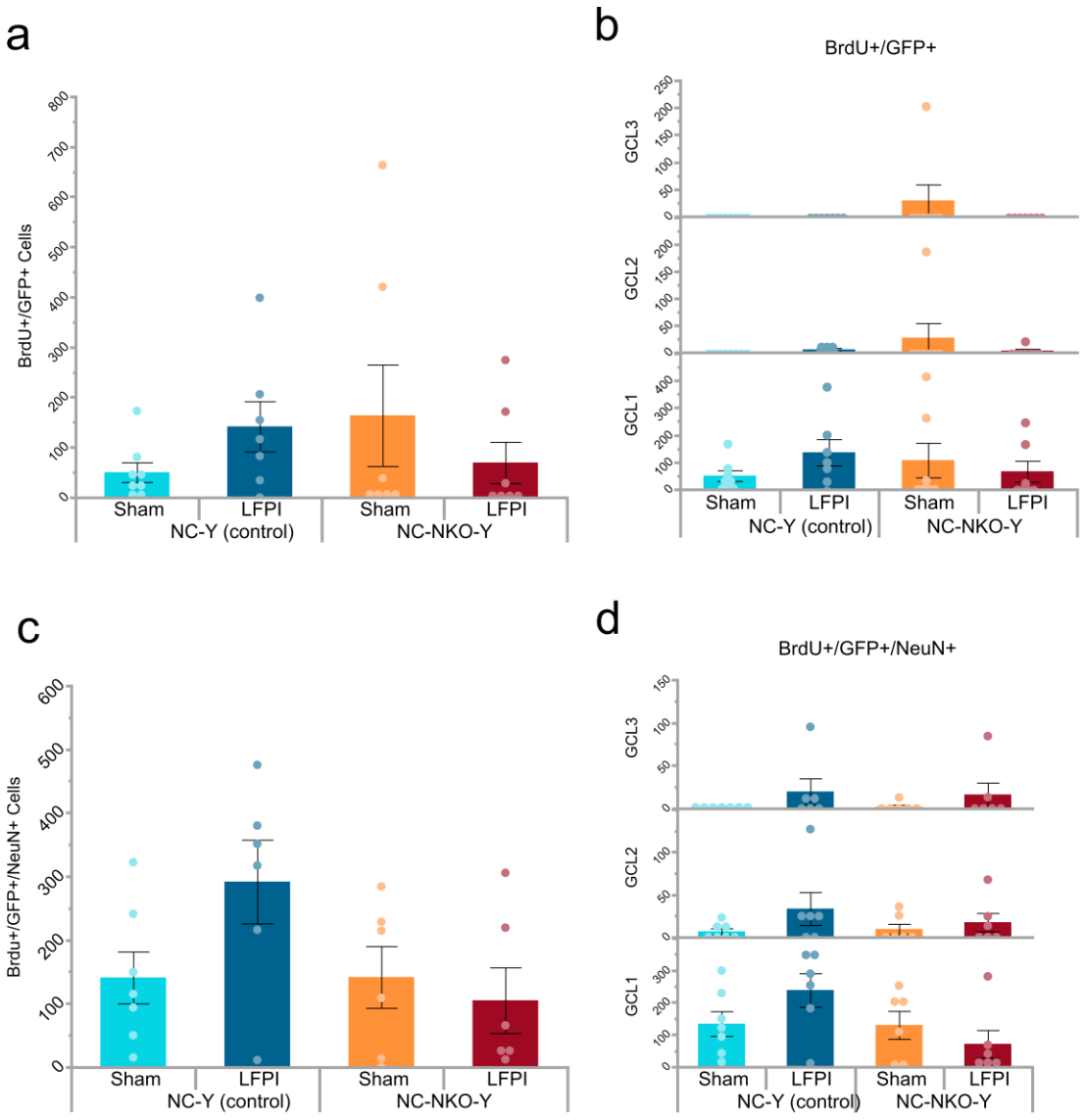

Figure 2.8. Loss of Notch1 Does Not Alter Injury-Induced Populations 8 WPI. Group means for stereologically calculated cell amounts are plotted for (**a**) BrdU+/GFP+ in all GCLS, (**b**) BrdU+/GFP+ separated by GCL, (**c**) BrdU+/GFP+/NeuN+ in all GCLs, and (**d**) BrdU+/GFP+/NeuN+ separated by GCL. No differences were observed between the different conditions.

2.3.5 Loss of *Notch1* Results in a Minor Reduction of Neuronal Differentiation Dependent on GCL

Outside of the injury-induced population but still within the injured environment, loss of Notch1 is expected to still cause alterations in proliferation. Examining the amount of GFP+/NeuN+ cells will inform if changes in proliferation results in a significant difference of mature neurons. At 4 weeks (**Figure 2.9**) into cell development there were no differences from injury [$F(1,16) = 1.067$; $p = 0.317$], genotype [$F(1,16) = 0.0046$; $p = 0.947$], or interactions [$F(1,16) = 0.067$; $p = 0.799$]. There were also no differences by injury for ***GFP+/NeuN+*** by GCL.

At 8 weeks (**Figure 2.10**) into cell development there were no overall differences in ***GFP+/NeuN+*** cells from injury [$F(1,24) = 1.351$; $p = 0.257$], genotype [$F(1,24 = 3.547$; $p = 0.072$], or interactions [$F(1,24) = 2.365$; $p = 0.137$], although similar to 4 WPI the effect of genotype was nearly present. When broken down by GCL, there was a difference by injury (**Figure 2.10b**). This difference specific to GCL2 shows that Notch1 loss within the injured environment does impact cell numbers, however this change is minor in comparison with the rest of the data.

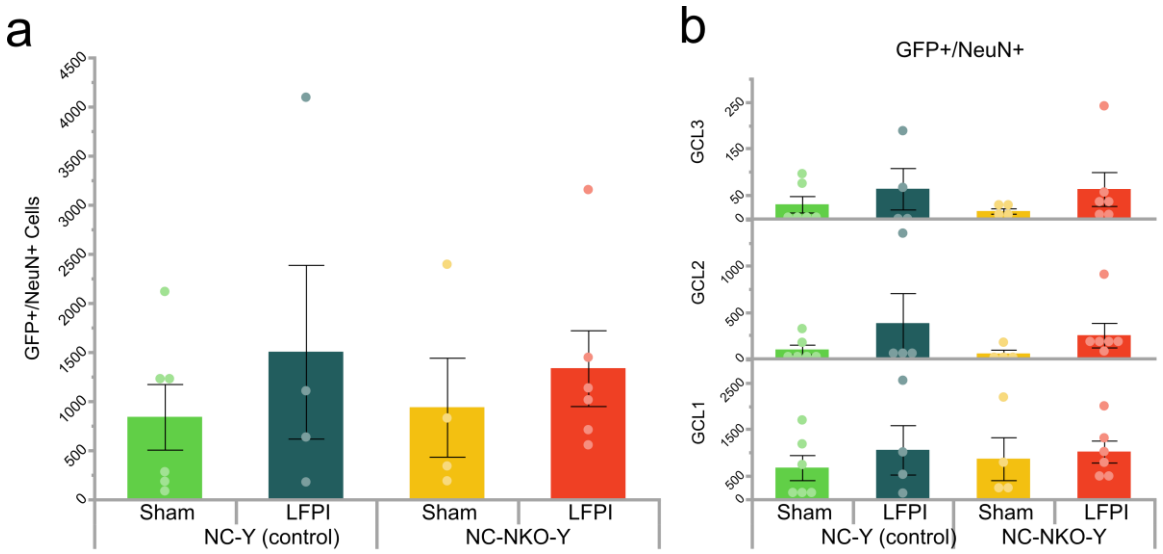

Figure 2.9. Loss of Notch1 Does Not Alter New Neuron Populations at 4 WPI. Group means for stereologically calculated cell amounts are plotted for (**a**) GFP+/NeuN+ in all GCLs and (**b**) GFP+/NeuN+ separated by GCL. No differences were observed between the separate conditions.

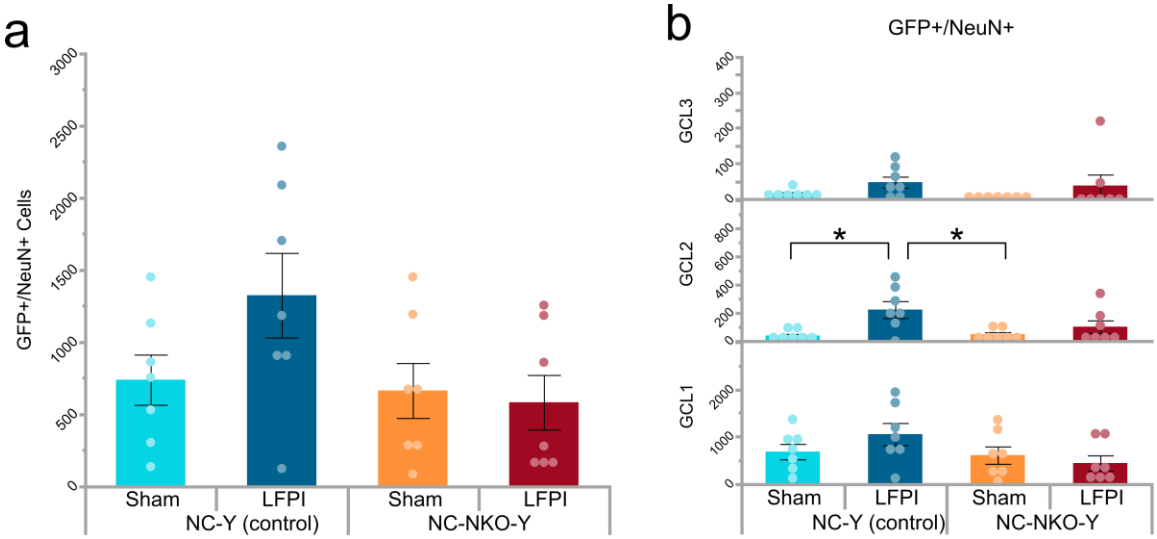

Figure 2.10. Loss of Notch1 Alters GCL2 New Neuron Populations at 8 WPI. Group means for stereologically calculated cell amounts are plotted for (**a**) GFP+/NeuN+ in all GCLS and (**b**) GFP+/NeuN+ separated by GCL. No differences were observed between the separate conditions except for a significant increase in cells residing in GCL2 of injured animals. Significance levels indicated by $*p < 0.05$.

2.4 Discussion

A neurogenic response in the adult mammalian brain commonly occurs after TBI (Gao et al., 2009). There have been many speculative theories as to why this response occurs and what are possible underlying consequences. In this study we wanted to investigate the role of Notch1 in the injury-induced neurogenic response. For the first set of experiments, we focused on the injury-induced cell proliferative response that is well recognized immediately after injury. We have previously reported in rats in the same injury model that this response occurs within the first week with the highest proliferative activity occurring two days after the injury (Sun et al., 2005). Our target dates were therefore 2 and 7 days after injury to interrogate the response occurring exactly one week out. The synthetic nucleoside BrdU was administered through i.p. injections on day 2 or day 7, two hours before animals were sacrificed. This paradigm allowed us to focus only on the proliferative response that occurred within that timeframe.

In the case of NC-Y (controls), we expected injury would result in significantly higher cell numbers at both 2- and 7-days post-injury compared to animals that received sham surgeries. The two regions in which cells were quantified were the granule cell layers and the hilus (**Table 2.6**). The hilus region typically does not have substantial amounts of proliferating cells at any given time, however after injury there is aberrant migration of NPCs or a glial cell response

(Chirumamilla et al., 2002; Rice et al., 2003; D. Sun et al., 2009; Urrea et al., 2007). The hilus at both 2 and 7 DPI had significantly more proliferating cells regardless of loss of Notch1. The GCLs at both 2 and 7 DPI did not have the typical increase in injury seen within the first week after TBI. This may have been due to variability in injury levels, as many ended up with injury levels that were borderline of a mild to moderate injury (Gao et al., 2009; Wang et al., 2016).

DPI	Region	Result
2 DPI	GCLs	-
2 DPI	Hilus	↑↓ from interaction between injury and cKO of Notch1
7 DPI	GCLs	↓ from Notch1 cKO
7 DPI	Hilus	↑ from injury

Table 2.6. Summary of Cell Proliferative Response with Notch1 Deletion. Separate DPI (left column) by region (middle column) with a generalized summary of results (right column) for each experimental group combination. Arrows indicate an increase or decrease.

At 7 DPI, the loss of Notch1 resulted in less cells, regardless if injured or not. Due to Notch1's role in maintaining proliferative pools and regulating the timing of neurogenesis, we expected loss of Notch1 would result in a loss of NSC pool maintenance and ultimately a reduction of the production in the neurogenic

responses long-term (Ables et al., 2010; Androutsellis-Theotokis et al., 2006; Imayoshi et al., 2010; Zhang et al., 2015). This study showed that by 7 DPI, animals with Notch1 knocked out in their NSC populations did have significantly fewer proliferating cells in the granule cell layers, regardless of injury status. Contrasting this, the cells in the hilus region were not significantly impacted with the loss of Notch1 in the NSC populations.

A few things to note from this study is that Notch1 was knocked out from the NSC/NPCs two weeks before injury, meaning during that time period maintenance of the stem cell pool was disrupted allowing for stem cell depletion (Ables et al., 2010). This would provide support to our findings that at least for the GCLs and one week out from injury, Notch1 cKO did result in a reduction of proliferating cells. Overall, Notch1 appears to play an important role in hippocampal adult neurogenesis for cells that migrate appropriately to the GCLs.

Long-term survival of injury-induced populations of cells are of importance in the neurogenic response. The cell type they differentiate into, how they exist with their surrounding environment, and general survival are all important factors that will influence the recovery after injury. New granule cells in the dentate gyrus have specific milestones of development that can serve as checkpoints for survival (Beining et al., 2017; Cole et al., 2019). With the interest on fully matured neurons, the period at 4 weeks from cell cycle exit is an excellent

time to look at survival of these cells as this is when a new GC is expected to begin expressing the mature neuronal marker NeuN. The injury-induced populations had significantly more BrdU+ cells, meaning, the proliferative response of cells survive long-term, and because there was a significantly higher number of cells with BrdU+/NeuN+, a substantial amount of these GCs became mature neurons. This supports our initial hypothesis that these cell numbers would remain elevated. This was observed at both 4 WPI and 8 WPI, so there is a continuation of this over time past the initial injury (**Table 2.7**).

Cell Phenotype	Result
4 WPI	
BrdU+	↑ from injury
GFP+	-
BrdU+ / GFP+	-
BrdU+ / NeuN+	↑ from injury
GFP+ / NeuN+	-
8 WPI	
BrdU+	↑ from injury
GFP+	↓ from injury
BrdU+ / GFP+	-
BrdU+ / NeuN+	↑ from injury
GFP+ / NeuN+	trend ↓ from Notch1 cKO

Table 2.7. Summary of Cell Response by Phenotype at 4- and 8- WPI. Separate cell phenotype combinations (left column) with a generalized summary of results (right column) for 4 WPI (top) and 8 WPI (bottom). Arrows indicate an increase or decrease.

GFP+ cells were informative in that they marked a subset of NSC/NPCs before injury that could be tracked later in time, and in the NC-NKO-Y, we know these specific cells had successful knockout of Notch1. At 4 WPI there were no differences between the groups for GFP+ cell populations, but by 8 weeks there was a large difference with both sham groups having many more GFP+ cells. Not all of the originally labeled GFP+ NSC/NPCs were anticipated to immediately exit the cell cycle to become new cells. The progenitor cells that stayed in the stem cell pool continuously divided, and the daughter cells would carry the GFP+ expression, as well. After injury at 8 weeks, the GFP+ cells were significantly depleted. One explanation for this is that the injury-induced neurogenic response resulted in what appears to be a depletion of the stem cell pool as a consequence long after the injury. The cells directly from the proliferative response after injury that differentiated into mature neurons did not show a difference, although it was close when comparing between genotypes. The knockout of Notch1 only occurred a couple weeks before injury so the population of cells actually inflicted by cKO may be small and therefore may not be representative of the effect or importance Notch1 is really serving. Cells outside of the injury-induced population were also calculated based on the number of GFP+/NeuN+ phenotype. The same trends were seen, and GCL2 showed that loss of Notch1 in the context of an injured environment does reduce the number of mature neurons. Comparing the results

of Brdu+/NeuN+ to Brdu+/GFP+/NeuN+, the only difference is it is a smaller population of cells and Brdu+/NeuN+ may include some cells that do not have Notch1 knocked out within that genotype group. If we select to compare against only mature neurons from the injury-induced population that do have Notch1 knocked out, we see a trend towards an effect of genotype and interaction between genotype and injury in the Brdu +/GFP+/NeuN+.

It's believed that an imbalance between maintenance and differentiation is how Notch1 activity can cause a reduction in neurogenesis, (Lugert et al., 2010), and this work supports this. There are a few other considerations for data interpretation. The transgenic mouse line only knocked out Notch1 in GFP-tagged Nestin+ cells. The Nestin+ population of cells includes astrocytes, as well, and there could be an underlying effect from this (Filippov et al., 2003; Fukuda et al., 2003). Another consideration is that variation in injury level can produce varied responses from the neurogenic population. Although most animals received a relatively consistent moderate injury, there was still minor variability leaning towards a more mild or severe injury. Variations in injury level can produce low survival rates or even mass cell death. The post-TBI environment must be taken under consideration, too, in that there may still be a hostile environment with a significant inflammatory response still occurring (Aungst et al., 2014; Sulhan et al., 2020). Last, one reason that may explain how there was no significant increase in

the 2 DPI and 7 DPI BrdU+ study versus the 4 WPI and 8 WPI BrdU+ and BrdU+/NeuN+ is the specific incorporation paradigm of BrdU. In the acute study, proliferating cells were only labeled two hours before sacrifice (single 100mg/kg i.p. injection) to see the active proliferation at the 2 hour time window before sacrificing. The longevity data was based off proliferating cells that were labeled continuously over the course of an entire week (50mg/kg i.p. injection every day for 7 days), which provides mixed information of cell proliferation and survival about new cells generated during the 1-7 days post-injury. The two cohorts had comparable injury levels and righting times, so TBI severity can be ruled out from explaining this difference.

To summarize these findings, Notch1 cKO reduces maintenance of the proliferative pool which ultimately leads to exhaustion of the pool that may have generated new neurons. This also shows that new neurons are continuously produced outside of that first post-injury week, and loss of Notch1 impacts their production. The number of mature neurons stay elevated long after injury, suggesting successful survival and synaptic incorporation into the local region. Reduction in mature neuron populations that are not directly part of the injury-induced response shows that loss of Notch1 from a subset of the NSC/NPC populations does have an impact on the balance of future cell populations. Our initial hypothesis predicted a significantly higher number of neurogenic cells

produced from injury, and knockout of Notch1 diminishing this result. The injury-dependent component of our hypothesis was supported from this data, with BrdU+ and BrdU+/NeuN+ cell numbers increased as a result of injury. Our Notch1 findings supported our hypothesis, but only with a decrease in cell number from Notch1 cKO in the GCLs at 7 DPI, and a trend in a decrease in cell number of GFP+/NeuN+ 8 WPI.

Chapter 3

Dendritic Arbors of Injury-Induced New Neurons and Recovery of Learning and Memory

3.1 Introduction

To increase our understanding of the contribution of injury-induced new neurons to recovery following TBI, it is paramount to examine these populations of cells in more detail. Not all of these new cells will survive to maturity ultimately contributing to the overall function of the hippocampus. Understanding the process of cell maturity heavily involves recognizing their morphological development. Separate stages of new GC development represent specific milestones that can be tied back to their establishment of synaptic plasticity with the surrounding environment (Zhao et al., 2006).

The new neurons in the dentate gyrus begin to form dendritic arbors that extend up into the molecular layer to receive perforant pathway inputs. Based on

the synaptotropic hypothesis, once a cell begins to stabilize, the arborization length decreases and branching increases as the cell reinforces communication throughout synaptic contacts. Notch1 is involved with synaptic plasticity and dendritic arborization modifications through decreasing branch length while increasing branch numbers, possibly engaging in the stabilization process directly (Berezovska et al., 1999; Redmond et al., 2000).

The distinct morphological stages tied to mature neuronal states and enhanced excitability and plasticity are around 4-8 weeks into maturity and was the target of these studies (Krzisch et al., 2016). Around 4 weeks, a new GC should be expressing the mature neuronal marker NeuN and should be at the latter end of dendritic and axonal growth and beginning of arbor modification as major synaptic connections are still being formed (Redell et al., 2020; Zhao et al., 2006). Around 8 weeks, a new GC should be indistinguishable from pre-existing mature GC neurons with the exception of a few synaptic modifications that are ongoing. This 8-week time point, also translated to 56-60 days, is the same time our lab has found innate cognitive and functional recovery occurring in animals with TBI (Sun et al., 2007, 2015; Weston et al., 2021). Previous studies of TBI have found that between 4-5 weeks after injury the new cells in the DG have significantly less dendritic complexity compared to cells from sham animals, with the exception of branch points most closely located to the soma (Ibrahim et al., 2016; Villasana et

al., 2015). Recovery is not evident around 4-5 weeks which could be expected to be associated with a lesser complex dendritic arbor. The 8 WPI period - when functional recovery is seen after injury - has not been investigated. Logically speaking if we expect morphology of these new cells to be a determinate for an essential role in recovery, we would hypothesize the arbor to show a significant increase in complexity to compensate for getting the region back to normal functioning capacity.

Due to a strong potential role Notch1 might play in the proliferative aspect of post-injury populations, it can be speculated that it is also involved in the dendritic arborization component of these new GCs because limiting Notch1 in physiological condition results in increased arbor extensions and less branching (Breunig et al., 2007; Ding et al., 2016). If Notch1 is involved in the dendritic morphological development at injury-induced neurons, eliminating it from these cells would be expected to result in an exacerbation of the decreased complexity compared to the injured control group around 4 WPI. By 8 WPI we would expect to see a continuation in reduced complexity with Notch1 cKO, instead of the recovered or heightened amount that is hypothesized for the case of injury.

Studies investigating dendritic development in DG new neurons found that while overexpression of Notch1 protein intracellular domain led to an increase in dendritic complexity, conditional knock out (cKO) of Notch1 resulted in reduced

dendritic complexity accompanied with a decrease in spatial learning and memory function (Alberi et al., 2011; Ding et al., 2016; Feng et al., 2017; Hallaq et al., 2015). This complements the hypothesis that reduced dendritic complexity around 4 weeks is associated with cognitive dysfunction and is related to modified Notch1 signaling. In these studies, control mice (NC-Y) and Notch1 cKOs (NC-NKO-Y) (**Appendix A**) received either a sham surgery or LFPI to examine innate cognitive recovery that we have observed in our rat models. Due to the prominent role Notch1 is thought to play in learning and memory, we expect animals with Notch1 knocked out to not recover on learning and memory tasks at 8 WPI compared to the injured controls. All learning and memory paradigms employed here will be used to assess recovery in relation to hippocampal-dependent learning and memory. Findings from these experiments will be informative if Notch1 is a new route to manipulate endogenous recovery after injury to enhance the recovery process.

The manipulation of Notch1 is expected to alter the morphological development of the injury-induced response and the ability to restore learning and memory function. The hypothesis for this set of studies is that injury will result in an increase in dendritic complexity by 8 WPI, however Notch1 cKO will prevent this increased complexity. We hypothesized 8 WPI injured animals will perform similar to sham animals as this is the predicted period of recovery. The animals

with Notch1 cKO (NC-NKO-Y) will not perform adequately in comparison to our controls (NC-Y), and the injured NC-NKO-Y will not return to a similar level of performance as the NC-Y sham animals.

3.2 Methods

Experimental Animals

Adult female and male transgenic NC-Y (control) and NC-NKO-Y (Notch1 cKO) mice were used in all studies (**Table 3.1; Appendix A**). For the morphology experiments a total of 38 mice were used and these same mice were included with cell stereology experiments (Chapter 2 – cell longevity data). Since these mice were the same used in the stereology experiments, they received i.p. BrdU injection single daily (50mg/kg) at 1-7 DPI. Experiments for Western blot data had a total of 22 mice and experiments for behavior had a total of 54 mice. Animals received sham surgery or LFPI (**Appendix B**) and mice were sacrificed at either 4- or 8-weeks post-injury (WPI) or at the conclusion of behavior experiments.

Group	4 WPI IHC	8 WPI IHC	WB	Behavior
NC-Y Sham	4	5	5	10
NC-Y LFPI	4	5	6	12
NC-NKO-Y Sham	4	5	6	16
NC-NKO-Y LFPI	4	7	6	16

Table 3.1. Total Animals Used for Separate Experiments. The number of animals used for each of the separate groups (left column) organized by the post-injury time and type of experiment.

Immunohistochemistry

For morphological assessment, the standard protocol for staining (**Appendix C**) was followed. In brief, mice were sacrificed at designated experiment post-injury weeks. Tissue was fixed with paraformaldehyde and sections were prepared. Sections were collected in sequence within a span of 800μm of the dentate gyrus, every 5th free floating section was collected for a total of 4 sections per animal. Sections were washed with PBS followed by application of a blocking solution and sequentially the primary antibody solution. Primary antibodies used were anti-GFP (1:2000; Invitrogen A11122), anti-NeuN (1:100; Millipore MAB377), and anti-BrdU (1:1500; Abcam AB6326). Secondary

antibodies used were biotinylated anti-rabbit (1:400; Vector Biolabs BA-1000), AlexaFluor 647 anti-mouse (1:200; Invitrogen A21235), and AlexaFluor 568 anti-rat (1:400; Invitrogen A11077). After ABC Elite kit, TSA™ Fluorescein Tyramide Reagent kit (1:50; AKOYA Biosciences SAT701001EA) was applied to amplify the fluorescent signal that allows for morphological reconstruction.

Microscopy and Morphology Analysis

Slides containing the triple labeled (BrdU/GFP/NeuN) sections were brought to the VCU Microscopy Facility and images were taken on a ZEISS confocal laser scanning microscope (LSM 710). For each animal, an average of 4 cells were imaged at 63x magnification. The requirement criteria for inclusion were that the cell had to be triple labeled for BrdU/GFP/NeuN, the entire dendritic arbor needed to be intact, and the soma needed to be located in the GCLs, preferentially GCL1. Z-stacks were taken to cover the entire cell structure with each stack 1 μm, and tiling was used when appropriate.

For morphology analysis, Z-stack image files were placed in the FIJI software plugin Neuroanatomy-SNT (Cole et al., 2019). Tracing of dendritic arbors began with designating the location of the soma and primary dendrites. Each subsequent branch was traced by manually selecting the next branch and then the SNT plugin performed the A*search algorithm to trace the rest of the branch path. This was

repeated until the entire morphology of the dendritic arbor of interest was traced. Since a Z-stack file could be used for this analysis, all morphology tracings were in 3D. The SNT software was also used for the analysis component. This included Sholl analysis with 10μm concentric spheres **(Figure 3.1a**), Path Order analysis (**Figure 3.1b**), and information was extracted from a quick measurement feature to analyze length and number of primary and terminal branches (**Figure 3.1c**) and total volumetric area (**Figure 3.1d**). For every analysis, the values from each individual cell for one animal was averaged, and then these averages from each animal were used for final analysis.

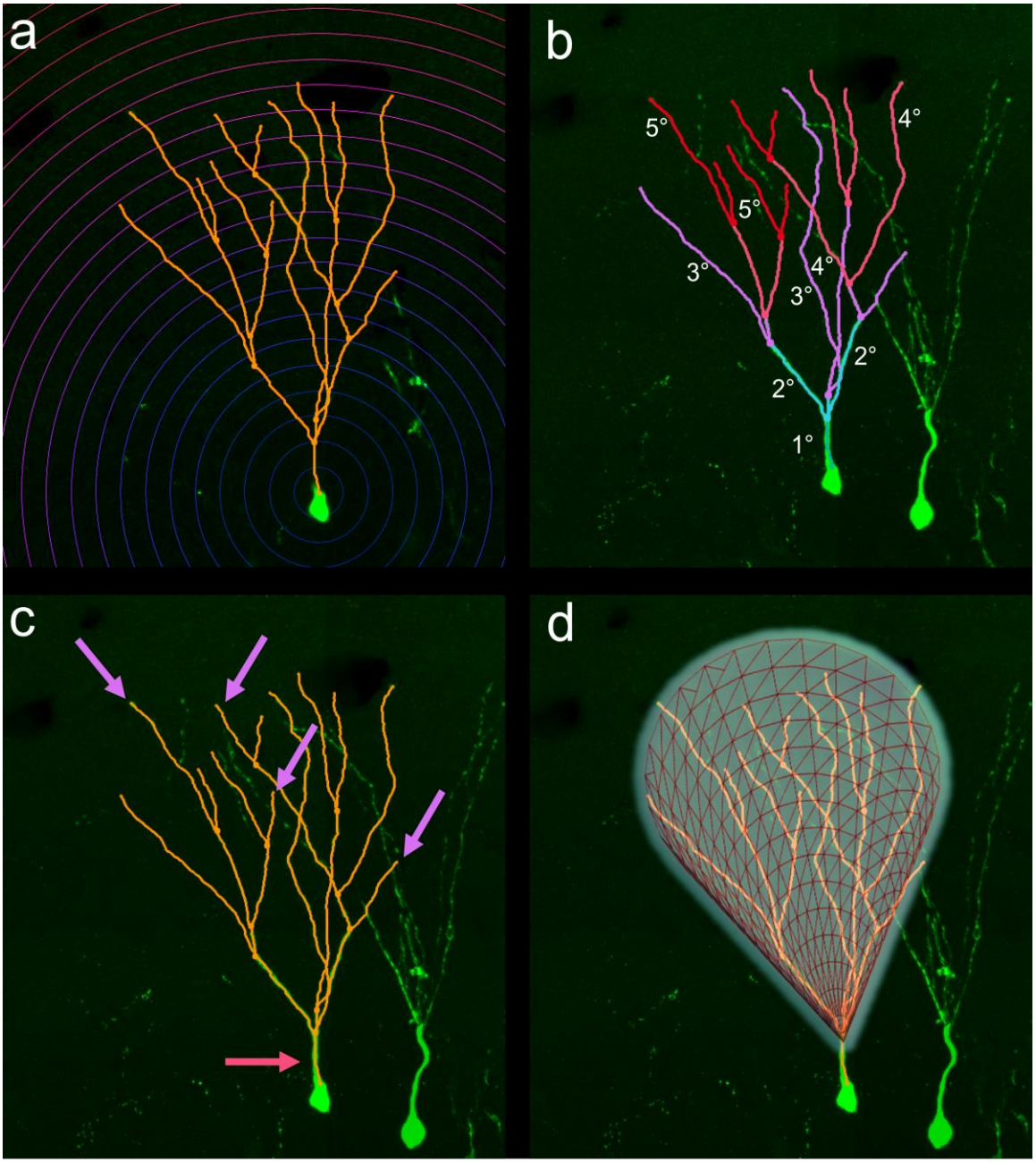

Figure 3.1. Dendritic Morphology Analysis Techniques. (**a**) ***Sholl*** analysis is the number of intersections a dendritic tree makes with separate concentric rings that extend out by 10μm from each other starting at the soma. (**b**) ***Path Order*** analysis is the hierarchical organization of a dendritic tree and is completely independent of distance measurements. The first dendrite coming off the soma is 1°, any branch coming off a 1° is a 2°, etc. (**c**) ***Terminal*** and ***Primary Branches*** are a way to assess the amount of end points a dendritic tree has (purple arrows) and how many starting branches (dark pink arrow). (**d**) ***Volume*** analysis is the total volumetric area the entire dendritic tree structure takes up in 3-Dimensional space.

Western Blots

Western blotting was used to assess synaptic protein expression at 8 weeks post-injury. Mouse hippocampal samples were lysed using lysis buffer (1x RIPA; Millipore, 20-188), 0.1% SDS (Bio-Rad, 1610416), 1% Triton X-100 (Sigma-Aldrich, T8787), mini cOmplete cocktail (Roche, 11836170001), 1mM EDTA (Quality Biological, 351-027-721)) and centrifuged at 16000g for 25 minutes at 4 °C. Supernatants were then boiled in Laemmli buffer (Bio-Rad, 1610747) and resolved using SDS-PAGE. After SDS-PAGE, protein was transferred to a low-fluorescence PVDF (Bio-Rad) and blocked with either 5% BSA in TBST (for PSD-95) or 1% Casein in TBS (for synaptophysin, Bio-Rad, 1610782). The following primary and secondary antibodies were used: anti-PSD95 (1:1000, Abcam, ab2723), anti-synaptophysin (1:50000, Abcam, ab32127), anti-mouse AlexFluor 647 (1:1000, Invitrogen, A21235), anti-rabbit AlexaFluor 647 (1:1000, Invitrogen, SA5-10327), anti-tubulin-rhodamine (1:5000, Bio-Rad, AbD22584).

Behavior

Open Field

The open field test assesses locomotor activity, anxiety, and willingness to explore (Hall & Ballachey, 1932). The open field apparatus consists of four chambers each measured at 40cm x 40cm x 35cm (Stoelting Co., Wood Dale, IL). For this test, all

quadrants were empty and dimly lit. Prior to and following each open field trial, 70% ethanol was used to deodorize the apparatus, allowing for complete evaporation of the ethanol before starting the next trial. Each trial consists of the animals being placed within the open field and allowed to explore for 10 minutes without prior habituation to the field. A video camera is placed above the apparatus for tracking purposes and ANY-maze 7.1 tracking software (Stoelting Co., Wood Dale, IL), collected data pertaining to: total distance traveled (m), latency to the edge of the open field (s), and latency to the center of the open field (s). The analysis of time spent in the edge or center of the open field is believed to be reflective of anxiety, with increased anxiety leading to a preference to stay towards the edge and the animal will have less locomotion.

Cognitive Functional Assessment

Animals were assessed with a battery of cognitive functional assessment including Novel Object Recognition (NOR) and Morris Water Maze (MWM) tests following protocols that we routinely used in our lab at 7-8 weeks following TBI. The NOR will assess working memory without spatial cues, whereas MWM will assess hippocampal-dependent spatial memory. NOR habituation occurred every day for two weeks straight beginning DPI 28, followed by NOR testing two days later. Standard MWM occurred 7 WPI – 8 WPI, and reverse MWM 8 WPI – 9 WPI.

Novel Object Recognition

The novel object recognition assay is performed in the same apparatus that is mentioned in the open field assay description. This assay is performed in three stages: 1) Habituation, 2) Familiarization, and 3) Novel Affiliation. Each animal is allowed to habituate to the NOR box for 5 minutes prior to the familiarization phase. Immediately following the end of the habituation phase, two identical objects (white jars) are placed opposite to each other at fixed points. After the objects are placed, the animal is allowed to explore for 10 minutes. Once the time has elapsed, the animal is returned to its cage and the apparatus as well as the objects are cleansed with 70% ethanol. The novel affiliation stage takes place 3 hours from the start of each trial. Similar to the familiarization phase, two objects are placed opposite to each other at fixed points. However, the bottom right object, or Object B, is replaced with a novel object, while the top left object, or Object A, remains the same object used during the familiarization phase. Likewise, the animal is again allowed to explore the chamber for ten minutes. The same video camera and software used during the open field assay collected data pertaining to: Object A and Object B exploratory time during the familiarization phase (s), Object A and Object B exploratory time during the novel affiliation phase (s), as well as the discrimination index during the novel affiliation phase.

Morris Water Maze

Considered one of the most robust behavioral assessments, the Morris Water Maze tests spatial learning and memory. The 180cm diameter circular pool was filled with water to a depth of 30cm. The water was made opaque using Crayola non-toxic white paint. A heater maintained the temperature of the water at 26±1°C. Extra-maze cues were present on the four walls surrounding the pool. A 25cm high, 10cm wide submerged platform was placed in the center of the SE quadrant of the pool. Each animal was placed on the hidden platform for 30s prior to the start of trials in order to habituate them prior to starting Day 1. Then, the animal was placed in a randomly assigned direction without repetition (N, S, E, W) for a total of four trials per day for five days. The animals were placed in the pool with their nose facing the side of the pool. Each trial lasted for a maximum of 90s, after which the animal was left on the hidden platform for 30s. If an animal failed to find the platform, the experimenter guided it there. At 24 hours after the final training trial, the probe trial was conducted without a platform in the pool. The latency to platform and proximity to platform were recorded (ANY-maze, San Diego Instruments, Inc., San Diego, CA).

The week following standard MWM, animals were tested in Reverse Morris Water Maze (RMWM) to assess cognitive flexibility. The platform was moved from the SE quadrant to the NW quadrant for each of the four training days. On

the fifth day, a 60 second probe trial was conducted to assess the animals' ability to learn the location of the platform. The latency to platform and proximity to platform were recorded.

Statistical Analysis

A repeated measures ANOVA (JMP Pro 16) was used for all Sholl analysis, Path Order analysis, and Morris Water Maze sequential days analysis. All other data was analyzed using ANOVA (JMP Pro 16) combined with Tukey HSD post hoc tests. The significance level was set to $\alpha = 0.05$ for all analyses performed, and averaged values are expressed as mean ± SEM.

3.3 Results

3.3.1 Injury-Induced DG New Neurons Have Altered Patterns of Dendritic Branching Near the Soma at 4 WPI

By 4 weeks after TBI the injury-induced cells should be expressing the mature neuronal marker NeuN and should be in the process of highly plastic restructuring of dendritic branching and spines. For these particular studies, morphology of BrdU+/GFP+/NeuN+ cells were assessed for differences contributed from either injury condition or absence of Notch1. The BrdU+ serves

to ensure the cell that was measured came directly from the injury-induced population, GFP+ allows to visualize the cell morphology, and NeuN+ to confirm the cell being measured is a mature neuron.

Sholl analysis is a technique used to describe morphological characteristics of a dendritic arbor from a neuron. Three-dimensional (3D) Sholl creates concentric spheres that continuously segment every 10μm in the direction further from the soma. Neuron arbor morphology at 4 WPI was analyzed using 3D Sholl (**Figure 3.2a**) and compared by separate groups, either just by injury or just by genotype. A repeated measures ANOVA was performed with NC-Y animals to compare the effect of injury on dendritic morphology of new neurons (**Figure 3.2b**). When examining the NC-Y animals, there was not an overall significant difference of morphology between sham and LFPI [$F(1,24) = 0.6180$; $p = 0.4617$] or from injury group by radius [$F(1,24) = 1.277$; $p = 0.190$]. However, there were significant differences specifically at radii closer to the soma with intersections at 40μm being significantly higher in the LFPI compared to sham ($p = 0.0213$*), intersections at 50μm significantly higher in LFPI than sham ($p = 0.0356$*), and the shams having more intersections at 80μm than the LFPI ($p = 0.0234$*).

For comparisons of Sholl data in NC-NKO-Y mice from sham and LFPI (**Figure 3.2c**), a repeated measures ANOVA was performed revealing there was no significant overall difference between groups [$F(1,24) = 1.774$; $p = 0.231$],

however there was a significant difference between group by radius [F(1,24) = 1.639; p = 0.0403*]. Similar to the NC-Y animals, the LFPI NC-NKO-Y group had more intersections closer to the soma than the sham NC-NKO-Y at both 20μm (p = 0.0268*) and 30μm (p = 0.0358*).

Sholl morphology data was additionally compared by the different genotypes. For sham NC-Y and sham NC-NKO-Y (**Figure 3.2d**), repeated measures ANOVA did not reveal a significant difference by genotype [F(1,24) = 0.751; p = 0.419], and no significant difference in genotype by radius [F(1,24) = 0.322; p = 0.999]. For LFPI NC-Y and LFPI NC-NKO-Y (**Figure 3.2e**), there were no statistically significant differences by genotype [F(1,24) = 0.319; p = 0.493], or genotype by radius [F(1,24) = 0.636; p = 0.902].

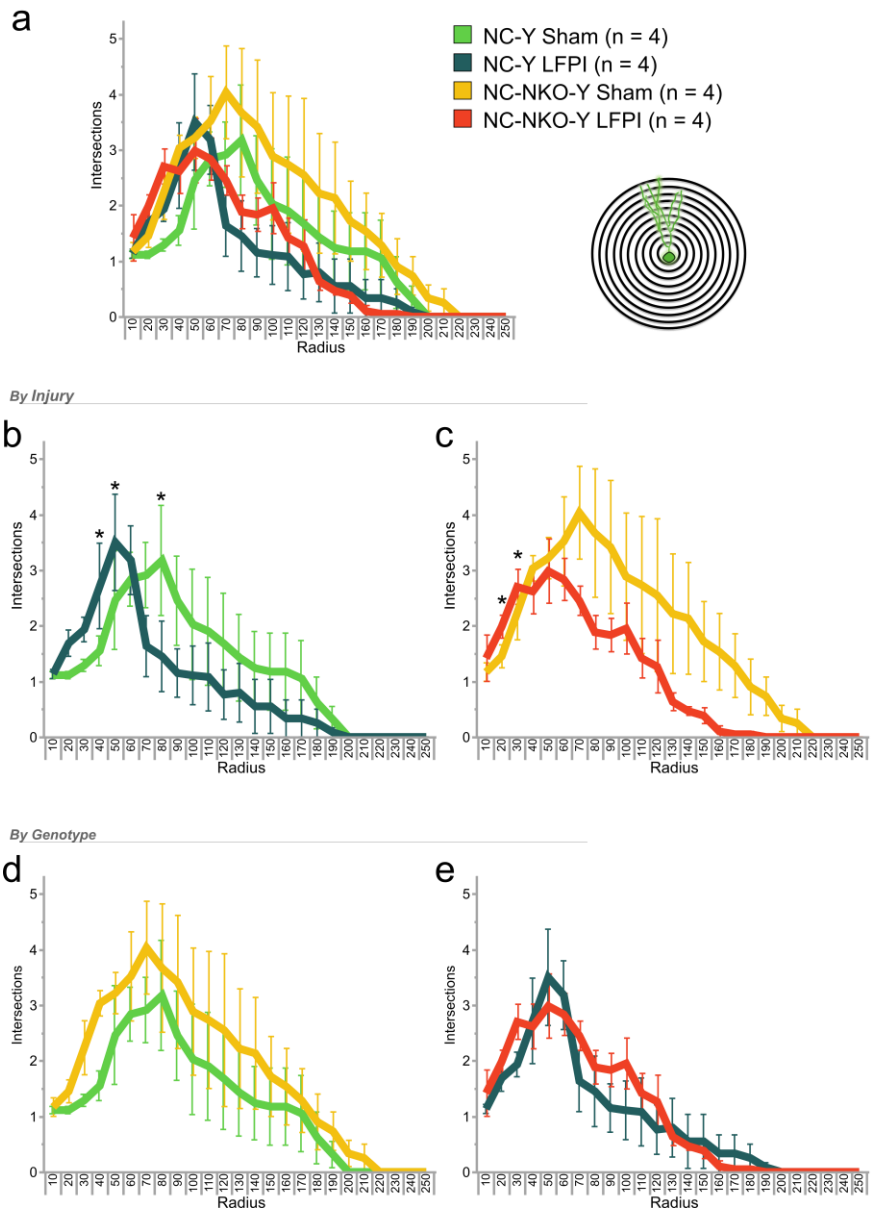

Figure 3.2. Sholl Morpohology 4 WPI is Altered from Injury. (**a**) Summary plot showing all 4 experimental groups together, the animal numbers used for each group, and a typical Sholl schematic. Comparisons were made either by injury groups (**b** and **c**) or by genotype groups (**d** and **e**). For each graph, the X-axis is the Sholl radii increasing in increments of 10µm with 0µm representing the location of the soma. Each intersection (Y-axis) is the number of times any dendritic branches on a specific neuron cross through a specific radius ring. Significance levels indicated by $*p < 0.05$.

Path Order is a separate type of measurement used to describe dendritic arbor morphology. A numeric system is used to organize the arbor with the order of branches coming off one another, beginning with any branch off a soma considered a first order (1°), any branch coming off a 1° is a second order (2°), any off a 2° is a third order (3°), and so on (**Figure 3.3a**). While Sholl analysis depends on continuing quantitative distances, Path Order is independent of distance and instead is focused on an overall hierarchy within the arbor.

A repeated measures ANOVA was performed with NC-Y animals to compare the effect of injury on Path Order (**Figure 3.3b**). There was no overall difference of morphology between sham NC-Y and LFPI NC-Y [$F(1,9) = 0.703$; $p = 0.434$] or from NC-Y injury group by radius [$F(1,9) = 1.041$; $p = 0.420$]. Similarly, there were no significant differences between sham NC-NKO-Y and LFPI NC-NKO-Y [$F(1,9) = 0.121$; $p = 0.740$] or from NC-NKO-Y injury group by radius [$F(1,9) = 0.451$; $p = 0.901$] (**Figure 3.3c**).

For Path Order comparisons by genotype, sham NC-Y and sham NC-NKO-Y (**Figure 3.3d**) did not differ as a result of genotype [$F(1,9) = 0.204$; $p = 0.668$] or genotype by path order [$F(1,9) = 0.476$; $p = 0.884$]. The LFPI NC-Y and LFPI NC-NKO-Y (**Figure 3.3d**) did not differ from genotype [$F(1,9) = 0.644$; $p = 0.453$] or genotype by path order [$F(1,9) = 0.773$ $p = 0.642$].

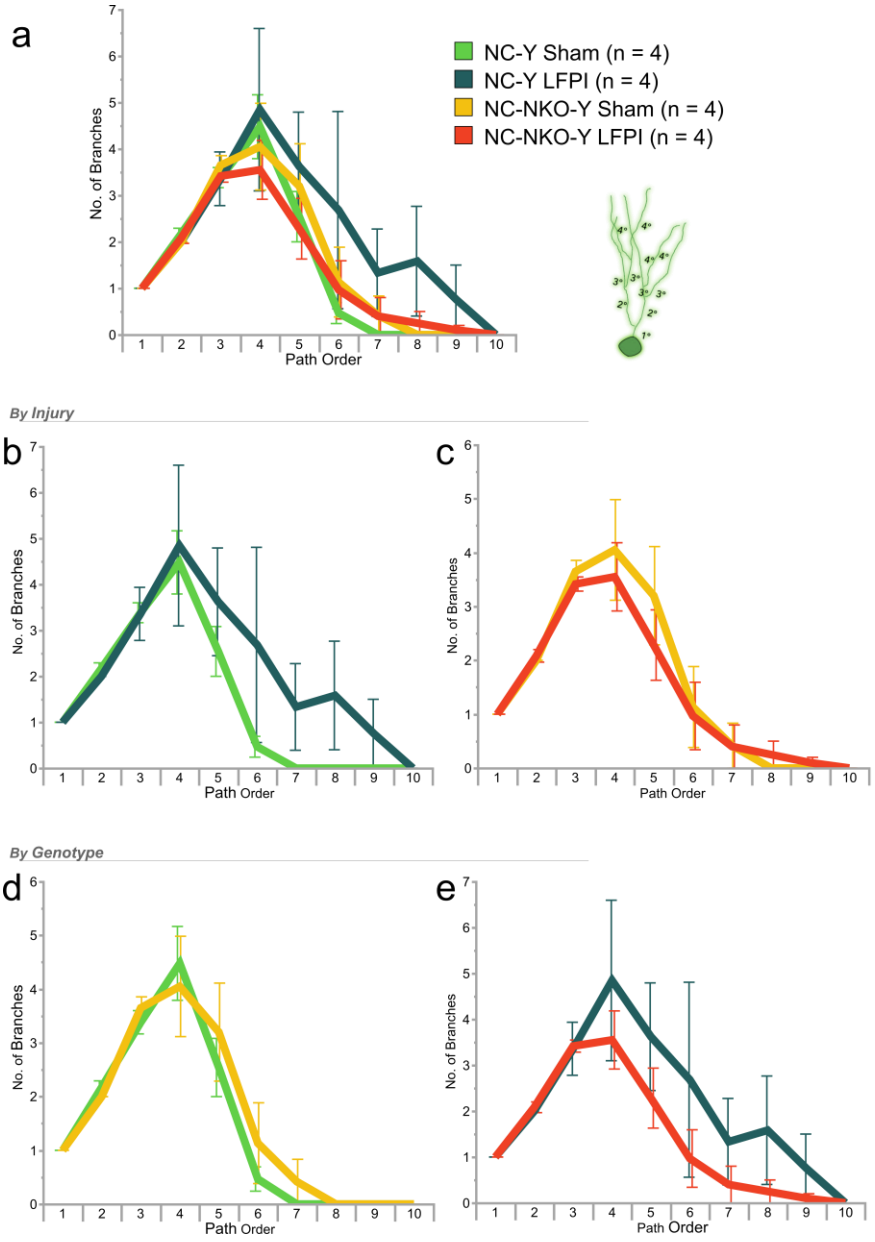

Figure 3.3. Path Order Analysis 4 WPI Demonstrates Absence of Morphology Alterations. (**a**) Summary plot showing all 4 experimental groups together, the animal numbers used for each group, and a typical schematic for path order designation. Comparisons were made either by injury groups (**b** and **c**) or by genotype groups (**d** and **e**). For each graph, the X-axis is the Path Order degree of branching. Each intersection (Y-axis) is the number of branches classified as a specific hierarchical degree.

There are a number of other quantitative ways to assess the morphological structure of a dendritic arbor. Volume span (**Figure 3.4a**) did not vary between any of the groups by genotype [$F(1,12) = 0.289$; $p = 0.601$], injury [$F(1,12) = 2.784$; $p = 0.121$], or interactions [$F(1,12) = 0.00$; $p = 0.998$]. Cable length (**Figure 3.4b**), the total summed length of each branch within an arbor, did not show differences of any groups from genotype [$F(1,12) = 0.0592$; $p = 0.812$], injury [$F(1,12) = 1.634$; $p = 0.224$], or interactions [$F(1,12) = 0.449$; $p = 0.515$]. The amount of primary branches (**Figure 3.4c**) had no significant difference from genotype [$F(1,12) = 0.0004$; $p = 0.985$], injury [$F(1,12) = 0.086$; $p = 0.775$], or interaction [$F(1,12) = 0.237$; $p = 0.635$], and the length of primary branches was not different either for genotype [$F(1,12) = 1.289$; $p = 0.278$], injury [$F(1,12) = 1.145$; $p = 0.306$], or an interaction [$F(1,12) = 1.675$; $p = 0.220$]. For terminal branches (**Figure 3.4d**), there were no significant differences in the amount from genotype [$F(1,12) = 0.500$; $p = 0.493$], injury [$F(1,12) = 0.346$; $p = 0.567$], or an interaction [$F(1,12) = 0.661$; $p = 0.432$]. Similarly, there were no differences in the length of terminal branches from genotype [$F(1,12) = 0.253$; $p = 0.624$], injury, although a close trend [$F(1,12) = 4.004$; $p = 0.0685$], or from an interaction [$F(1,12) = 0.266$; $p = 0.616$].

In summary, the Sholl morphology data indicated that at 4 WPI, LFPI changed new neuron dendritic arbors by increasing the branch number close to the soma. This pattern of increased intersections changing from injured groups to

sham NC-Y groups as branches get further away from the soma replicates findings from other studies evaluating Sholl data 4 weeks after injury. The NC-NKO-Y groups showed this same pattern of increased branching near the soma with injury.

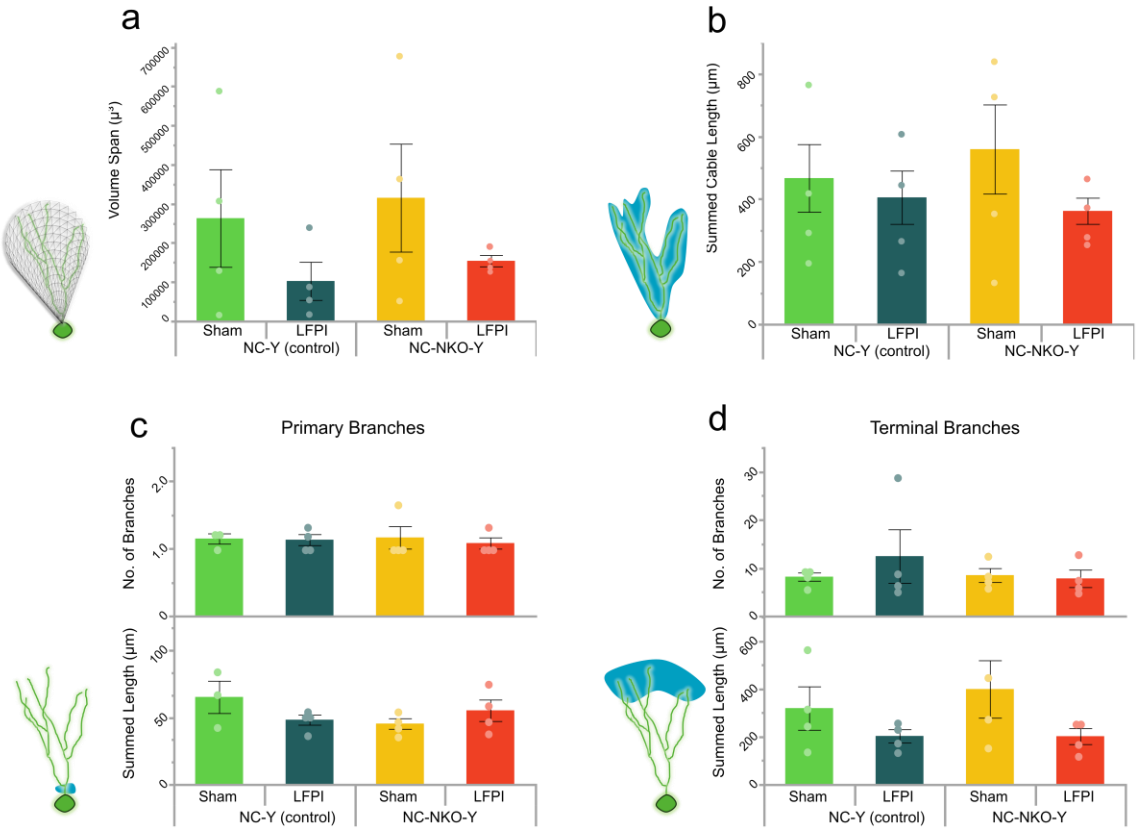

Figure 3.4. 4 WPI General Morphology Analysis Reveals No Changes. Morphological analysis by volume span, cable length, primary branches, and terminal branches, with representative schematics on left. (**a**) Volume span is the total cubic area an entire dendritic arbor expands. (**b**) Cable length is the total of all branches summed together. (**c**) The number (top) and length (bottom) of primary branches and (**d**) the number (top) and length (bottom) of terminal branches.

3.3.2 Loss of *Notch1* Results in a Divergence in Dendritic Complexity of New Neurons within the Context of Injury at 8 WPI

Eight weeks after injury any injury-induced new neurons that survived should have a mature neuronal phenotype with a stabilized dendritic arbor structure and plateauing alterations in synaptic spines. The same analysis techniques used to assess 4 WPI dendritic morphology were also used to investigate 8 WPI dendritic morphology. Sholl analysis was conducted on 8 WPI morphology data (**Figure 3.5a**). Repeated measures ANOVA showed there was no difference by injury when comparing sham NC-Y to LFPI NC-Y [$F(1,24) = 0.0097$; $p = 0.924$] (**Figure 3.5b**) or from injury by radius [$F(1,24) = 1.235$; $p = 0.216$]. When each radii was evaluated a very similar pattern of results was apparent with LFPI NC-Y having significantly more intersections than sham NC-Y at 40μm ($p = 0.003$**), and then sham NC-Y having significantly more intersections than LFPI NC-Y at 80μm ($p = 0.0172$*). A dramatic difference was evident when comparing sham NC-NKO-Y to LFPI NC-NKO-Y (**Figure 3.5c**) with a main effect from injury [$F(1,24) = 5.151$; $p = 0.0466$*] and an effect of injury by radius [$F(1,24) = 3.817$; $p < 0.0001$**]. At radii closer to the soma the LFPI NC-NKO-Y group had significantly more intersections than sham NC-NKO-Y at 10μm ($p = 0.0187$*), 20μm ($p = 0.0046$**), and 30μm ($p = 0.0091$**). At radii further away from the soma there was

a considerable change in that the sham NC-NKO-Y had significantly more intersections than the LFPI NC-NKO-Y at 70μm (p = 0.0003**), 80μm (p = 0.0248*), 90μm (p = 0.0327*), 100μm (p = 0.0158*), and 140μm (p = 0.0108*).

Sholl for 8 WPI data was compared by genotypes. Sham NC-Y and sham NC-NKO-Y (**Figure 3.5d**) were extremely similar by injury [F(1,24) = 0.0508; p = 0.827] and injury by radius [F(1,24) = 0.415; p = 0.993]. On the other hand, LFPI NC-Y and LFPI NC-NKO-Y (**Figure 3.5e**) did have a main effect by genotype with the controls having significantly more intersections [F(1,24) = 5.145; p = 0.0467*].

Path order for 8 WPI was assessed by injury and genotypes (**Figure 3.6a**). The sham NC-Y did not show a main effect compared to the LFPI NC-Y [F(1,9) = 3.726; p = 0.0897] (**Figure 3.6b**), however the LFPI NC-Y did have significantly higher order branching than sham NC-Y when compared from injury by path order [F(1,9) = 2.717; p = 0.0087**]. Specifically, LFPI NC-Y had more branches than sham NC-Y at 5° (p = 0.0201*) and 6° (p = 0.0030**) path orders. The sham NC-NKO-Y and LFPI NC-NKO-Y data were almost identically flipped compared to the NC-Y (**Figure 3.6c**). The sham NC-NKO-Y showed a main effect of injury by having more branches compared to LFPI NC-NKO-Y [F(1,9) = 8.533; p = 0.0153*] and when analyzed injury by radius [F(1,9) = 3.626; p = 0.0007**]. Specifically, the increase in branches were seen at path orders 4° (p = 0.0004**) and 5° (p = 0.0003**).

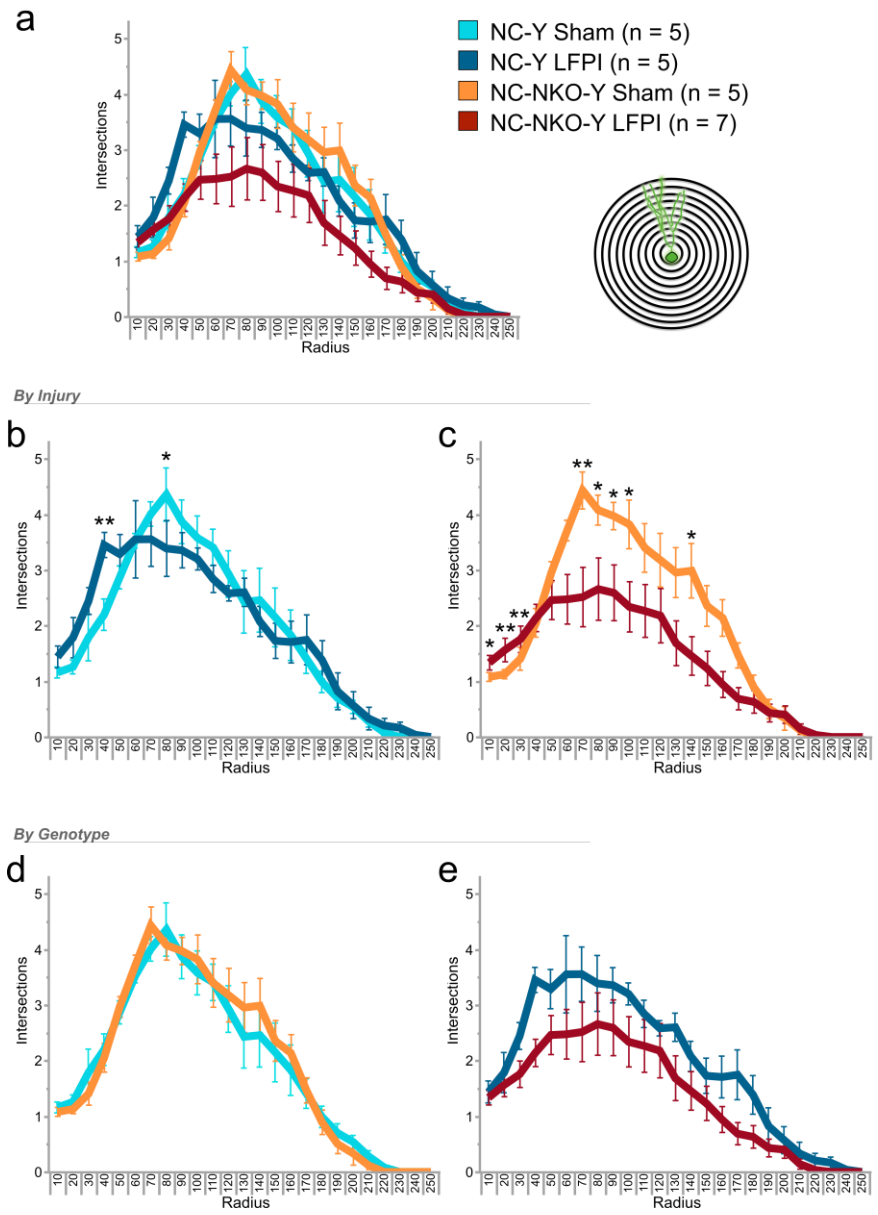

Figure 3.5. Sholl Morphology 8 WPI is Altered by Condition. (**a**) Summary plot showing all 4 experimental groups together, the animal numbers used for each group, and a typical Sholl schematic. Comparisons were made either by injury groups (**b** and **c**) or by genotype groups (**d** and **e**). For each graph, the X-axis is the Sholl radii increasing in increments of 10µm with 0µm representing the location of the soma. Each intersection (Y-axis) is the number of times any branches on a specific neuron cross through a specific radius ring. Significance levels indicated by $*p < 0.05$ and $**p < 0.005$.

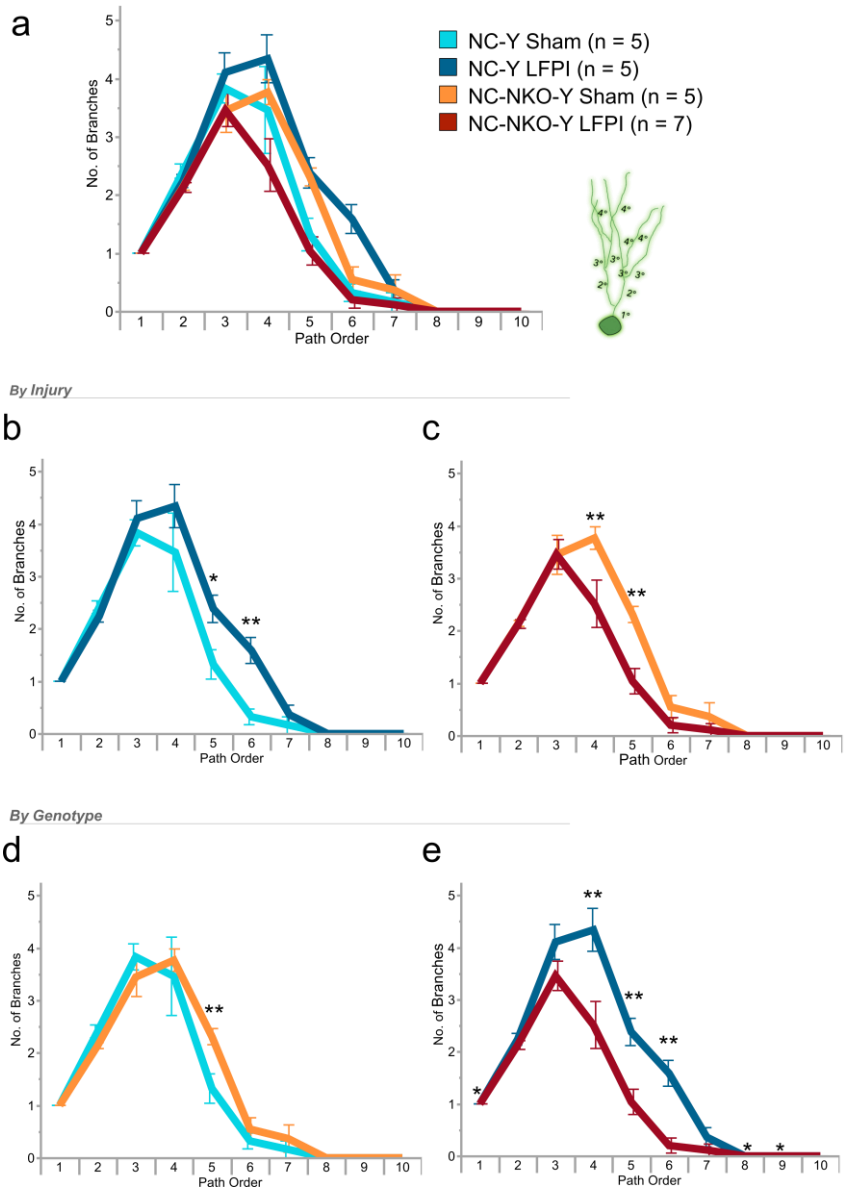

Figure 3.6. Path Order Analysis 8 WPI is Altered by Condition. (**a**) Summary plot showing all 4 experimental groups together, the animal numbers used for each group, and a typical schematic for path order designation. Comparisons were made either by injury groups (**b** and **c**) or by genotype groups (**d** and **e**). For each graph, the X-axis is the Path Order degree of branching. Each intersection (Y-axis) is the number of branches classified as a specific hierarchical degree. Significance levels indicated by $*p < 0.05$, $**p < 0.005$.

When path orders were compared by genotypes for 8 WPI, the sham NC-Y did not differ from the sham NC-NKO-Y (**Figure 3.6d**) by genotype [$F(1,9) = 0.468$; $p = 0.513$] or genotype by path order [$F(1,9) = 1.516$; $p = 0.159$]. When assessed through individual path orders, there was a significant difference seen at 5° with more branches in the sham NC-NKO-Y than sham NC-Y ($p = 0.0032$**). The largest difference was seen with LFPI NC-Y having significantly more branches than LFPI NC-NKO-Y (**Figure 3.6e**) by genotype [$F(1,9) = 18.03$; $p = 0.0017$**] and genotype by path order [$F(1,9) = 6.427$; $p < 0.0001$**]. The increase in branches were seen at path orders 1° ($p = 0.0375$*), 4° ($p < 0.0001$**), 5° ($p = 0.0037$**), 6° ($p = 0.0022$**), 8° ($p = 0.0375$*), and 9° ($p = 0.0375$*).

Volume span (**Figure 3.7a**) did not have a main effect of genotype [$F(1,18) = 1.657$; $p = 0.214$] or injury [$F(1,18) = 3.292$; $p = 0.0863$], however there was an interaction between genotype and injury [$F(1,18) = 5.124$; $p = 0.0362$*]. Tukey's post-hoc test revealed significantly more volume is covered by sham NC-NKO-Y compared to LFPI NC-NKO-Y ($p = 0.0352$*). The total cable length (**Figure 3.7b**) ANOVA analysis showed no changes by genotype [$F(1,18) = 2.743$; $p = 0.115$], injury [$F(1,18) = 2.797$; $p = 0.112$], or an interaction [$F(1,18) = 3.062$; $p = 0.0972$]. Primary branch (**Figure 3.7c**) length was not altered by injury [$F(1,18) = 0.706$; $p = 0.412$], genotype [$F(1,18) = 0.015$; $p = 0.903$], or an interaction [$F(1,18) = 0.931$; $p = 0.347$], however the number of primary branches was effected by injury [$F(1,18) =$

5.023; $p = 0.0379$*], but not genotype [F(1,18) = 0.118; $p = 0.735$], and no interaction [F(1,18) = 0.0087; $p = 0.927$]. Terminal branch (**Figure 3.7d**) length analysis showed no differences by injury [F(1,18) = 2.144; $p = 0.160$], genotype [F(1,18) = 1.284; $p = 0.272$], or interactions [F(1,18) = 2.277; $p = 0.149$]. The number of terminal branches were significantly different, with a main effect by genotype [F(1,18) = 5.739; $p = 0.0277$*], an interaction [F(1,18) = 13.11; $p = 0.0020$**], but not by injury [F(1,18) = 0.167; $p = 0.687$]. The LFPI NC-Y group had significantly more terminal branches than the LFPI NC-NKO-Y group ($p = 0.0017$*).

To summarize, the morphology data indicated both Notch1 cKO and LFPI have a significant impact on dendritic arbor shape. The NC-Y Sholl data showed no difference between sham and LFPI except for intersections near the soma, in which the morphology pattern followed the 4 WPI, and path order revealed LFPI results in a higher complexity of branching. The opposite was found for the NC-NKO-Y data, in which LFPI results in a significant reduction of complexity based on both Sholl and path order analyses, and the volume span of NC-NKO-Y shams was much larger than the injured. The path order data also revealed that LFPI NC-NKO-Y had significantly less complex branching than the LFPI NC-Y, suggesting an important role for Notch1 in the morphological development of injury-induced new neurons.

Due to the relevance of dendritic spines to dendritic morphology, spine density was measured for 8 WPI injury-induced new neurons (**Figure 3.8a and** b). There were no significant differences from injury $F(1,17) = 0.227$; $p = 0.639$], genotype $F(1,17) = 0.0267$; $p = 0.872$], and no interactions $F(1,17) = 0.199$; $p = 0.661$]. Total protein levels were measured with Western blots for the synaptic proteins synaptophysin (presynaptic) and PSD95 (postsynaptic). For PSD95 total protein (**Figure 3.8c**), there was no significant difference from injury [$F(1,18) = 0.131$; $p = 0.722$], from genotype [$F(1,18) = 1.695$; $p = 0.209$], or from an interaction [$F(1,18) = 0.914$; $p = 0.352$]. For synaptophysin (**Figure 3.8d**), there was no significant difference by injury, although very close [$F(1,18) = 0.407$; $p = 0.059$], no difference by genotype [$F(1,18) = 0.0026$; $p = 0.960$], however there was an interaction between injury and genotype [$F(1,18) = 4.533$; $p = 0.0473$*]. Tukey's postdoc test revealed a difference between the sham and LFPI groups in NC-Y animals with the injured group having significant lower expression ($p = 0.0405$*).

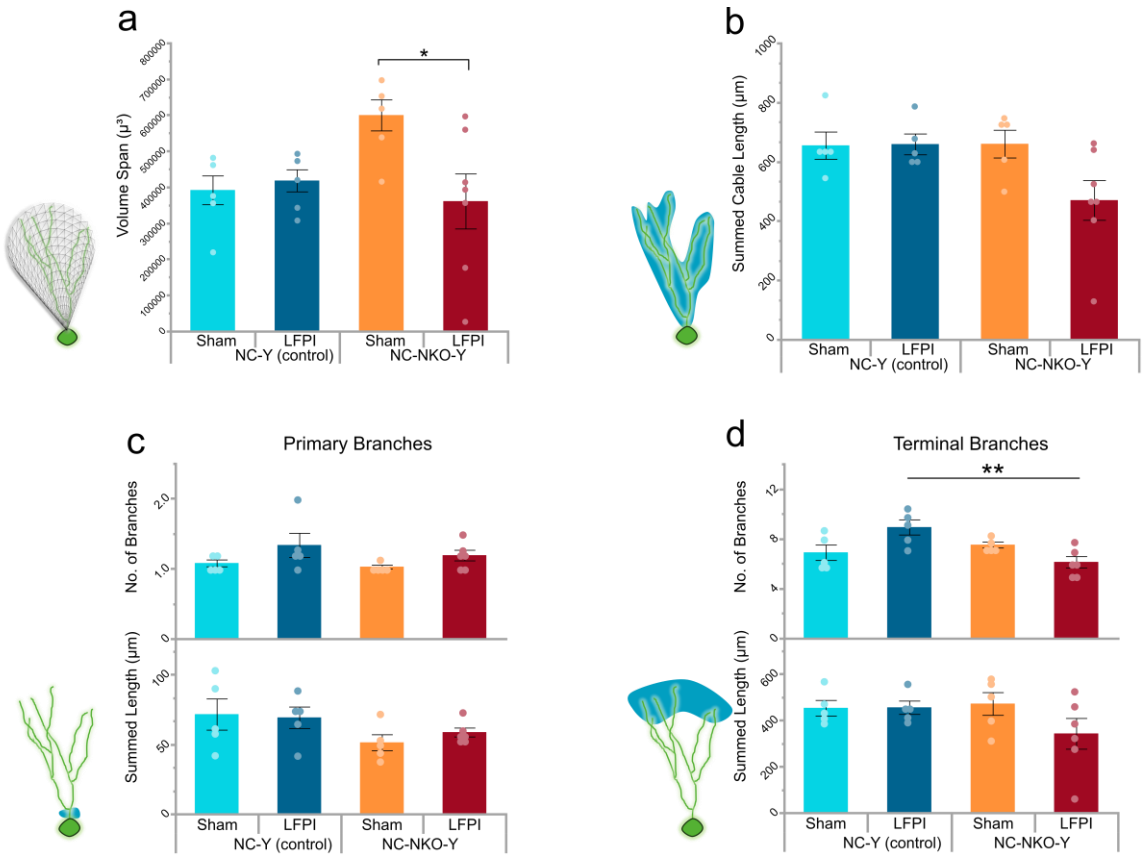

Figure 3.7. 8 WPI General Morphology Analysis Reveals Changes from cKO of Notch1. Morphological analysis by volume span, cable length, primary branches, and terminal branches, with representative schematics on left. (**a**) Volume span is the total cubic area an entire dendritic arbor expands. (**b**) Cable length is the total of all branches summed together. (**c**) The number (top) and length (bottom) of primary branches and (**d**) the number (top) and length (bottom) of terminal branches. Significance levels indicated by *$p < 0.05$, **$p < 0.005$.

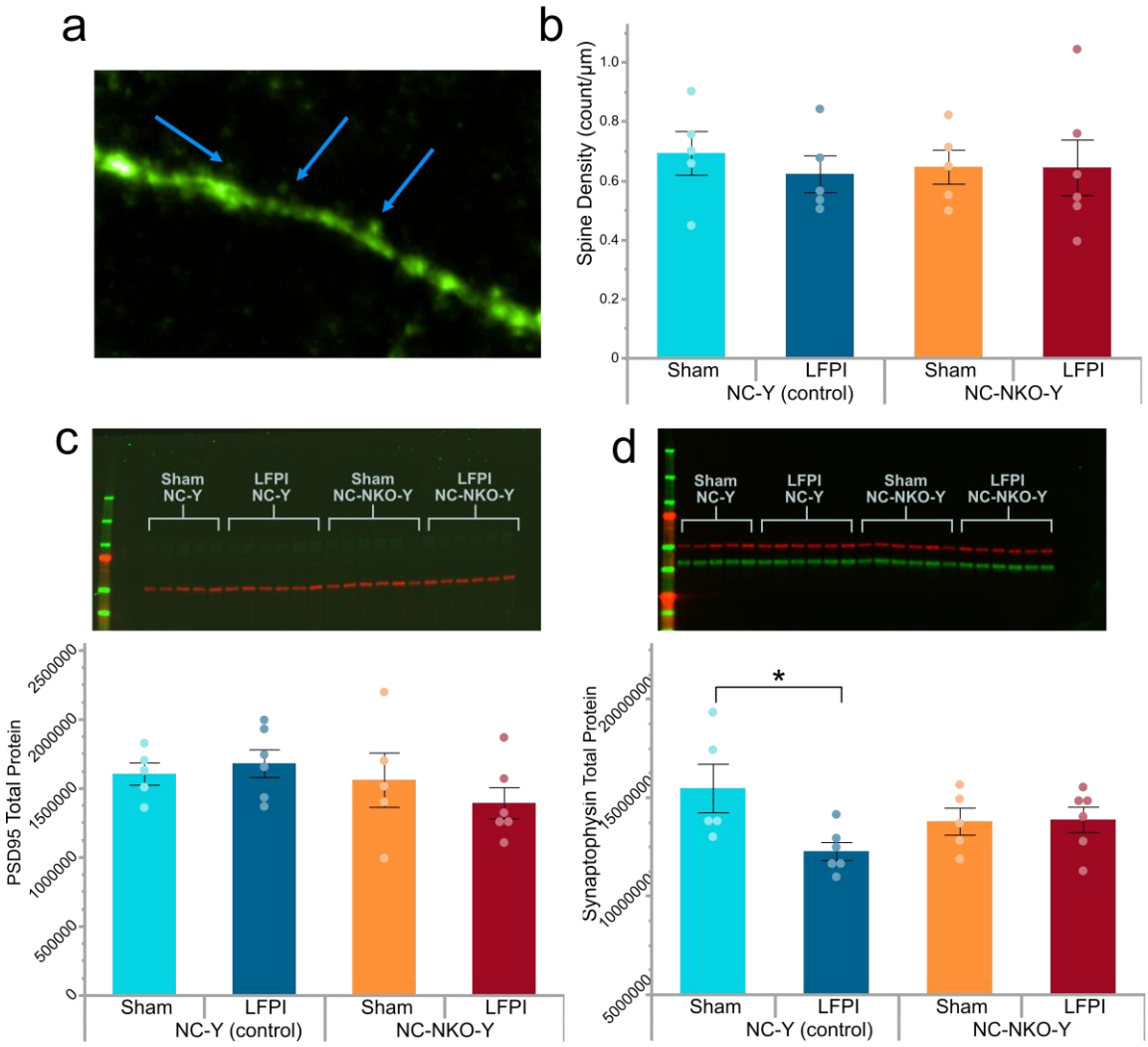

Figure 3.8. Spine Density and Synaptic Plasticity 8 WPI. (**a**) The number of spines per segment of a dendrite were analyzed. Blue arrows point to example spines from a dendritic segment. (**b**) Comparisons of spine density means across groups. (**c**) Total PSD95 protein values with ladder above. (**d**) Total Synaptophysin protein values with ladder above. For Western blot data control lanes were anti-tubulin-rhodamine. Significance level indicated by *$p < 0.05$.

3.3.3 Memory Performance Shifts Substantially Due to *Notch1* Loss with or without Injury

The Morris Water Maze (MWM) is a commonly used behavioral test for learning and memory. The animals in these studies underwent 6 days of standard MWM latency testing followed by a probe trial. Beginning the day after the standard testing probe trial, they underwent 6 days of reverse MWM latency testing followed by a reverse MWM probe trial. Repeated measures ANOVA analyses were performed to compare by injury within each genotype, and separately genotype within each injury group.

For NC-Y animals (**Figure 3.9a left**), latency to platform on standard MWM testing did not have a significant difference by injury [$F(1,5) = 1.684$; $p = 0.209$] or injury by day [$F(1,5) = 1.399$; $p = 0.231$]. There was a significant change on day 3 with sham NC-Y slightly slower than LFPI NC-Y, however ($p = 0.0137$*). The latency to platform on reverse MWM testing (**Figure 3.9a right**) had no significant differences between sham NC-Y and LFPI NC-Y [$F(1,5) = 1.553$; $p = 0.227$] and no significant differences from injury by day [$F(1,5) = 0.665$; $p = 0.651$].

For NC-NKO-Y animals (**Figure 3.9b left**), latency to platform on standard MWM testing revealed a main effect of injury [$F(1,5) = 6.268$; $p = 0.018$*] with the sham NC-NKO-Y having a significantly shorter latency to finding the platform compared to LFPI NC-NKO-Y. There was no interaction of injury by day, however

[F(1,5) = 1.122; p = 0.351]. Similarly, latency to platform on reverse MWM (**Figure 3.9b right**) had a main effect of injury [F(1,5) = 10.972; p = 0.0024**], but no effect from injury by day [F(1,5) = 0.797; p = 0.554].

Comparisons were also made on genotypes with injury groups separated. For sham animals (**Figure 3.10a left**), latency to platform on standard MWM testing was not significantly different from genotype [F(1,5) = 2.052; p = 0.165] or genotype by day [F(1,5) = 1.281; p = 0.277]. Reverse MWM testing (**Figure 3.10a right**) showed much different results with sham NC-NKO-Y animals performing significantly quicker than sham NC-Y [F(1,5) = 16.303; p = 0.0005**]. Analysis for genotype by day on reverse testing did not differ [F(1,5) = 0.330; p = 0.894].

The LFPI (**Figure 3.10b left**) NC-Y animals performance on standard MWM testing did not differ from LFPI NC-NKO-Y [F(1,5) = 0.487; p = 0.491] or from genotype by day [F(1,5) = 1.291; p = 0.272]. On reverse MWM (**Figure 3.10b right**) LFPI NC-Y animals performed the same as LFPI NC-NKO-Y [F(1,5) = 0.118; p = 0.734] and same for genotype by day [F(1,5) = 1.275; p = 0.279].

On standard MWM probe trial (**Figure 3.11a**), ANOVA analysis showed no effect of injury [F(1,50) = 2.396; p = 0.128], genotype [F(1,50) = 1.415; p = 0.239], and no interactions [F(1,50) = 0.0462; p = 0.831]. On reverse MWM probe trial (**Figure 3.11b**), ANOVA analysis showed no effect of injury [F(1,50) = 0.529; p = 0.470], genotype [F(1,50) = 0.004; p = 0.952], and no interactions [F(1,50) = 2.059; p = 0.158].

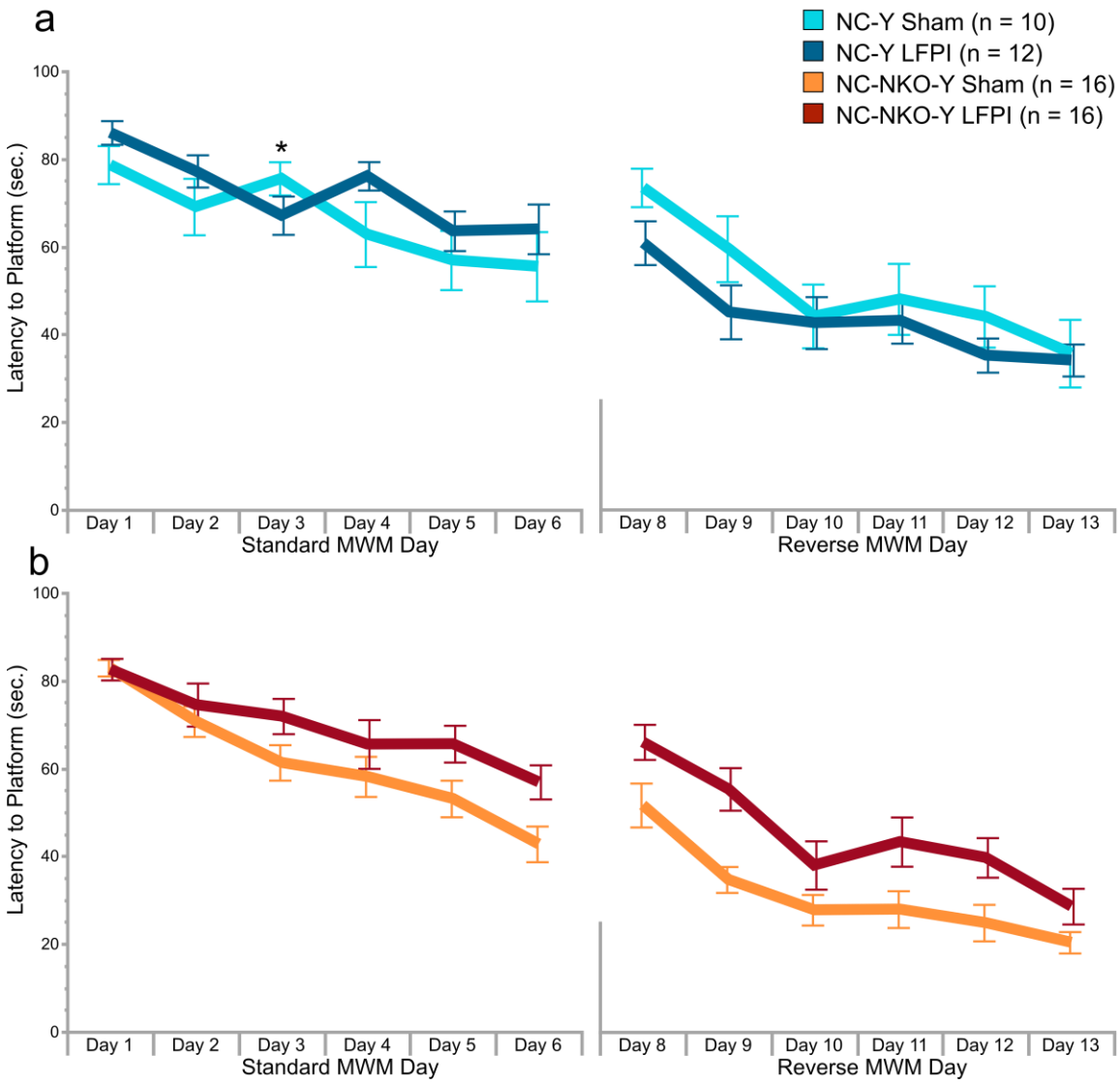

Figure 3.9. Latency to Platform on MWM Standard and Reverse Testing: Compared by Injury. (**a**) NC-Y (control) animals comparing injury conditions on latency performance with standard test days on the left x-axis and reverse test days on the right x-axis. (**b**) NC-NKO-Y (Notch1 cKO) animals comparing injury conditions, standard test days on left and reverse test days on right. Injured NC-NKO-Y animals showed a significant deficit in finding the platform compared to sham NC-NKO-Y. Significance levels indicated by $*p < 0.05$.

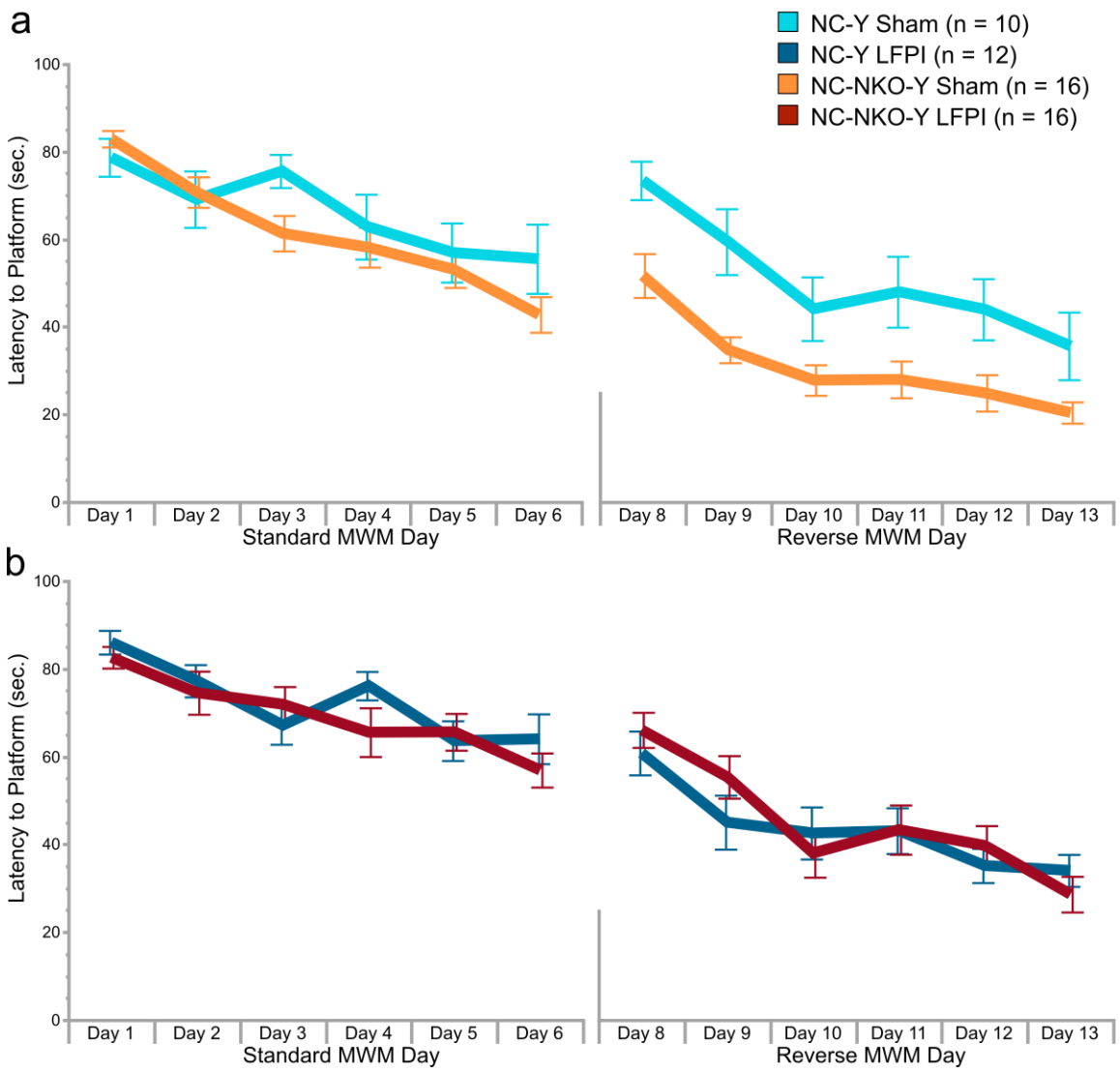

Figure 3.10. Latency to Platform on MWM Standard and Reverse Testing: Compared by Genotype. (**a**) Sham animals comparing genotypes on latency performance with standard test days on the left x-axis and reverse test days on the right x-axis. (**b**) LFPI animals comparing genotypes, standard test days on left and reverse test days on right. Sham NC-NKO-Y animals showed a significant deficit in latency to platform compared to sham NC-Y animals on reverse test days.

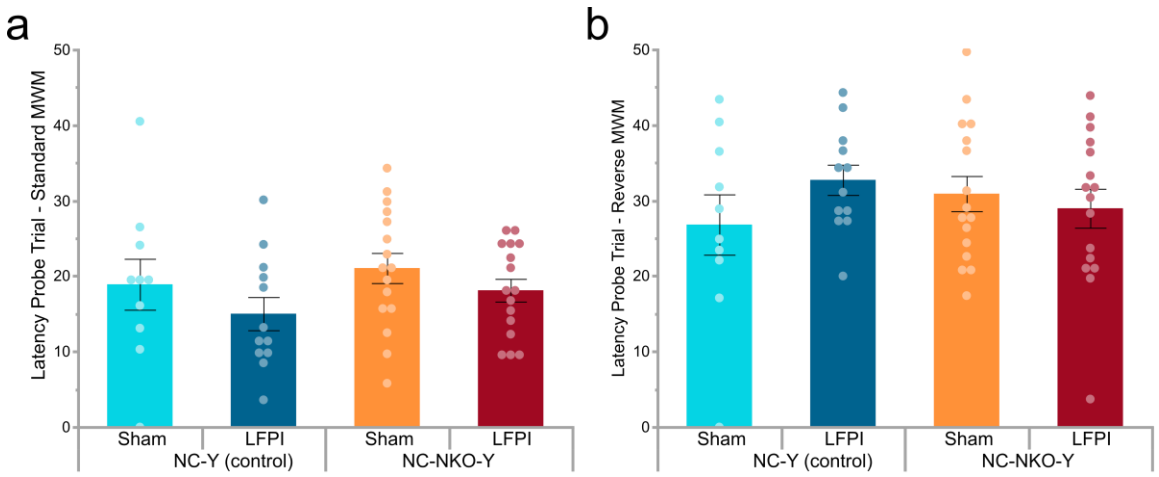

Figure 3.11. Latency to Platform MWM Probe Trials. (**a**) All four groups compared on latency performance with standard test days (**b**) All four groups compared on latency performance with reverse test days. No differences were seen on either standard or reverse probe trials.

A component of MWM tasks includes proximity to the platform which is the average of how close an animal is to the platform on any given day. For NC-Y animals, there was no effect on standard (**Figure 3.12a left**) MWM days [$F(1,5) = 1.643$; $p = 0.215$] and no changes from injury by day [$F(1,5) = 2.119$; $p = 0.069$]. When comparing by each individual testing day the sham NC-Y were significantly closer to the platform on day 3 ($p = 0.0153$*) but LFPI NC-Y were significantly closer to the platform on day 5 ($p = 0.0484$*). On reverse MWM days (**Figure 3.12a right**) there was no difference between sham NC-Y and LFPI NC-Y from injury [$F(1,5) = 1.729$; $p = 0.203$] and no difference from injury by day [$F(1,5) = 0.731$; $p = 0.602$].

On standard MWM days the sham NC-NKO-Y (**Figure 3.12b left**) were significantly closer to the platform than the LFPI NC-NKO-Y [$F(1,5) = 4.889$; $p = 0.0348$*], but there was no effect from injury by day [$F(1,5) = 0.686$; $p = 0.635$]. For reverse MWM days there were similar results (**Figure 3.12b right**) with the sham NC-NKO-Y being significantly closer to the platform than the LFPI NC-NKO-Y [$F(1,5) = 5.422$; $p = 0.0268$*], but no effect from injury by day [$F(1,5) = 0.533$; $p = 0.751$].

Comparisons were also made on genotypes with injury groups separated. For sham animals (**Figure 3.13a left**), proximity platform on standard MWM testing was not significantly different from genotype [$F(1,5) = 1.456$; $p = 0.239$] or genotype by day [$F(1,5) = 1.28$; $p = 0.277$]. Reverse MWM testing (**Figure 3.13a right**) showed sham NC-NKO-Y animals being in closer proximity than sham NC-Y [$F(1,5) = 5.336$; $p = 0.0298$*]. Analysis for genotype by day on reverse testing did not differ [$F(1,5) = 0.318$; $p = 0.902$].

The LFPI groups were not significantly different in their proximity to the platform on standard MWM days (**Figure 3.13b left**), in fact, they were extremely similar [$F(1,5) = 0.0004$; $p = 0.984$]. The genotype by day comparisons did not differ either [$F(1,5) = 1.081$; $p = 0.374$]. Reverse MWM days (**Figure 3.13b right**) had no differences between the LFPI NC-Y and LFPI NC-NKO-Y [$F(1,5) = 1.223$; $p = 0.279$], and no differences from genotypes by day [$F(1,5) = 1.843$; $p = 0.109$].

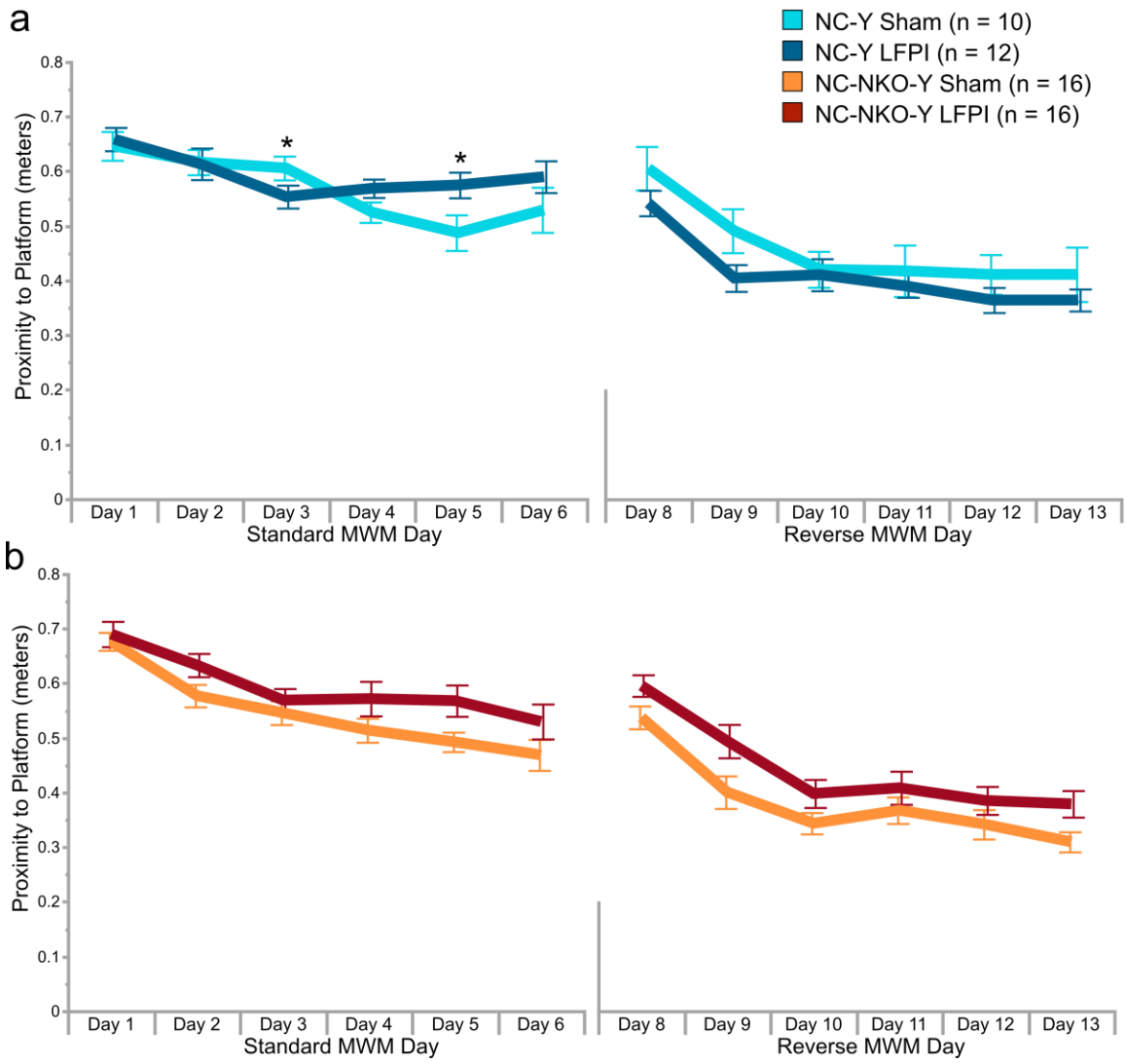

Figure 3.12. Proximity to Platform on MWM Standard and Reverse Testing: Compared by Injury. (**a**) NC-Y (control) animals comparing injury conditions on proximity from the platform with standard test days on the left x-axis and reverse test days on the right x-axis. (**b**) NC-NKO-Y (Notch1 cKO) animals comparing injury conditions, standard test days on left and reverse test days on right. Significance levels indicated by $*p < 0.05$.

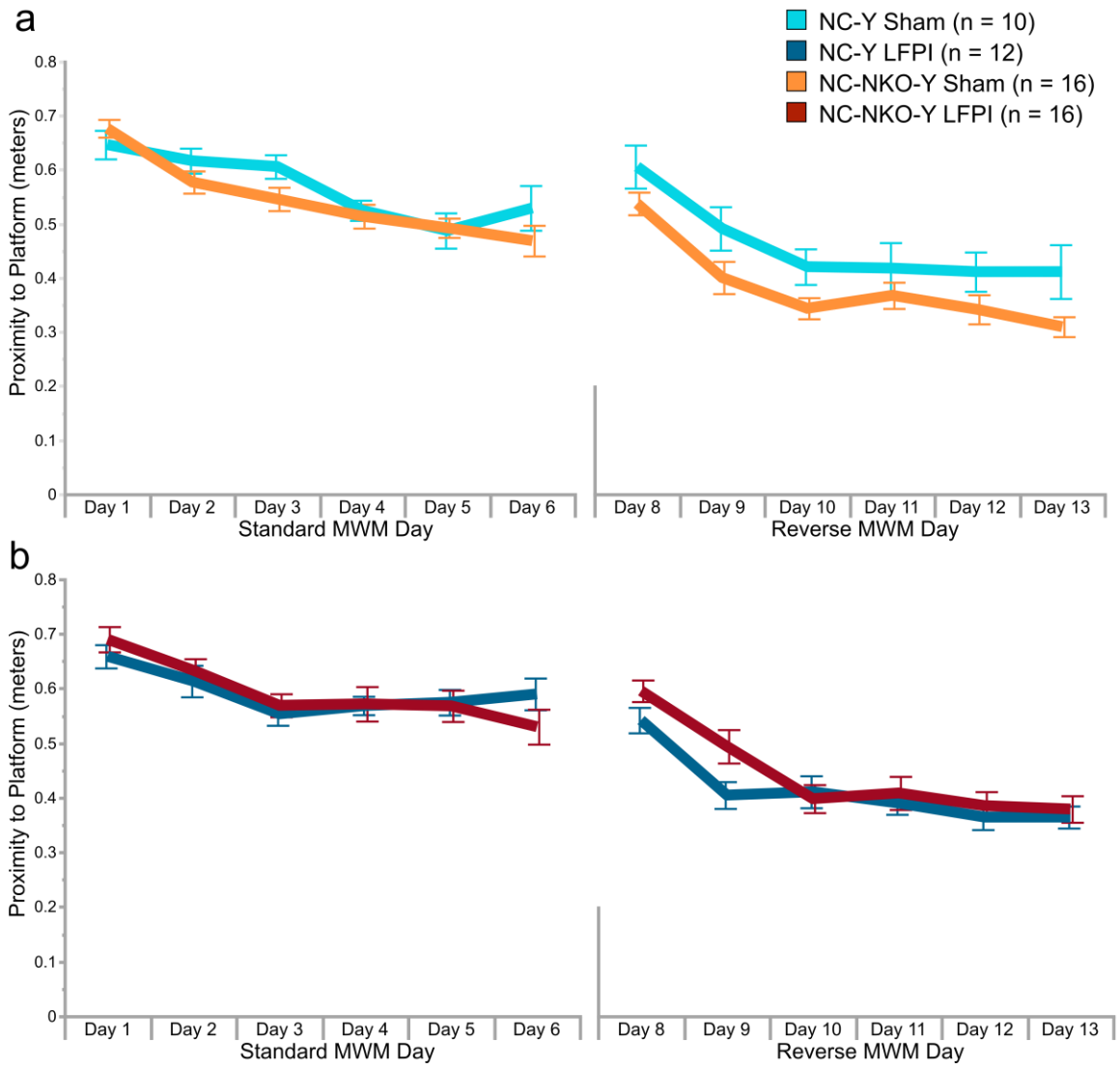

Figure 3.13. Proximity to Platform on MWM Standard and Reverse Testing: Compared by Genotype. (**a**) NC-Y (control) animals comparing genotypes on proximity from the platform with standard test days on the left x-axis and reverse test days on the right x-axis. (**b**) NC-NKO-Y (Notch1 cKO) animals comparing genotypes, standard test days on left and reverse test days on right.

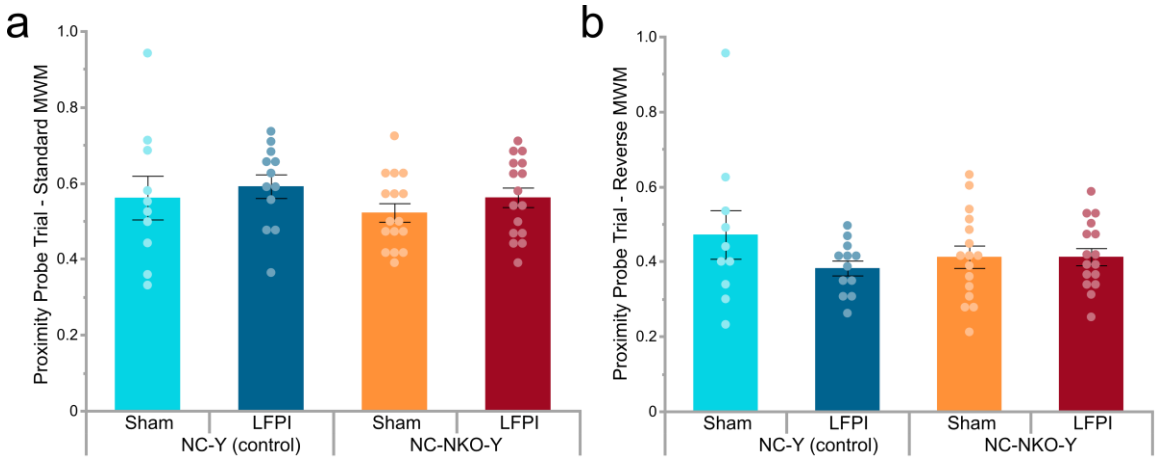

Figure 3.14. Proximity to Platform MWM Probe Trials. (**a**) All four groups compared on proximity with standard test days (**b**) All four groups compared on proxmity with reverse test days. No differences were seen on either standard or reverse probe trials.

The proximity to platform standard MWM days (**Figure 3.14a**) had no effect of injury [$F(1,50) = 1.089$; $p = 0.302$, no effect of genotype [$F(1,50) = 1.044$; $p = 0.312$, and no interaction [$F(1,50) = 0.022$; $p = 0.884$. Similarly, the proximity to platform reverse MWM days (**Figure 3.14b**) had no effect of injury [$F(1,5) = 1.682$; $p = 0.201$, no effect by genotype [$F(1,50) = 0.180$; $p = 0.673$, and no interaction [$F(1,50) = 1.696$; $p = 0.199$. Another form of measurement on the MWM tasks is to look at the average swim speeds by group. On the standard probe trial (**Figure 3.15a**) there was a significant effect by genotype [$F(1,50) = 14.205$; $p = 0.0004$**), no effect by injury [$F(1,50) = 0.0009$; $p = 0.977$], and no interaction [$F(1,50) = 3.549$; $p = 0.0654$].

Tukeys posthoc analysis revealed a difference between sham NC-Y and sham NC-NKO-Y ($p = 0.0016$**), and a difference between LFPI NC-Y and sham NC-NKO-Y ($p = 0.0388$*). During the reverse probe trial (**Figure 3.15b**) there was also an effect by genotype [F(1,50) = 16.236; $p = 0.0002$**], and no effect from injury [F(1,50) = 1.1247; $p = 0.294$] and no interaction [F(1,50) = 2.777; $p = 0.102$]. On the reverse probe trial, Tukey's posthoc analysis revealed a difference in swim speed between sham NC-Y and sham NC-NKO-Y ($p = 0.0015$**) and between LFPI NC-Y and NC-NKO-Y ($p = 0.0029$**).

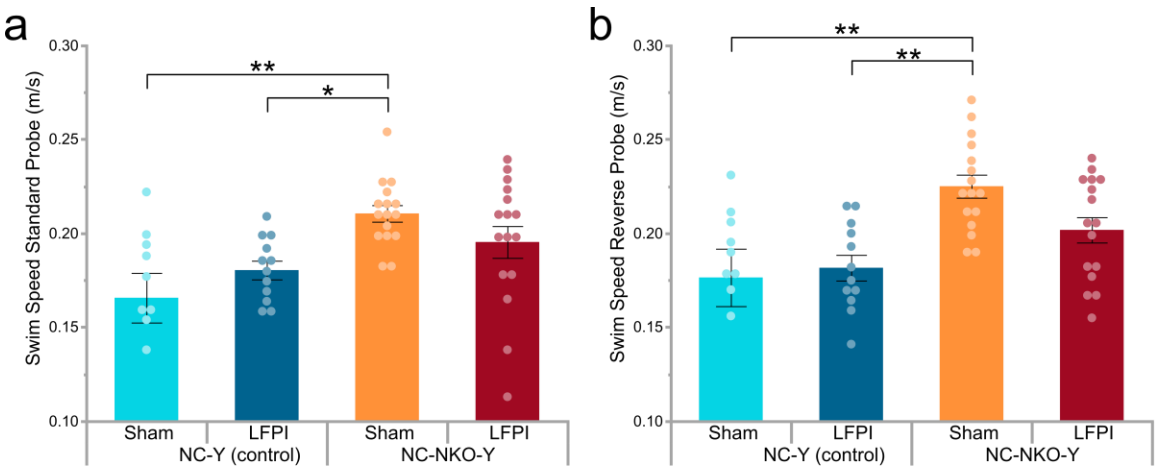

Figure 3.15. Swim Speed on Probe Trials Reveals Variation by Genotype. (**a**) All four groups compared by their swim speed on the standard test days and (**b**) all four groups compared by their swim speed on the reverse test days. NC-NKO-Y sham animals were reportedly faster at swimming compared to NC-Y (control) animals. Significance levels indicated by *p < 0.05, **p < 0.005.

3.3.4 Other Forms of Behavioral Tests

The animals used in these studies went through other tasks in addition to MWM. Open field is one of the most common ways to measure locomotor and anxiety behaviors in test animals. The injured animals spent significantly more time in the center (**Figure 3.16a**) compared to sham animals [$F(1,49) = 4.677$; $p = 0.0355$*]. For center latency there was no difference by genotype [$F(1,49) = 1.437$; $p = 0.237$] and no interaction [$F(1,49) = 0.389$; $p = 0.535$]. The injured groups spent significantly less time on the edge (**Figure 3.16b**) than the sham groups [$F(1,49) = 7.619$; $p = 0.0081$**], and there was no effect by genotype, however it was trending towards an effect [$F(1,49) = 3.521$; $p = 0.0666$], and there was no interaction [$F(1,49) = 0.016$; $p = 0.899$]. Tukey's posthoc analysis revealed that the sham NC-NKO-Y and the LFPI NC-Y differed significantly with the sham NC-NKO-Y animals spending more time near the edge ($p = 0.0083$**). The total distance traveled (**Figure 3.16c**) within the open field was significantly higher in injured groups compared to sham groups [$F(1,50) = 12.392$; $p = 0.0009$**]. There was no difference in distant traveled by genotype [$F(1,50) = 0.986$; $p = 0.326$] and no interaction [$F(1,50) = 0.0097$; $p = 0.922$]. Tukey's posthoc analysis revealed a significantly shorter distance traveled in the open field by sham NC-NKO-Y compared to LFPI NC-NKO-Y ($p = 0.0466$*) and sham NC-NKO-Y compared to LFPI NC-Y ($p =$

0.0099**). The open field data suggested that the injured animals had increased anxiety regardless of genotype.

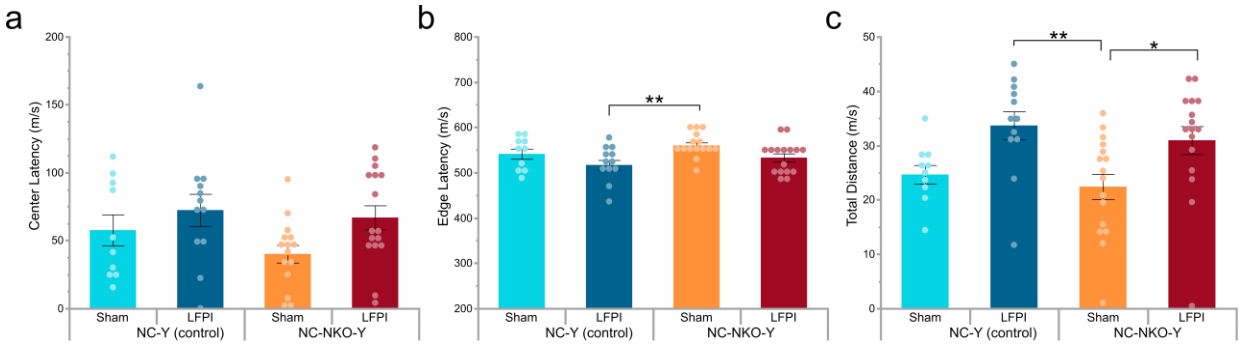

Figure 3.16. Open Field Test Locomotor Activity Reveals Anxiety-Like Behaviors in Injured Animals. Groups compared by the amount of time they spent in the (**a**) center of the open field, (**b**) edge of the open field, or (**c**) the total distance traveled around in the open field. Significance levels indicated by *p < 0.05, **p < 0.005.

Novel object recognition is a behavioral task used to test recognition learning and memory function (**Figure 3.17**). For this specific study, there were no differences in time spent with the familiar object by injury [F(1,49) = 0.372; p = 0.545], genotype [F(1,49) = 0.0287; p = 0.866], or interactions [F(1,49) = 0.0237; p = 0.878]. There were no differences in time spent with the novel object by injury [F(1,49) = 0.0248; p = 0.875], genotype [F(1,49) = 0.901; p = 0.347], or interactions [F(1,49) = 1.305; p = 0.259]. There were no differences on the discrimination index

by injury [F(1,50) = 0.321; p = 0.574], genotype [F(1,50) = 3.109; p = 0.084], or interactions [F(1,50) = 0.367; p = 0.548].

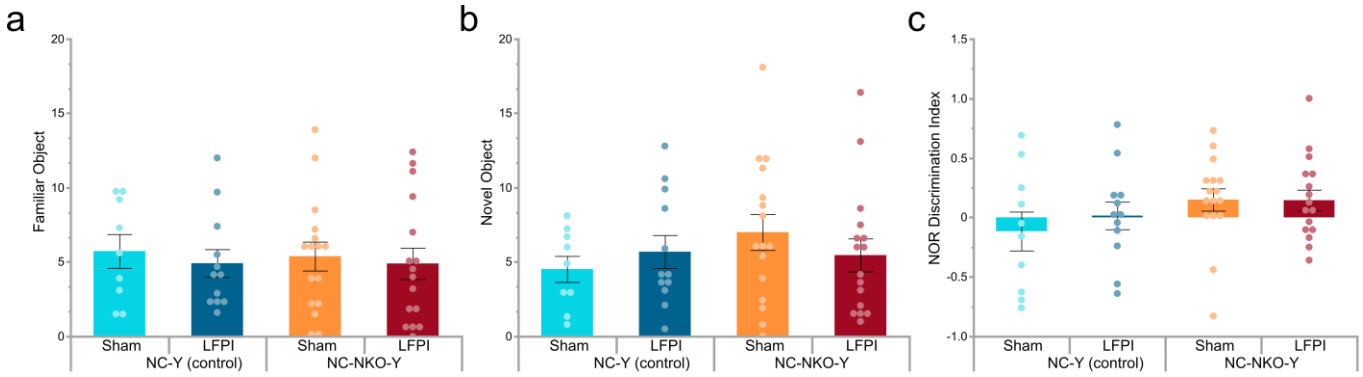

Figure 3.17. Novel Object Recognition Outcomes are Analogous. Groups compared by the amount of time they spent with the (**a**) familiar object or (**b**) novel object. A discrimination index (**c**) was calculated based on time spent with the familiar and novel objects. There were no differences between any of the groups.

3.4 Discussion

Learning and memory associated with hippocampal function is one of the most frequent complaints and impairments among TBI patients (Chohan et al., 2015). The discovery of an endogenous process that occurs as a direct result of TBI provides an opportunity to address the learning and memory dysfunction after injury. Injury-induced neurogenesis in the adult brain results in an increase in

new neurons that are likely contributing to functional recovery after injury (Blaiss et al., 2011; Chirumamilla et al., 2002; Sun et al., 2007; Sun et al., 2015; Zhao et al., 2018). Understanding these cells and how they incorporate into the local region will help aid in ways to regulate and influence this response for improved recovery.

This body of work investigated new neuron morphological development to distinguish neuroplastic changes occurring during the time of recovery and outcomes of performance on learning and memory tasks. Additionally, the role of Notch1 was assessed to understand implications it has on these two components of recovery. We hypothesized Notch1 to play an essential role in dendritic complexity and for loss of Notch1 to diminish any enhanced complexity we predicted for injury-induced populations of cells. We expected injured animals to perform similar to sham animals on learning and memory tasks as this relates to our past findings, and for Notch1 cKO to result in absence of this performance recovery (Chirumamilla et al., 2002; Sun et al., 2007; Sun et al., 2015).

Behavioral function is connected to synaptic plasticity, and one of the foundations of plasticity are the changes in synaptic contacts over periods of time. When the newborn cells start to mature and develop their dendritic arbors, they exhibit a large amount of structural flexibility. Characteristics of synaptic contact alteration include activity dependent changes in synaptic strength,

neurotransmitter release quantity, receptor insertion or removal, or elimination of dendritic spine/axonal boutons, which on a circuitry vantage could result in complete remodeling of connectivity. The new neurons derived from these regions establish functional synapses within the circuitry once they mature and continue to refine these contacts several months after. The hippocampus is one of the most vulnerable regions impaired following TBI as it involves significant cell loss reflected in the cognitive dysfunction outcomes (Smith et al., 1997; Sun et al., 2015). For injury-induced new cells to integrate they would have to adapt to this post-injury environment. Survival and successful synaptic integration would need to compensate for these changes. These experiments were designed to closely examine the morphological patterns of new GC neurons and the role of Notch1 in these patterns.

A number of parameters were used to assess the morphology of injury-induced new neuron dendritic arbors (**Table 3.2**). All cells measured were from the injury-induced population that became mature neurons, with or without Notch1 knocked out. Sholl analysis is a well-established tool to objectively study the shape and complexity of a dendritic arbor based on fixed distances away from the soma (O'Neill et al., 2015; Ratliff et al., 2020; Wu et al., 2004). We also used more novel means to study branch arbor structures including path order analysis, length and number of branches, and volume (Beining et al., 2017).

	Comparisons by Injury		Comparisons by Genotype	
	NC-Y	**NC-NKO-Y**	**sham**	**LFPI**
	sham vs. LFPI	**sham vs. LFPI**	**NC-Y vs. NC-NKO-Y**	**NC-Y vs. NC-NKO-Y**
4 WPI				
Sholl	LFPI ↑ near soma	LFPI ↑ near soma	-	-
Path Order	-	-	-	-
Volume Span	-	-	-	-
Summed length	-	-	-	-
No. of primary branches	-	-	-	-
Summed primary branch length	-	-	-	-
No. of terminal branches	-	-	-	-
Summed terminal branch length	-	-	-	-
8 WPI				
Sholl	LFPI ↑ near soma	LFPI ↑ near soma LFPI ↓ overall	-	-
Path Order	LFPI	LFPI ↓	NC-NKO-Y minor ↑	LFPI ↓
Volume Span	-	sham ↑	-	-
Summed length	-	-	-	-
No. of primary branches	-	-	-	-
Summed primary branch length	-	-	-	-
No. of terminal branches	-	-	-	NC-NKO-Y ↓
Summed terminal branch length	-	-	-	-

Table 3.2. Summary of Neurogenic Cell Population Morphology. Separate comparisons by injury condition (left) and by genotype (right) with a generalized summary of morphology results (far left column) for 4 WPI (top) and 8 WPI (bottom). Arrows indicate an increase or decrease.

The increase in dendritic complexity from LFPI NC-Y animals compared to sham NC-Y was anticipated as part of the original hypothesis. Conversely, conditionally knocking out Notch1 from NSCs/NPCs resulted in more dendritic branching, however in the case of an injury-induced population there are significantly fewer branches in the new neurons. This result may have to do with the environment that injury incites and how the loss of Notch1 in neurogenic populations does not coordinate well with, while in an uninjured environment the loss of Notch1 results in a response that appears to be beneficial. Notch1 is known to increase branch numbers, so the question is why is branch complexity increasing in our model if Notch1 is knocked out? There is no change from genotype for shams by Sholl analysis and hardly any change by path order analysis, which could possibly be explained by a compensatory mechanism keeping up with normal patterning needed for new developing cells. However, since injury prevents this from happening, the role of Notch1 appears to be essential only in the case of injury.

The alterations in morphology relate well to the outcomes of the learning and memory tasks in these studies. Notch1 knock out resulted in more branching, and these same animals had better performance on MWM, however if a NC-NKO-Y animal was injured there were far fewer branches and a learning deficit on MWM performance. This only partially supports our initial hypothesis, as we

predicted NC-NKO-Y animals would generally perform worse on MWM and have reduced branching, regardless of injury.

Animals in this study underwent a series of learning and memory tasks to assess the innate recovery response after injury and if Notch1 plays a significant role in this function (**Table 3.3**). Days 56 - 60 after injury is a timeframe when we have observed this innate cognitive recovery in the past (Chirumamilla et al., 2002; Sun et al., 2007; Sun et al., 2015). On the MWM tasks here, standard MWM days 1 – 6 were performed on post-injury days 56 – 61, so we hypothesized to see recovery of performance similar to our past findings. In the NC-Y animals, the sham and injured animals performed similarly suggestive of learning and memory function recovered in the injured animals. The animals did not perform MWM tasks before the innate recovery period covering post-injury days 56 – 61, so without data of MWM performance earlier than the innate recovery period it is difficult to assess if this is true recovery or if there was never a deficit in these particular animals.

The NC-NKO-Y animals with an injury performed substantially worse on MWM compared to sham NC-NKO-Y supporting our hypothesis on the effect of Notch1 cKO with regards to injury. This could not be contributed from injury severity differences between groups, as they remained relatively consistent with one another. Unexpectedly, during the reverse MWM task which measures cognitive flexibility, the NC-NKO-Y sham animals found the platform

significantly quicker than the NC-Y sham animals. This almost suggests a beneficial aspect to loss of Notch1, which could be supported by the literature that shows upregulated Notch1 in Alzheimer's disease models results in worse cognitive abilities (Galeano et al., 2018).

	Comparisons by Injury		Comparisons by Genotype	
	NC-Y sham vs. LFPI	**NC-NKO-Y** sham vs. LFPI	**sham** NC-Y vs. NC-NKO-Y	**LFPI** NC-Y vs. NC-NKO-Y
MWM				
Latency to Platform	-	LFPI ↑ latency	NC-NKO-Y ↓ latency	-
Proximity to Platform	-	Sham proximity	NC-NKO-Y ↑proximity	-
Swim Speed	-	-	NC-NKO-Y ↑ speed	-
Open Field				
Center Latency	-	-	-	-
Edge Latency	-	-	-	-
Total Distance	-	LFPI ↑ total distance	-	-
NOR				
Familiar Object	-	-	-	-
Novel Object	-	-	-	-
Discrim. Index	-	-	-	-

Table 3.3. Summary of Learning and Memory Behavioral Assay Outcomes. Separate comparisons by injury condition (left) and by genotype (right) with a generalized summary of behavior results (far left column) for Morris Water Maze (top), Open Field (middle), and Novel Object Recognition (bottom). Arrows indicate an increase or decrease.

On the component of MWM task looking at proximity to the platform, the NC-NKO-Y shams were always closer than the injured NC-NKO-Y animals, and were closer than sham NC-Y on the reverse MWM days. These results may have more to do with swim speed of the animal groups, as the NC-NKO-Y shams swam significantly faster than almost all other groups. One possible explanation for this is that Notch1 is a candidate for anxiety and stress related models (Steine et al., 2016). However, Notch1 is upregulated in connection to anxiety, and based on our open field data, NC-NKO-Y shams stayed away from the center of the field for the greatest amount of time. One study using a similar NC-NKO mouse line found no difference in behavior in association with mood disturbances (Steine et al., 2013). The experiments in this dissertation used two separate lines of transgenic mice composed of slightly different genetic backgrounds. This may have contributed to the differences seen between genotype, however both lines are made from a similar combination of 129X1/SvJ backcrossed to C57BL/J6 for several generations.

Even though the results presented here are robust and support the importance of Notch1 in the injury recovery process, there are some things to take under consideration. The injury severity and type of injury could result in different dendritic morphology patterns, for example a more severe injury could result in less dendritic complexity (Villasana et al., 2015). Another item to consider

are the measurement categories, especially because neuron morphology differs substantially even within the same animal (Cole et al., 2019). Some studies outside the context of TBI have separated out morphology of GCs based on which GC layer their soma is located in, for example, if they are located in the suprapyramidal blade or infrapyramidal blade. Even though we quantified how many cells have one primary dendrite versus two, it may be beneficial in the future to separate these into two separate categories, especially because injury is known to lead to more primary dendritic branch numbers. Even with all these caveats, the findings of the experiments conducted for this dissertation complement each other such that these extra forms of analysis may not be necessary.

Chapter 4

Conclusions, Discussions, and Directions

4.1 Summary

Models of traumatic brain injury in adult mammalian brains have continuously shown that injury promotes a neurogenic response, specifically within the dentate gyrus of the hippocampus. A lot of effort has been put into understanding the purpose and reason for a neurogenic response to occur as a result of injury, especially because the amount of proliferation that manifests may differ dependent on the injury model and the severity of injury. In the case of these studies, we were directly interested in a mixed model at a moderate level not only because the lateral fluid percussion injury (FPI) is an excellent representation of what occurs in a real-life traumatic brain injury, but also because the data using this model has been reliable showing a neurogenic response.

Work from our lab has followed this line of research over the past several years, being one of the first research groups to recognize an injury-induced proliferative response (Sun et al., 2005). The research in this field, including work continuing from our lab, has come a significant way in working to understand this response. A powerful method to dive deeper into understanding this process is to start targeting specific proteins or cellular mechanisms that could be playing an important role in the response.

Notch1 signaling is prevalently used during the development stages of the brain. It is most commonly known for its role in maintaining proliferative stem cell pools and differentiation and maturation of cells preferentially into glial cells as development continues. With the discovery of adult neurogenesis, several research groups started to focus on developmental neurobiology because it appeared a majority of the same mechanisms and processes would be recapitulated, albeit specifically in the few neurogenic regions that still exist in the brain. Notch1 is an example of a protein that has been shown to serve the same functions in the adult neurogenic region as the embryonic development phases. Since Notch1 maintains the neurogenic stem cell and proliferative pools, it can be predicted that any outside cue manipulating the production of new cells in these adult neurogenic regions could involve changes in Notch1 signaling.

In these experiments, we wanted to know if Notch1 plays a significant role in the injury-induced response in the DG of the hippocampus. We were specifically interested in the response when Notch1 is conditionally knocked out of neurogenic populations in the adult mammalian brain. To target the neurogenic populations these experiments used a transgenic mouse strain that only knocks out Notch1 in nestin expressing cells. To summarize, this model allowed for specific manipulation of only the adult neurogenic niches, even more specifically the NSCs/NPCs within these regions.

The mouse lines were developed with a tamoxifen-inducible Cre-lox system which allowed control of knocking out Notch1 from the NSCs/NPCs. After injury, animals were included in separate cohorts either focused on cell population alterations, morphology of NSCs/NPCs, synaptic protein expression, or cognitive learning and memory behavioral paradigms. These experiments were hypothesized to result in injury-induced new cells contributing to recovery after injury, and this would be evident through the survival and morphology of these new cells in association with learning and memory task performance, and Notch1 plays a critical role in this process. The conditional knockout of Notch1 was hypothesized to result in an increase of cells leaving the stem cell pool, reduced dendritic complexity of new neurons, and reduced ability to perform on learning and memory tasks.

The hypothesis of the Notch1 knockout did not manifest. Instead, on our learning and memory studies and morphology studies, it was evident that the knockout of Notch1 in a NSC/NPC population within the DG of the hippocampus almost appeared beneficial. A number of studies have found significant increases in the expression of Notch1 in brains from patients with later stages of Alzheimer's disease, and this includes the DG of the hippocampus (Ethell, 2010; Galeano et al., 2018; Lazarov & Marr, 2010; Nagarsheth et al., 2006). Even more specifically, cleavage leading to Notch1 intracellular domain (NICD, active form of Notch) was increased in brains of patients with sporadic AD. Notch1 activation may accelerate Aβ associated pathology and cognitive decline, however it is important to note that chronic NICD expression in wildtype animals has no effect on spatial learning and memory retention (Ables et al., 2009).

With regards to TBI, the NC-NKO-Y animals with injury did have a significant deficit in learning and memory tasks, supporting this component of the initial hypothesis. Notch1 is believed to be neuroprotective after injury (Wang et al., 2015). The premise of the hypothesis for this study was based on new neurons undergoing synaptic plasticity dependent on Notch1. The deficits seen with NC-NKO-Y may not be directly related to synaptic locations, especially considering the surprising NC-NKO-Y sham results. One study showed that Notch1 signaling enhances angiogenesis and is involved with vascular repair after TBI, promoting

blood vessel formation and tissue repair after brain injury (Ran et al., 2015). With Notch1 knocked out, this recovery mechanism would not be able to occur causing continuous secondary injuries to the hippocampus. Endothelial cells specifically use Notch as a negative regulator in angiogenesis, which may be a component of vasculature repair after injury in coordination with VEGF (Nakayama et al., 2013). On the other hand, chronic activation of Notch leads to pro-angiogenesis levels resulting in abnormalities with impaired blood flow and thicker vessel walls, which is another theory behind the increased Notch association with AD (Galeano et al., 2018).

Another possibility for the unexpected NC-NKO-Y sham results may have to do with communication of neighboring glial cells. Astrocytes communicate to NSCs through Notch1, and nestin is a negative regulator for neuronal differentiation. There are complex relationships between nestin and Notch1 signaling, and since these experiments were done in mouse lines specific to Notch1 cKO in nestin+ cells, there may be an underlying explanation (Wilhelmsson et al., 2019). In this study, the authors reported that a small amount of nestin expressing progenitor cells show characteristics of astrocytes and do not express NeuN once they mature. They also found that in adult brains, nestin is expressed in astroglial cells of the hippocampus, and can be re-expressed in reactive astrocytes under pathophysiological conditions. In this study, the number of proliferating cells did

not change when they knocked out nestin in the hippocampus. The same goes for the amount of neuroblasts, immature neurons, proliferating neuroblasts, and no alterations to the total NSC/NPC pool number, either. Even though they saw no changes to proliferation, the number of mature neurons downstream were changed. The loss of nestin led to a reduction in Notch signaling with astrocytes, leading to more neurons. Additionally, their nestin cKO had impaired long-term memory with object recognition tasks. A decrease of nestin in astrocytes led to internalization and the breakdown of Notch1 ligand Jagged1, resulting in nothing to bind to the extracellular domain of Notch1 to trigger Notch signaling.

The results in this dissertation could be explained by a similar unexpected mechanism involving Notch in the experimental animals (NC-Y and NC-NKO-Y). Notch cross-talks with several other pathways, for example lef-1, fox01, and smad1 (Alberi et al., 2013). Another interaction of Notch1 is with CREB, relating back to learning and memory. Inhibitory effects of Notch1 on CREB relies on gamma-secretase cleavage, and one group showed that application of gamma-secretase inhibitors enhanced long-term memory, and Notch1 antagonizes CREB (Dash et al., 2005; Hallaq et al., 2015). It's possible the loss of Notch1 disrupts long-term memory, but not short-term memory. More support for a nonconanical pathway is P75 interacts with Notch for dendritic arborization, and this is an example of how the dendritic tiling process is thought to be more complicated than originally

thought, especially when associated studies show Notch actually limits the number and length of neurites (Giniger, 2012; Salama-Cohen et al., 2006).

After injury, there is damage to the majority of the hippocampus and in particular, the FPI model is known to lead to large numbers of cell death (Carbonell & Grady, 1999). There is a compounding process of deafferentation in the DG cell dendrites due to entorhinal cortex loss with the FPI model. It is possible the loss of Notch1 in NC-NKO-Y injured animals is resulting in the inability to form synaptic contacts, especially with the massive cell death in the injured environment and progressive deafferentation. The only group to have a significant increase in volume of their dendritic branch pattern were the NC-NKO-Y sham animals, suggesting the contact-dependent inhibition role of Notch in neurite growth is prevented. In the case of injury, we do not see the volume increase in NC-NKO-Y animals and this could be explained from the loss of surrounding cell density. In a study looking at Notch1's role in cortical development, the size of a dendritic field depends on local cell to cell interactions and overall neuronal density (Šestan, Artavanis-Tsakonas & Rakic, 1999). An upregulation in Notch resulted in an increase in interneuron contacts, in which they hypothesized Notch serves a prominent role in transitioning dendritic branching related to neuronal growth to dendritic branching maturity (Šestan, Artavanis-Tsakonas & Rakic, 1999). It's possible Notch1 may help with spatial

distribution after injury, so the loss of Notch1 may result in a cluster of overlapping cells with inappropriate synaptic contacts and locations. When introducing a TBI, a large number of changes occur and not having Notch1 signaling to promote spatial distribution could be detrimental for injury recovery. The reduced complexity of injury-induced new neurons from NC-NKO-Y animals may be a result of factors involving more generalized alterations of the GCLs after injury. The migration of cells after TBI observed in these experiments would result in less tissue for new cells to extend their dendrites through the molecular layers. Molecular layer shrinkage after injury could also explain the morphology results, with the same concept that the dendrites have less tissue to expand through.

The experiments in this dissertation used both sexes. Although the data did not show sex-related differences, it's still an important component to discuss for the development of future experiments. Notch sex differences exist, but are barely evident and most are in relation to embryology. Past work on embryogenesis has shown sex differences with Notch1. In a study examining sexually dimorphic differences in the genome of bovine embryos, an increase in oxygen levels results in higher expression of Notch1 in cultures female embryos compared to male embryos (Taqi et al., 2019). Additionally, the expression of Notch1 was elevated in male embryos exposed to oxidative stress. An earlier study examined the transcription factor AP-2 family of genes due to its essential roles in development,

especially in the brain (Coelho et al., 2005). The various AP-2 factors are suggested to regulate various neural specific genes. In developing *Drrosophila* legs, the sole AP-2 family gee for this species is activated by Notch signaling in epithelial cells. Notch is also involved in the development of ectopic sensory bristles, showing its involvement in neurogenesis. The study found Notch1 is co-expressed at low levels in a small population of cells possibly including nascent neurons in the DG, supporting a potential role for Notch signaling in AP-2 regulation. The study also identified sexually dimorphic AP-2 expression in neurons of other regions, including the olfactory region which is another adult neurogenic zone. Notch activation occurs in the skeleton which can cause cell-context dependent alteraations in the physiology of the skeleton. Since sex is a determining factor in skeletal structure, this suggests Notch may be involved in sex-dependent skeletal remodeling. One study found juvenile mice females had a greater number of osteocytes than their male littermates, and this was an age-dependent decline. When assessing the inactivation of Notch, they found there was no effect on osteocyte number and it did not influence bone loss (Canalis et al., 2017). Another study that ties into the morphology of neurons found that the widespread environmental neurotoxic contaminant methylmercury causes significantly more impairment in a sex-dependent manner, with male fetuses having more severe alterations (Edoff et al., 2017). This study relates to Notch-dependent morphology

with alterations from assault on the brain, similar to the work presented in this dissertation, however we did not observe any differences between the sexes on the morphology studies. Future work will need to address sex differences with more detailed cell quantification, morphological analysis, and behavior paradigm approaches.

Finally, it is important to mention the issues that can arise with neurogenic recovery in adults after brain injury. Treatments pose a risk, but the endogenous responses can, as well. The characterization of seizures or epilepsy developing long after injury is suggestive of incorrect circuitry repair. Some other issues could be scar tissue and tumors as a result of faulty recovering. Nevertheless, understanding the capabilities of the neurogenic population and what mechanisms manipulate it may benefit TBI recovery and other neurological diseases such as Alzheimer's and mood disorders. In this dissertation, the experiments set forth have shown Notch1 serves an important role for injury-induced new neurons and relevant outcomes. The populations of injury-induced new neurons, morphological development aiding in synaptic plasticity and connectivity, and learning and memory recovery are all components of the role of Notch1.

4.2 Future Directions

The work in this dissertation examined injury-induced cell populations and longevity, morphology of new neurons, learning and memory task capabilities, and synaptic proteins. These experiments serve a foundation for understanding Notch1's critical role in the injury-induced neurogenic response, however there are a few directions for future studies that will elucidate this further.

4.2.1 LTP and Cellular Function

Previous work from our lab has studied the capacity for long-term potentiation at different post-injury times using field electrophysiology recordings (Weston et al., 2021). These experiments were conducted with our commonly used rat model of LFPI. Recordings were taken along the perforant pathway from the entorhinal cortex to the molecular layers to assess LTP contributed to the new injury-induced population of neurons. At 30 DPI, there was a significant deficit in the capacity for LTP, however at 60 DPI this capacity was similar to sham levels suggesting recovery of this circuitry function had occurred. The timing of LTP capacity recovery coordinated with our findings of our rat model. On behavioral tasks assessing learning and memory after injury, recovery was seen on MWM at 60 DPI (Sun et al., 2007, 2015a).

In this dissertation, learning and memory on MWM was assessed, however experiments on the functional recovery from a LTP standpoint were not replicated. Studies to address this gap will be conducted in the near future by repeating the perforant pathway LTP experiments in the NC-Y (control) and NC-NKO-Y (Notch1 cKO) transgenic mice. Animals will receive either sham or LFPI, and the recordings will be conducted 8 WPI, similar to the post-injury behavior, cell population, and morphology assessment studies from this dissertation.

The hypothesis of this future work is capacity for LTP will follow the same patterns of plasticity seen in the morphology data and performance seen in the behavior data. For the NC-Y, LFPI is expected to have a comparable outcome on these electrophysiological recordings as the sham, or even slightly elevated capacity similar to the rat 60 DPI data results (Weston et al., 2021). This result would provide supportive evidence of injury-induced new neurons in innate recovery after TBI. The NC-NKO-Y that will receive sham surgeries are hypothesized to also have a similar level of capacity for LTP, or possibly even heightened complementing the morphology and behavior data. However, the NC-NKO-Y LFPI group is hypothesized to show a significant deficit in the capacity for LTP 8 WPI. These results would tie together the cell morphology results to a broader cell network function and the more global behavioral function.

4.2.2 Markers for Synaptic Plasticity

In this dissertation, hippocampal tissue was isolated to quantify synaptic marker proteins. This was especially important as previous studies show Notch1 colocalizes with PSD95 and is believed to participate in synaptic plasticity (Alberi et al., 2011; Brai et al., 2015). The data from this dissertation examined PSD95 (postsynaptic density marker) and synaptophysin (presynaptic). Unexpectedly, there was no difference in PSD95 total protein, but there was a difference in synaptophysin total protein, specifically between the NC-Y sham and LFPI.

It's possible Notch1 is not essential for PSD95 per the results, and the similar levels seen in the NC-Y may represent and complement recovery at 8 WPI as seen in both the morphology data and behavior data. The decrease in presynaptic markers within the hippocampus after injury could be attributed to a number of causes, including long-lasting effects of loss of cells after injury, alterations in synaptic function with other cells of the hippocampus, or indirect effects such as post-injury seizure activity causing significant network rewiring (Chen et al., 2018; Folweiler et al., 2018; Hunt et al., 2011; Lowenstein et al., 1992; Reeves et al., 2000; Vascak et al., 2017). It's difficult to determine the most probable cause without a repertoire of further studies. Ongoing work is underway to assess total protein of other synaptic markers in hopes of teasing out synaptic plasticity post-injury. These proteins include GAD-6 to assess the production of the major inhibitory

transmitter GABA, VGLUT1 to assess glutamate transport, and a new PSD-95 primary antibody as the sensitivity of the current one used for this study is less than optimal.

An important distinction with the Western blot total protein data is experiments were conducted not only with DG tissue, but instead with the entire hippocampal tissue. This could mean alterations in other regions such as CA3, CA1, the subiculum, may have had a robust result overshadowing any change in synaptic proteins just within the DG. To address this point, studies are in progress utilizing fluorescence-activated cell sorting (FACS) and single cell RNAseq. The goal of this experiment is to isolate all GFP expressing cells within the hippocampus, targeting only the NSC/NPC populations within the DG. Once isolated, single cell RNAseq will be conducted to reveal several synaptic plasticity proteins and pathway components. If successful, this experiment will be able to tell exactly what components of synaptic plasticity are directly altered in the NSC/NPC populations as a result of LFPI and Notch1 cKO.

4.2.3 Assessment of Immature Neurons

The experiments conducted in this dissertation focused on 4 WPI and 8 WPI, however significant alterations and milestones in morphology also occur at 2 WPI. At 2 WPI, new cells typically are differentiated into immature neurons

beginning to grow and transition to a mature phenotype (Cole et al., 2019; Gonçalves et al., 2016; Trinchero et al., 2017). This is also the transition when axons enter CA3, dendritic protrusions grow, and spine growth begins (Zhao et al., 2006). The protein DCX is a distinct neuronal migration protein expressed specifically in immature neurons (Folweiler et al., 2018). Future experiments will examine the same endpoints of cell populations and morphology in this DCX+ population of cells 2 WPI, hopefully providing a better understanding of the overall maturation process of the injury-induced population and the role of Notch1.

Appendix A

Transgenic Mouse Models

Housing

Both female and male mice were housed in an animal facility with controlled temperature and humidity, a 12-hour light-dark cycle, ad libitum access to food and water, and weekly cage changes. All experimental mice were bred, genotyped, then transferred from the Virginia Commonwealth University Transgenic/Knockout Mouse Core. Experiments began when the mice were 6-8 weeks of age and housed in the animal facility until sacrifice for experiments. All procedures followed the NIH Guide for the Care and Use of Laboratory Animals (NIH Publications No. 80-23, 1996) and were approved by the Virginia Commonwealth University Institutional Animal Care and Use Committee.

Strain Details

Tamoxifen (TAM) inducible Cre-Lox system transgenic mouse lines were used in these studies (**Figure A.1**). Cre-recombinase has an estrogen receptor specific to tamoxifen as a ligand for control over Cre-induction. Stock strains for breeding were obtained from the Jackson Laboratories. Three separate strains were used to create two lines of experimental mice. A control line (NC-Y) was derived from nestin-CreER (Jax. Stock No: 012906) and R26R-EYFP (Jax. Stock No: 006148) to produce eYFP expression in cells that are expressing the neural stem cell protein nestin, an intermediate filament protein expressed at neural stem cell precursor and progenitor stages. In addition to this control line, a Notch1 conditional knockout (NC-NKO-Y) was made from Notch1flox (Jax. Stock No: 007181), the nestin-CreER, and R26R-EYFP lines to produce both eYFP expression and knockout of Notch1 in nestin+ cells.

Genotype identification was conducted through the VCU Transgenic/Knockout Mouse Core and subsequently transferred for experiments. For the acute proliferation 2 DPI and 7 DPI studies in Chapter 2, the NC-NKO-Y was the only line used. The Notch1 cKO mice had a Cre+ genotype, and the control mice for these studies had a Cre- genotype. For all other experiments only Cre+ mice were used from NC-NKO-Y (Notch1 cKO) and NC-Y (control). To induce the expression of Cre, mice began receiving TAM (180mg/kg in 10%

EtOH/sunflower oil) through intraperitoneal injection (i.p.) for six consecutive days. Two weeks after the last i.p. injection experiments began and animals started receiving surgery.

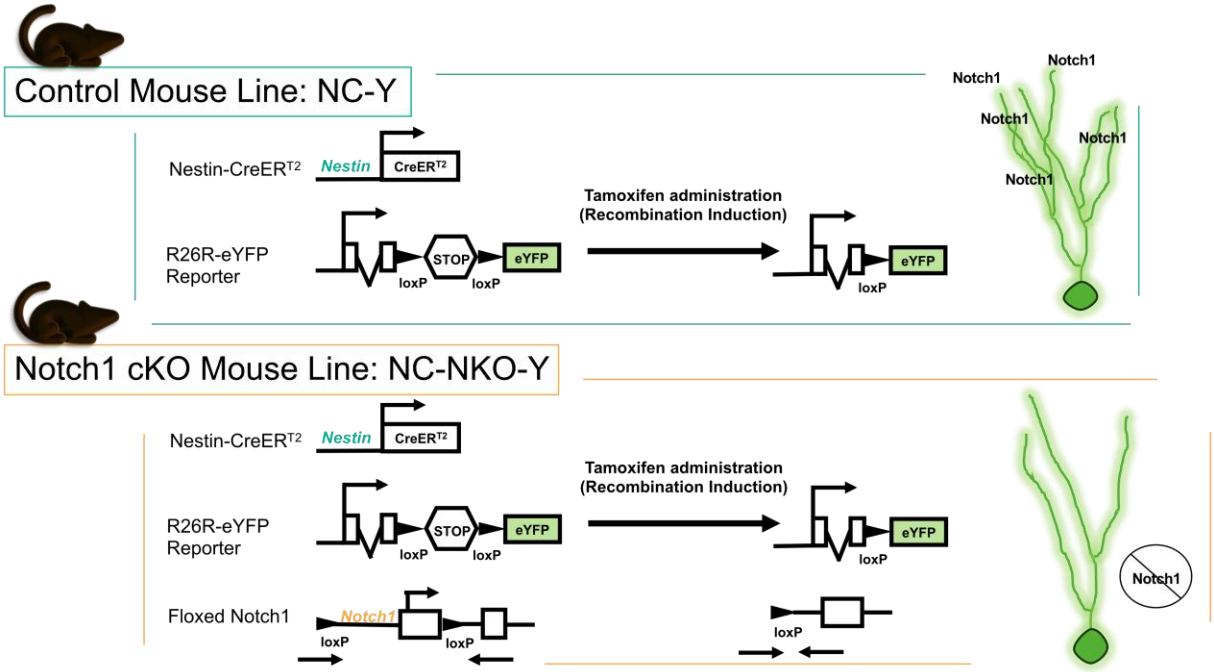

Figure A.1. Transgenic Mouse Lines Used for Experiments. Schematic of the two mouse lines used for experiments illustrating the different components of the strains the lines were derived from and the outcome once the Cre-lox system recombination is induced.

Appendix B

Injury Model and Surgery

Procedure

Animals received a moderate lateral fluid percussion injury (LFPI) or sham surgery two weeks after Cre induction (8-10 weeks old). FPI replicates clinical TBI without the skull fracture (Mahmood et al., 2013). The main purpose is that FPI is a combination of producing a focal cortical contusion and a diffuse subcortical injury. It produces the common neurobehavioral and cognitive deficits associated with TBI, including working memory deficits. Initially, mice were placed in an acrylic induction chamber to anesthetize using 4% isoflurane. The mice were positioned in a ventilated stereotaxic frame to stabilize their heads and to provide a continuous flow of 2.5% isoflurane in O2. A midline incision was made to expose the skull in both sham and LFPI animals. After creating the midline incision in LFPI mice, a craniectomy was made using a 2.7mm trephine over the left parietotemporal bone halfway between lambda and bregma sutures (Figure A.2a). A Luer-slip style hub was manufactured using a 20-gauge needle cap. The hub

was placed on the craniectomy site with cyanoacrylate and reinforced with dental acrylic to the skull. Anesthesia was turned off and animals were placed in recovery cages on heated pads and with access to food and water. After a two-hour recovery, mice were anesthetized with 4% isoflurane immediately before injury. The Luer-slip style hub was filled with 0.9% saline and connected to a pre-calibrated FPI device and a pulse target of 1.83 ATM was administered to induce a moderate traumatic brain injury (Figure A.2b). Immediately after injury animals were placed on a heated pad and monitored for recovery and righting time. After monitoring righting time, the mice were anesthetized and the hub was removed. Sham control animals received the same surgical procedure, however without the craniectomy and fluid pulse. After sham surgery or injury, the incision site was sutured and animals were returned to their cage. Animals received post-operative care and monitoring and hydrogel supplement was added to their home cages to aid in hydration.

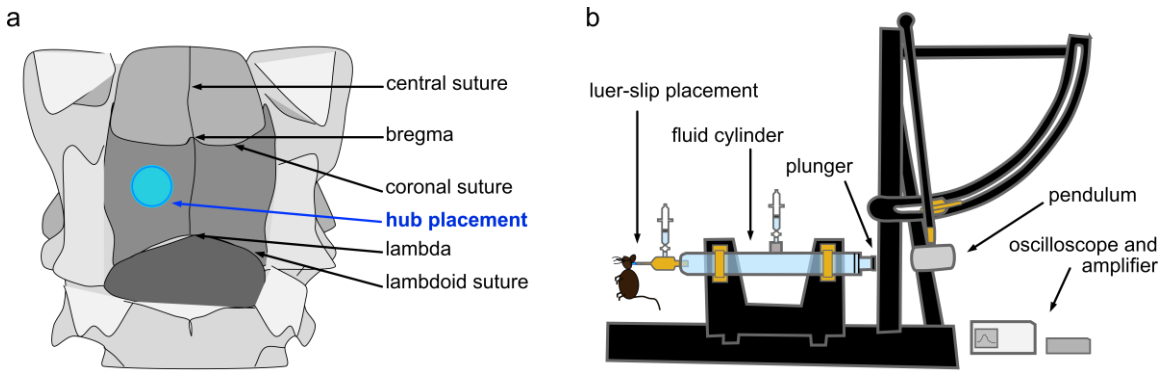

Figure A.2. Mouse Injury Preparation and Administration. (a) Lateral hub placement between bregma and lambda. (b) Fluid Percussion Injury device used to administer injury through the hub placement site.

Surgical Data by Experimental Cohort

Surgical Data Chapter 2 – Acute Proliferation 2 DPI and 7 DPI

The animals in this set of data were sacrificed 2- or 7-days post-injury and used for cell quantification acute proliferation data.

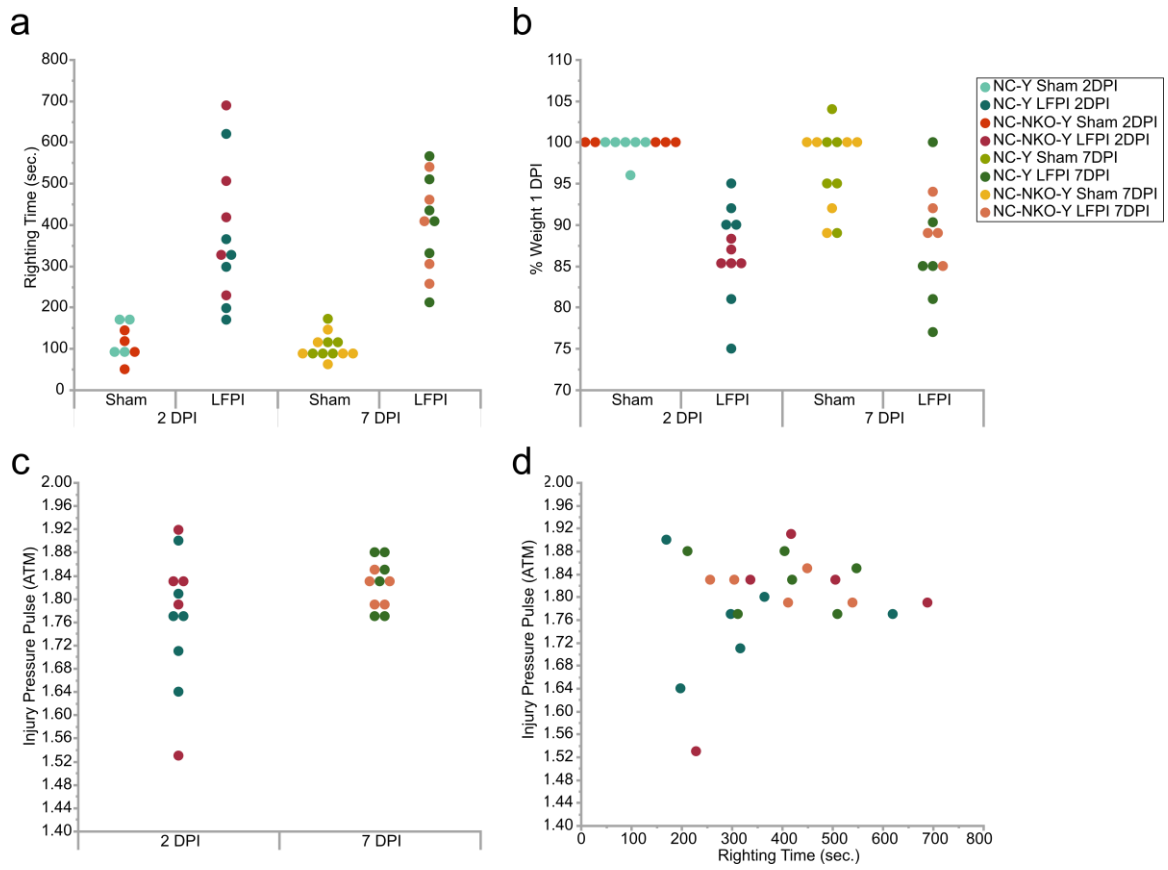

Figure A.3. 2DPI and 7DPI Surgical Data. NC-Y and NC-NKO-Y are differentiated through color index located on the right. (**a**) Righting time is plotted for both sham and LFPI animals. (**b**) The total % body weight of mice 1 DPI compared to their weight the day of surgery. (**c**) Injury levels for the LFPI groups. (**d**) Injury levels plotted with righting time.

Surgical Data Chapters 2 & 3 – Injury-Induced Cells 4 WPI and 8 DPI

The same animals sacrificed 4- and 8-weeks post-injury were used for cell quantification data from Chapter 2 and morphology data from chapter 3.

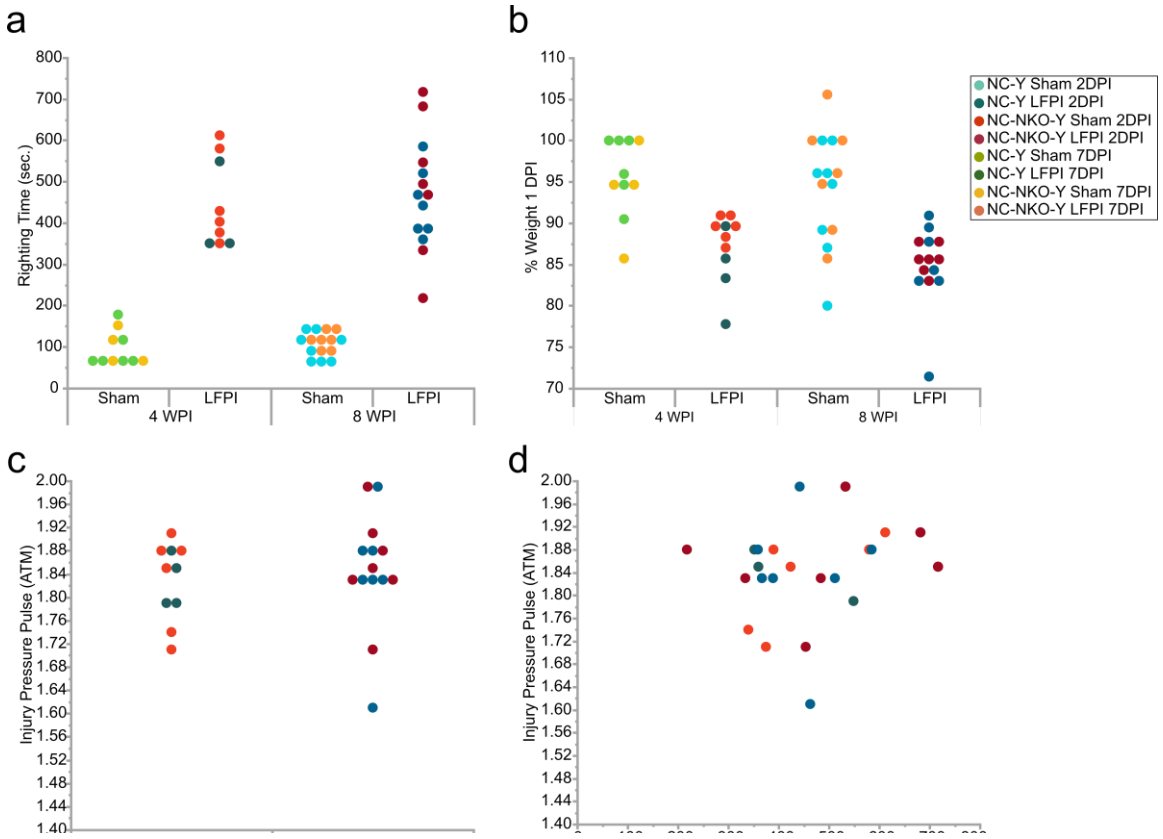

Figure A.4. 4 WPI and 8 WPI Surgical Data. NC-Y and NC-NKO-Y are differentiated through color index located on the right. (**a**) Righting time is plotted for both sham and LFPI animals. (**b**) The total % body weight of mice 1 DPI compared to their weight the day of surgery. (**c**) Injury levels for the LFPI groups. (**d**) Injury levels plotted with righting time.

Surgical Data Chapter 3 – Behavior Cohort

The animals in this set of data were sacrificed about 8 weeks after injury and used only for behavior.

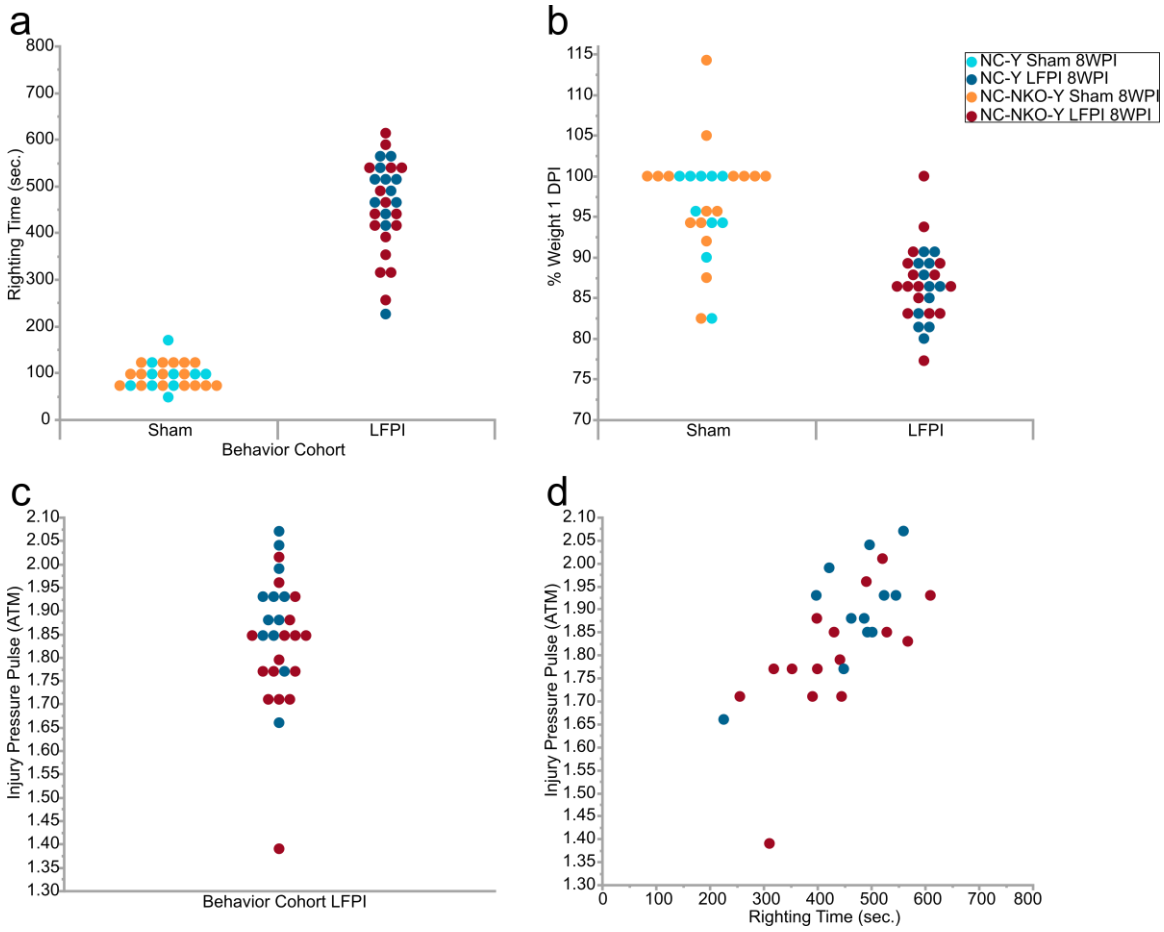

Figure A.5. Behavior Cohort Data. NC-Y and NC-NKO-Y are differentiated through color index located on the right. (**a**) Righting time is plotted for both sham and LFPI animals. (**b**) The total % body weight of mice 1 DPI compared to their weight the day of surgery. (**c**) Injury levels for the LFPI groups. (**d**) Injury levels plotted with righting time.

Surgical Data Chapter 3 – Western Blot Cohort

The animals in this set of data were sacrificed 8 weeks post-injury and used only for protein isolation.

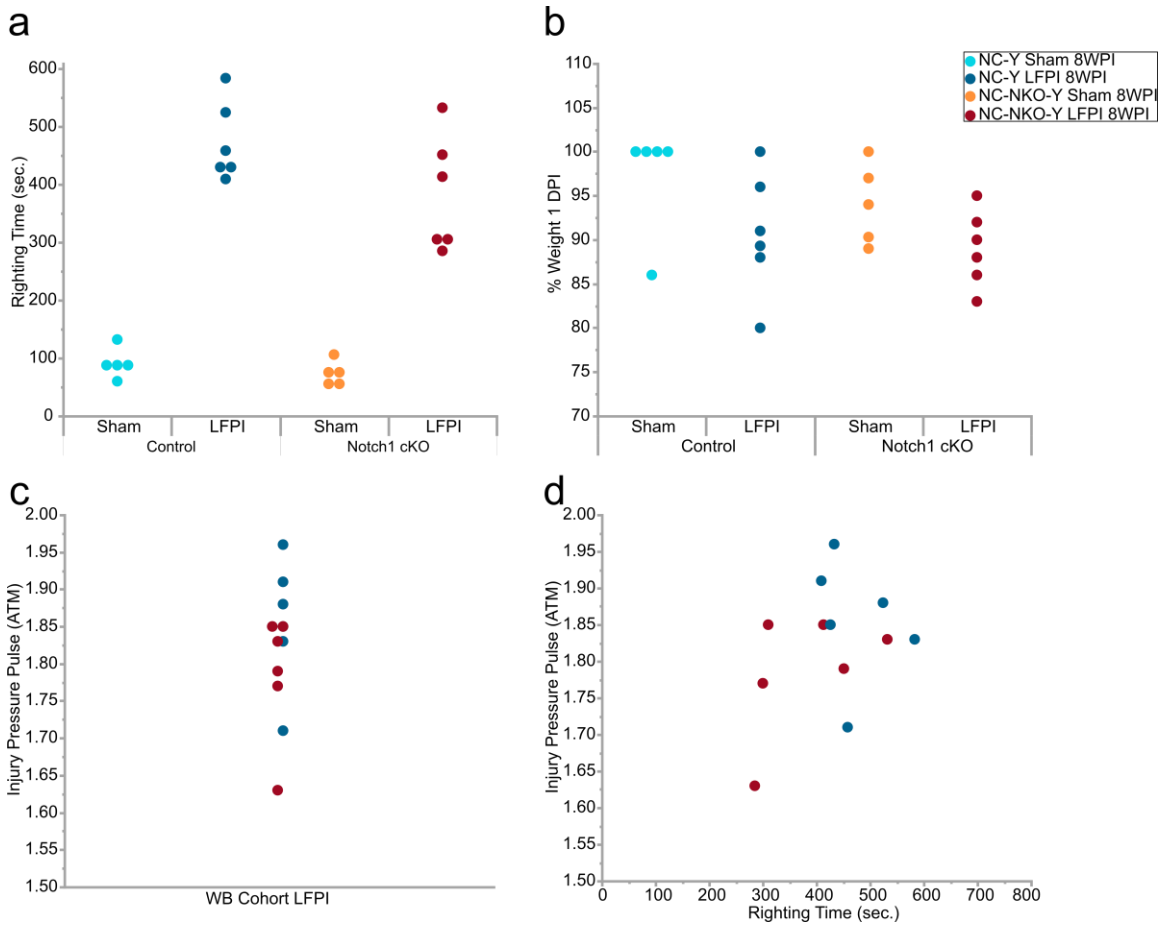

Figure A.6. Western Blot Surgical Data. NC-Y and NC-NKO-Y are differentiated through color index located on the right. (**a**) Righting time is plotted for both sham and LFPI animals. (**b**) The total % body weight of mice 1 DPI compared to their weight the day of surgery. (**c**) Injury levels for the LFPI groups. (**d**) Injury levels plotted with righting time.

Appendix C

Tissue Processing and Staining for Experiments

Transcardial Perfusions

Mice used in these studies were anesthetized and transcardially perfused with phosphate buffer saline (PBS) followed by 4% paraformaldehyde. This fixation process modifies tertiary and quaternary structures of proteins. The brains were collected and post-fixed for 24 hours in 4% paraformaldehyde, and stored at 4°C in PBS+0.05% sodium azide until processed for experiments. Paraformaldehyde-fixed brains were cut into 50 μm sections with a Leica VT1000 S vibrating microtome and stored in 48-well plates containing PBS+0.05% sodium azide at 4°C until further use.

Immunohistochemistry

Tissue Collection

Fixed free-floating sections were collected based on individual experiment goals and placed in separate wells of a 48-well plate (Figure A.7). A preliminary

wash of the sections was done by filling the wells with phosphate buffer saline (PBS), and then placed on a shaker for 10 minutes at room temperature. This was repeated three times for 10-minute intervals with fresh PBS.

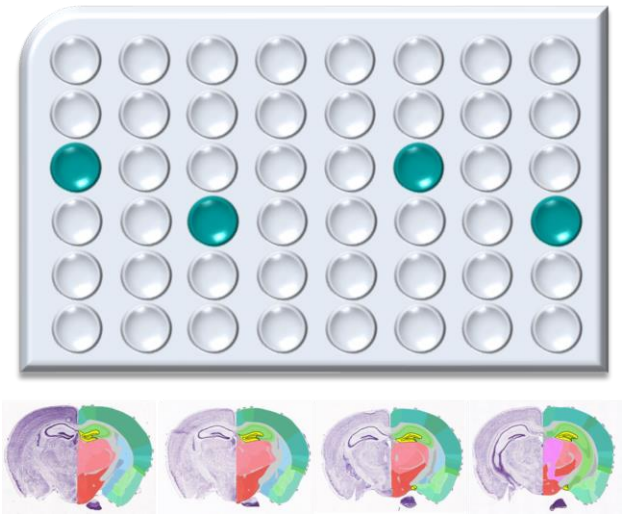

Figure A.7. Tissue Collection. Diagram of a 48-well storage plate with highlighted wells that section samples were taken from and would be transferred to an experiment 48-well plate. This example shows 4 coronal sections (50μm) representing an 800μm span of a hippocampus from one mouse. Coronal sections taken from Allen Brain Institute Mouse Brain Atlas.

Blocking

A blocking solution was prepared from serum, a detergent, and any other reagents necessary dependent on the experiment. To prevent non-specific binding of antibodies to tissue or Fc receptors, sections were blocked with 3% goat serum. To block endogenous biotin when using a biotin-based detection system, 2% VECTASTAIN® Avidin-Biotin Complex (ABC) Elite Kit reagent A was added to

the solution. The goat serum and reagent A were added to PBS with a detergent made up from 0.3% Triton X-100. Detergents solubilize membrane proteins by mimicking the lipid-bilayer environment, forming mixed micelles consisting of lipids and detergents and detergent micelles containing proteins. This blocking solution was placed in wells (150ul/well) containing tissue sections and the plate was placed on a shaker for 30 minutes at room temperature.

Primary Antibody

After blocking, a primary solution containing 1x PBS with 0.3% Triton X-100, 3% goat serum, 2% ABC Elite kit reagent B (second step of blocking endogenous biotin), and the appropriate concentration of primary antibody was added to each well (150ul/well) and left on a shaker overnight (~16 hours) at 4°C.

Peroxidase Activity

On the second day of staining the 48 well plate was taken out of 4°C and each well was rinsed with 1x PBS for 10 minutes at room temperature. To block endogenous peroxidase activity, sections were incubated in 1% H2O2 at this point for 30 minutes at room temperature. After H2O2 incubation, sections were washed with 1x PBS for 5 minutes and this was repeated 3 times with fresh PBS.

Secondary Antibody

After rinsing the sections, a secondary antibody solution containing 1.5% goat serum, 1x PBS, and the appropriate secondary concentrations were added to each well (150ul/well) and placed on a shaker for 4 hours at room temperature. After the secondary antibody incubation period the sections were rinsed with PBS at room temperature for 10 minutes.

Avidin-Biotin Complex System

Experiments involved the use of ABC kit for biotin conjugation. This kit was prepared at 1:400 reagent A, 1:400 reagent B, and 1x PBS. The kit solution was applied for 1 hour at room temperature. Following ABC kit, the sections were rinsed with 1x PBS and placed on a shaker for 10 minutes at room temperature. This wash step was repeated 3 times with fresh PBS.

Enzyme Substrate

Depending on the experiment, 3,3'-Diaminobenzidine (DAB) or AKOYA BIOSCIENCES® tyramide signal amplification (TSA) kit was used to pair with biotin conjugated secondary antibodies. The DAB was prepared as a liquid with 1-part 50x DAB concentrate, 1 part 0.5% H_2O_2, and 50 parts PBS. The DAB was washed off the sections with PBS after 10 minutes or when the reaction was visible

with light microscopy. For the TSA kit, preparation was made at a concentration of 1:50 with the provided fluorescein and the provided diluent. The solution was applied to the wells and left on the sections for 12 minutes. The TSA kit was washed off with 1x PBS for 10 minutes on a shaker at room temperature.

Denature for BrdU Samples

To label bromodeoxyuridine (BrdU) the sections require a denaturing step before the rest of the protocol is conducted. The sections are denatured with 2N HCl at 37°C for 30 minutes. Sections are allowed to drop to room temperature before washing off the HCl with several rinses of PBS.

Slide Preparation

Tissue mounting on slides was performed with VECTASHIELD® Vibrance™ antifade mounting medium (#H-1700). Sections were carefully transferred from the 48- well plate to a *Superfrost Plus* microscope slide (Fisherbrand™ 12-550-15) and coverslipped (Fisherfinest® 12-544-14). Sections were allowed to cure overnight at 4°C while protected from light. Clear nail polish was applied to seal coverslip edges and slides were stored in a slide box at either 4°C or -20°C until needed for experiments.

Appendix D

Experiment Timeline Details

Tamoxifen was administered at 180mg/kg through intraperitoneal injection for six consecutive days to induce recombination of the Cre-lox system in transgenic mice used for these experiments (Ables et al., 2010; Basak et al., 2012; Whitfield et al., 2015). A two-week period of rest was created starting after the last day of injections. This allowed the mice to recover from the side effects of tamoxifen while simultaneously allowing time for continuous activity of eYFP reporter expression and for knocking out Notch1 in NC-NKO-Y mice. After this two-week period, mice were either subjected to a sham surgery or a lateral fluid percussion injury. To label injury-induced proliferating cells, BrdU was administered at 50mg/kg through i.p. injections every day for the first 7 days after sham surgery or injury unless noted differently. Animals were continuously monitored until the appropriate planned date of sacrifice for experiments.

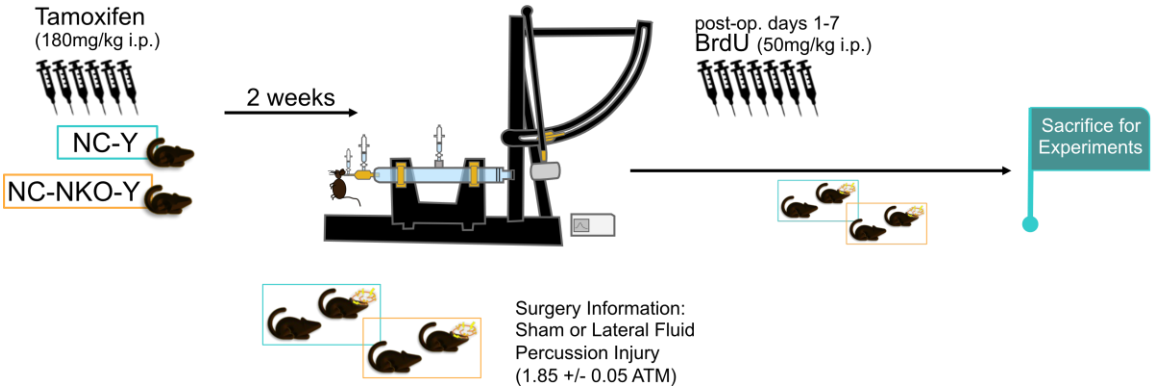

Figure A.8. Diagram of Animal Procedures. Diagram of procedures to prepare animals for experiments. Initially, animals receive 6 i.p. injections of tamoxifen. Animals are injured or receive sham surgery 2 weeks later. BrdU i.p. injections are administered days 1-7 after injury or surgery.

References

Aasebø, I. E. J., Blankvoort, S., & Tashiro, A. (2011). Critical maturational period of new neurons in adult dentate gyrus for their involvement in memory formation. *European Journal of Neuroscience*, *33*(6), 1094–1100. https://doi.org/10.1111/j.1460-9568.2011.07608.x

Abbott, L. C., & Nigussie, F. (2020). Adult neurogenesis in the mammalian dentate gyrus. In *Journal of Veterinary Medicine Series C: Anatomia Histologia Embryologia* (Vol. 49, Issue 1, pp. 3–16). Blackwell Publishing Ltd. https://doi.org/10.1111/ahe.12496

Ables JL, Breunig JJ, Eisch AJ, Rakic P. Not(ch) just development: Notch signalling in the adult brain. Nat Rev Neurosci. 2011 May;12(5):269-83. doi: 10.1038/nrn3024. PMID: 21505516; PMCID: PMC3159580.

Ables, J. L., DeCarolis, N. A., Johnson, M. A., Rivera, P. D., Gao, Z., Cooper, D. C., Radtke, F., Hsieh, J., & Eisch, A. J. (2010). Notch1 Is Required for Maintenance of the Reservoir of Adult Hippocampal Stem Cells. *Journal of Neuroscience*. https://doi.org/10.1523/JNEUROSCI.4721-09.2010

Aguirre, A., Rubio, M. E., & Gallo, V. (2010). Notch and EGFR pathway interaction regulates neural stem cell number and self-renewal. *Nature*, *467*(7313), 323–327. https://doi.org/10.1038/nature09347

Aimone JB, Wiles J, Gage FH. Computational influence of adult neurogenesis on memory encoding. Neuron. 2009 Jan 29;61(2):187-202. doi: 10.1016/j.neuron.2008.11.026. PMID: 19186162; PMCID: PMC2670434.

Aimone JB, Wiles J, Gage FH. Potential role for adult neurogenesis in the encoding of time in new memories. Nat Neurosci. 2006 Jun;9(6):723-7. doi: 10.1038/nn1707. PMID: 16732202.

Alberi, L., Hoey, S. E., Brai, E., Scotti, A. L., & Marathe, S. (2013). Notch signaling in the brain: In good and bad times. *Ageing Research Reviews*, *12*(3), 801–814. https://doi.org/10.1016/j.arr.2013.03.004

Alberi, L., Liu, S., Wang, Y., Badie, R., Smith-Hicks, C., Wu, J., Pierfelice, T. J., Abazyan, B., Mattson, M. P., Kuhl, D., Pletnikov, M., Worley, P. F., & Gaiano, N. (2011). Activity-Induced Notch Signaling in Neurons Requires Arc/Arg3.1 and Is Essential for Synaptic Plasticity in Hippocampal Networks. *Neuron*. https://doi.org/10.1016/j.neuron.2011.01.004

Almeida-Suhett CP, Prager EM, Pidoplichko V, Figueiredo TH, Marini AM, Li Z, Eiden LE, Braga MF. Reduced GABAergic inhibition in the basolateral amygdala and the development of anxiety-like behaviors after mild traumatic brain injury. PLoS One. 2014 Jul 21;9(7):e102627. doi: 10.1371/journal.pone.0102627. PMID: 25047645; PMCID: PMC4105413.

Altman J, Das GD. Autoradiographic and histological studies of postnatal neurogenesis. I. A longitudinal investigation of the kinetics, migration and transformation of cells incorporating tritiated thymidine in neonate rats, with special reference to postnatal neurogenesis in some brain regions. J Comp Neurol. 1966 Mar;126(3):337-89. doi: 10.1002/cne.901260302. PMID: 5937257.

Altman J, Das GD. Autoradiographic and histological evidence of postnatal hippocampal neurogenesis in rats. J Comp Neurol. 1965 Jun;124(3):319-35. doi: 10.1002/cne.901240303. PMID: 5861717.

Altman, J. (1962). Are New Neurons Formed in the Brains of Adult Mammals? In *New Series* (Vol. 135, Issue 3509).

Androutsellis-Theotokis, A., Leker, R. R., Soldner, F., Hoeppner, D. J., Ravin, R., Poser, S. W., Rueger, M. A., Bae, S.-K., Kittappa, R., & McKay, R. D. G. (2006). Notch signalling regulates stem cell numbers in vitro and in vivo. *Nature*, *442*(7104), 823–826. https://doi.org/10.1038/nature04940

Arvidsson A, Collin T, Kirik D, Kokaia Z, Lindvall O. Neuronal replacement from endogenous precursors in the adult brain after stroke. Nat Med. 2002 Sep;8(9):963-70. doi: 10.1038/nm747. Epub 2002 Aug 5. PMID: 12161747.

Aungst, S. L., Kabadi, S. v, Thompson, S. M., Stoica, B. a, & Faden, A. I. (2014). Repeated mild traumatic brain injury causes chronic neuroinflammation, changes in hippocampal synaptic plasticity, and associated cognitive deficits. *Journal of*

Cerebral Blood Flow and Metabolism : Official Journal of the International Society of Cerebral Blood Flow and Metabolism, *34*(7), 1223–1232. https://doi.org/10.1038/jcbfm.2014.75

Bakker A, Kirwan CB, Miller M, Stark CE. Pattern separation in the human hippocampal CA3 and dentate gyrus. Science. 2008 Mar 21;319(5870):1640-2. doi: 10.1126/science.1152882. PMID: 18356518; PMCID: PMC2829853.

Basak, O., Giachino, C., Fiorini, E., MacDonald, H. R., & Taylor, V. (2012). Neurogenic Subventricular Zone Stem/Progenitor Cells Are Notch1-Dependent in Their Active But Not Quiescent State. *Journal of Neuroscience*. https://doi.org/10.1523/JNEUROSCI.0455-12.2012

Becker S, Wojtowicz JM. A model of hippocampal neurogenesis in memory and mood disorders. Trends Cogn Sci. 2007 Feb;11(2):70-6. doi: 10.1016/j.tics.2006.10.013. Epub 2006 Dec 14. PMID: 17174137.

Beining, M., Jungenitz, T., Radic, T., Deller, T., Cuntz, H., Jedlicka, P., & Schwarzacher, S. W. (2017). Adult-born dentate granule cells show a critical period of dendritic reorganization and are distinct from developmentally born cells. *Brain Structure and Function*, *222*(3), 1427–1446. https://doi.org/10.1007/s00429-016-1285-y

Berezovska, O., McLean, P., Knowles, R., Frosh, M., Lu, F. M., Lux, S. E., & Hyman, B. T. (1999). Notch1 inhibits neurite outgrowth in postmitotic primary neurons. *Neuroscience*. https://doi.org/10.1016/S0306-4522(99)00157-8

Bergami M, Masserdotti G, Temprana SG, Motori E, Eriksson TM, Göbel J, Yang SM, Conzelmann KK, Schinder AF, Götz M, Berninger B. A critical period for experience-dependent remodeling of adult-born neuron connectivity. Neuron. 2015 Feb 18;85(4):710-7. doi: 10.1016/j.neuron.2015.01.001. Epub 2015 Feb 5. PMID: 25661179.

Blaabjerg, M., & Zimmer, J. (2007). The dentate mossy fibers: structural organization, development and plasticity. In *Progress in Brain Research* (Vol. 163). Elsevier. https://doi.org/10.1016/S0079-6123(07)63005-2

Blaiss, C. A., Yu, T.-S., Zhang, G., Chen, J., Dimchev, G., Parada, L. F., Powell, C. M., & Kernie, S. G. (2011). Temporally Specified Genetic Ablation of Neurogenesis Impairs Cognitive Recovery after Traumatic Brain Injury. *Journal of Neuroscience*, *31*(13), 4906–4916. https://doi.org/10.1523/JNEUROSCI.5265-10.2011

Brai, E., Marathe, S., Astori, S., Fredj, N. ben, Perry, E., Lamy, C., Scotti, A., & Alberi, L. (2015). Notch1 Regulates Hippocampal Plasticity Through Interaction with the Reelin Pathway, Glutamatergic Transmission and CREB Signaling. *Frontiers in Cellular Neuroscience*, *9*(November), 1–15. https://doi.org/10.3389/fncel.2015.00447

Breunig, J. J., Silbereis, J., Vaccarino, F. M., Sestan, N., & Rakic, P. (2007). Notch regulates cell fate and dendrite morphology of newborn neurons in the postnatal dentate gyrus. *Proceedings of the National Academy of Sciences*, *104*(51), 20558–20563. https://doi.org/10.1073/pnas.0710156104

Brunner J, Neubrandt M, Van-Weert S, Andrási T, Kleine Borgmann FB, Jessberger S, Szabadics J. Adult-born granule cells mature through two functionally distinct states. Elife. 2014 Jul 24;3:e03104. doi: 10.7554/eLife.03104. PMID: 25061223; PMCID: PMC4131194.

Bye, N., Carron, S., Han, X., Agyapomaa, D., Ng, S. Y., Yan, E., Rosenfeld, J. v., & Morganti-Kossmann, M. C. (2011). Neurogenesis and glial proliferation are stimulated following diffuse traumatic brain injury in adult rats. *Journal of Neuroscience Research*, *89*(7), 986–1000. https://doi.org/10.1002/jnr.22635

Canalis E, Schilling L, Zanotti S. Effects of Sex and Notch Signaling on the Osteocyte Cell Pool. J Cell Physiol. 2017 Feb;232(2):363-370. doi: 10.1002/jcp.25433. Epub 2016 Jun 7. PMID: 27192486; PMCID: PMC5325059.

Carbonell WS, Grady MS. Evidence disputing the importance of excitotoxicity in hippocampal neuron death after experimental traumatic brain injury. Ann N Y Acad Sci. 1999;890:287-98. doi: 10.1111/j.1749-6632.1999.tb08005.x. PMID: 10668434.

Chambers RA, Potenza MN, Hoffman RE, Miranker W. Simulated apoptosis/neurogenesis regulates learning and memory capabilities of adaptive neural networks. Neuropsychopharmacology. 2004 Apr;29(4):747-58. doi: 10.1038/sj.npp.1300358. PMID: 14702022.

Chen, Y. H., Kuo, T. T., Huang, E. Y. K., Hoffer, B. J., Chou, Y. C., Chiang, Y. H., Ma, H. I., & Miller, J. P. (2018). Profound deficits in hippocampal synaptic plasticity after traumatic brain injury and seizure is ameliorated by prophylactic levetiracetam. *Oncotarget*, *9*(14), 11515–11527. https://doi.org/10.18632/oncotarget.23923

Chirumamilla, S., Sun, D., Bullock, M. R., & Colello, R. J. (2002). Traumatic brain injury induced cell proliferation in the adult mammalian central nervous system. *J.Neurotrauma*, *19*(6), 693–703. https://doi.org/10.1089/08977150260139084

Chohan, M. O., Bragina, O., Kazim, S. F., Statom, G., Baazaoui, N., Bragin, D., Iqbal, K., Nemoto, E., & Yonas, H. (2015). Enhancement of Neurogenesis and Memory by a Neurotrophic Peptide in Mild to Moderate Traumatic Brain Injury. *Neurosurgery*, *76*(2), 201–215. https://doi.org/10.1227/NEU.0000000000000577

Christensen BK, Colella B, Inness E, Hebert D, Monette G, Bayley M, Green RE. Recovery of cognitive function after traumatic brain injury: a multilevel modeling analysis of Canadian outcomes. Arch Phys Med Rehabil. 2008 Dec;89(12 Suppl):S3-15. doi: 10.1016/j.apmr.2008.10.002. PMID: 19081439.

Christidi, F., Bigler, E. D., McCauley, S. R., Schnelle, K. P., Merkley, T. L., Mors, M. B., Li, X., Macleod, M., Chu, Z., Hunter, J. v., Levin, H. S., Clifton, G. L., & Wilde, E. A. (2011). Diffusion Tensor Imaging of the Perforant Pathway Zone and Its Relation to Memory Function in Patients with Severe Traumatic Brain Injury. *Journal of Neurotrauma*, *28*(5), 711–725. https://doi.org/10.1089/neu.2010.1644

Clelland, C. D., Choi, M., Romberg, C., Clemenson, G. D., Fragniere, A., Tyers, P., Jessberger, S., Saksida, L. M., Barker, R. A., Gage, F. H., & Bussey, T. J. (2009). A functional role for adult hippocampal neurogenesis in spatial pattern separation. *Science*, *325*(5937), 210–213. https://doi.org/10.1126/science.1173215

Coelho DJ, Sims DJ, Ruegg PJ, Minn I, Muench AR, Mitchell PJ. Cell type-specific and sexually dimorphic expression of transcription factor AP-2 in the adult mouse brain. Neuroscience. 2005;134(3):907-19. doi: 10.1016/j.neuroscience.2005.04.060. PMID: 16009501.

Cole, J. D., Espinueva, D., Seib, D. R., Cooke, M. B., Cahill, S. P., O'Leary, T., Kwan, S. S., & Snyder, J. S. (2019). *Adult-born hippocampal neurons undergo extended development and are morphologically distinct from neonatally-born neurons*. *40*(30), 5740–5756. https://doi.org/10.1101/702746

Coronado VG, McGuire LC, Sarmiento K, Bell J, Lionbarger MR, Jones CD, Geller AI, Khoury N, Xu L. Trends in Traumatic Brain Injury in the U.S. and the public health response: 1995-2009. J Safety Res. 2012 Sep;43(4):299-307. doi: 10.1016/j.jsr.2012.08.011. Epub 2012 Aug 25. Erratum in: J Safety Res. 2014 Feb;48:117. PMID: 23127680.

Danielson NB, Kaifosh P, Zaremba JD, Lovett-Barron M, Tsai J, Denny CA, Balough EM, Goldberg AR, Drew LJ, Hen R, Losonczy A, Kheirbek MA. Distinct Contribution of Adult-Born Hippocampal Granule Cells to Context Encoding.

Neuron. 2016 Apr 6;90(1):101-12. doi: 10.1016/j.neuron.2016.02.019. Epub 2016 Mar 10. PMID: 26971949; PMCID: PMC4962695.

Dash, P. K., Mach, S. A., & Moore, A. N. (2001). Enhanced neurogenesis in the rodent following traumatic brain injury. *Journal of Neuroscience Research*, *63*(4), 313–319. https://doi.org/10.1002/1097-4547(20010215)63:4<313::AID-JNR1025>3.0.CO;2-4

Dash, P. K., Moore, A. N., & Orsi, S. A. (2005). Blockade of γ-secretase activity within the hippocampus enhances long-term memory. *Biochemical and Biophysical Research Communications*, *338*(2), 777–782. https://doi.org/10.1016/j.bbrc.2005.10.006

Ding, X.-F., Gao, X., Ding, X.-C., Fan, M., & Chen, J. (2016). Postnatal dysregulation of Notch signal disrupts dendrite development of adult-born neurons in the hippocampus and contributes to memory impairment. *Scientific Reports*, *6*(1), 25780. https://doi.org/10.1038/srep25780

Dmytriyeva O, Belmeguenai A, Bezin L, Soud K, Drucker Woldbye DP, Gøtzsche CR, Pankratova S. Short erythropoietin-derived peptide enhances memory, improves long-term potentiation, and counteracts amyloid beta-induced pathology. Neurobiol Aging. 2019 Sep;81:88-101. doi: 10.1016/j.neurobiolaging.2019.05.003. Epub 2019 May 13. PMID: 31255922.

Edoff K, Raciti M, Moors M, Sundström E, Ceccatelli S. Gestational Age and Sex Influence the Susceptibility of Human Neural Progenitor Cells to Low Levels of

MeHg. Neurotox Res. 2017 Nov;32(4):683-693. doi: 10.1007/s12640-017-9786-x. Epub 2017 Jul 29. PMID: 28756503; PMCID: PMC5602033.

Eriksson, P. S., Perfilieva, E., Björk-Eriksson, T., Alborn, A.-M., Nordborg, C., Peterson, D. A., & Gage, F. H. (1998). Neurogenesis in the adult human hippocampus. *Nature Medicine*, *4*(11), 1313–1317. https://doi.org/10.1038/3305

Ethell, D. W. (2010). An amyloid-notch hypothesis for Alzheimer's disease. *Neuroscientist*, *16*(6), 614–617. https://doi.org/10.1177/1073858410366162

Feng, S., Shi, T., Qiu, J., Yang, H., Wu, Y., Zhou, W., Wang, W., & Wu, H. (2017). Notch1 deficiency in postnatal neural progenitor cells in the dentate gyrus leads to emotional and cognitive impairment. *FASEB J., 1530-6860 (Electronic)*. https://doi.org/10.1096/fj.201700216RR

Ferrari-Toninelli G, Bonini SA, Bettinsoli P, Uberti D, Memo M. Microtubule stabilizing effect of notch activation in primary cortical neurons. Neuroscience. 2008 Jun 26;154(3):946-52. doi: 10.1016/j.neuroscience.2008.04.025. Epub 2008 Apr 22. PMID: 18495362.

Filippov V, Kronenberg G, Pivneva T, Reuter K, Steiner B, Wang LP, Yamaguchi M, Kettenmann H, Kempermann G. Subpopulation of nestin-expressing progenitor cells in the adult murine hippocampus shows electrophysiological and morphological characteristics of astrocytes. Mol Cell Neurosci. 2003 Jul;23(3):373-82. doi: 10.1016/s1044-7431(03)00060-5. PMID: 12837622.

Finkelstein, E. A., Corso, P. S., & Miller, T. R. (2006). The incidence and economic burden of injuries in the United States. *Oxford University Press*, *9*(2006), 2007–2007. https://doi.org/10.1016/j.biocon.2007.07.012

Folweiler, K. A., Samuel, S., Metheny, H. E., & Cohen, A. S. (2018). Diminished dentate gyrus filtering of cortical input leads to enhanced area ca3 excitability after mild traumatic brain injury. *Journal of Neurotrauma*, *35*(11), 1304–1317. https://doi.org/10.1089/neu.2017.5350

Fraser, E., Downing, M., Biernacki, K., McKenzie, D., & Ponsford, J. (2019). Cognitive Reserve and Age Predict Cognitive Recovery Following Mild to Severe Traumatic Brain Injury. *Journal of Neurotrauma*, neu.2019.6430. https://doi.org/10.1089/neu.2019.6430

Fukuda S, Kato F, Tozuka Y, Yamaguchi M, Miyamoto Y, Hisatsune T. Two distinct subpopulations of nestin-positive cells in adult mouse dentate gyrus. J Neurosci. 2003 Oct 15;23(28):9357-66. doi: 10.1523/JNEUROSCI.23-28-09357.2003. Erratum in: J Neurosci. 2004 Jan 7;24(1):24. PMID: 14561863; PMCID: PMC6740569.

Gaiano N, Fishell G. The role of notch in promoting glial and neural stem cell fates. Annu Rev Neurosci. 2002;25:471-90. doi: 10.1146/annurev.neuro.25.030702.130823. Epub 2002 Mar 25. PMID: 12052917.

Galeano, P., Leal, M. C., Ferrari, C. C., Dalmasso, M. C., Martino Adami, P. v., Farías, M. I., Casabona, J. C., Puntel, M., do Carmo, S., Smal, C., Arán, M., Castaño, E. M.,

Pitossi, F. J., Cuello, A. C., & Morelli, L. (2018). Chronic Hippocampal Expression of Notch Intracellular Domain Induces Vascular Thickening, Reduces Glucose Availability, and Exacerbates Spatial Memory Deficits in a Rat Model of Early Alzheimer. *Molecular Neurobiology*, *55*(11), 8637–8650. https://doi.org/10.1007/s12035-018-1002-3

Gao, X., Enikolopov, G., & Chen, J. (2009). Moderate traumatic brain injury promotes proliferation of quiescent neural progenitors in the adult hippocampus. *Experimental Neurology*, *219*(2), 516–523. https://doi.org/10.1016/j.expneurol.2009.07.007

Ge, S., Sailor, K. A., Ming, G. L., & Song, H. (2008). Synaptic integration and plasticity of new neurons in the adult hippocampus. *Journal of Physiology*, *586*(16), 3759–3765. https://doi.org/10.1113/jphysiol.2008.155655

Ge, S., Yang, C. hao, Hsu, K. sen, Ming, G. li, & Song, H. (2007). A Critical Period for Enhanced Synaptic Plasticity in Newly Generated Neurons of the Adult Brain. *Neuron*, *54*(4), 559–566. https://doi.org/10.1016/j.neuron.2007.05.002

Giniger, E. (2012). Notch signaling and neural connectivity. *Current Opinion in Genetics and Development*, *22*(4), 339–346. https://doi.org/10.1016/j.gde.2012.04.003

Gonçalves, J. T., Bloyd, C. W., Shtrahman, M., Johnston, S. T., Schafer, S. T., Parylak, S. L., Tran, T., Chang, T., & Gage, F. H. (2016). In vivo imaging of dendritic pruning

in dentate granule cells. *Nature Neuroscience*, *19*(6), 788–791. https://doi.org/10.1038/nn.4301

Goodman T, Trouche S, Massou I, Verret L, Zerwas M, Roullet P, Rampon C. Young hippocampal neurons are critical for recent and remote spatial memory in adult mice. Neuroscience. 2010 Dec 15;171(3):769-78. doi: 10.1016/j.neuroscience.2010.09.047. Epub 2010 Sep 29. PMID: 20883747.

GoodSmith D, Chen X, Wang C, Kim SH, Song H, Burgalossi A, Christian KM, Knierim JJ. Spatial Representations of Granule Cells and Mossy Cells of the Dentate Gyrus. Neuron. 2017 Feb 8;93(3):677-690.e5. doi: 10.1016/j.neuron.2016.12.026. Epub 2017 Jan 26. PMID: 28132828; PMCID: PMC5300955.

Gould E, Gross CG. Neurogenesis in adult mammals: some progress and problems. J Neurosci. 2002 Feb 1;22(3):619-23. doi: 10.1523/JNEUROSCI.22-03-00619.2002. PMID: 11826089; PMCID: PMC6758509.

Gridley T, Groves AK. Overview of genetic tools and techniques to study Notch signaling in mice. Methods Mol Biol. 2014;1187:47-61. doi: 10.1007/978-1-4939-1139-4_4. PMID: 25053480; PMCID: PMC4591040.

Gupta, A., Elgammal, F. S., Proddutur, A., Shah, S., & Santhakumar, V. (2012). Decrease in tonic inhibition contributes to increase in dentate semilunar granule cell excitability after brain injury. *Journal of Neuroscience*, *32*(7), 2523–2537. https://doi.org/10.1523/JNEUROSCI.4141-11.2012

Gupta, A., Proddutur, A., Chang, Y. J., Raturi, V., Guevarra, J., Shah, Y., Elgammal, F. S., & Santhakumar, V. (2020). Dendritic morphology and inhibitory regulation distinguish dentate semilunar granule cells from granule cells through distinct stages of postnatal development. *Brain Structure and Function*, *225*(9), 2841–2855. https://doi.org/10.1007/s00429-020-02162-y

Hafting, T., Fyhn, M., Molden, S., Moser, M. B., & Moser, E. I. (2005). Microstructure of a spatial map in the entorhinal cortex. *Nature*, *436*(7052), 801–806. https://doi.org/10.1038/nature03721

Hainmueller, T., & Bartos, M. (2020). Dentate gyrus circuits for encoding, retrieval and discrimination of episodic memories. In *Nature Reviews Neuroscience* (Vol. 21, Issue 3, pp. 153–168). Nature Research. https://doi.org/10.1038/s41583-019-0260-z

Hall, C., & Ballachey, E. L. (1932). A study of the rat's behavior in a field. A contribution to method in comparative psychology. University of California Publications in Psychology, 6, 1–12.

Hallaq, R., Volpicelli, F., Cuchillo-Ibanez, I., Hooper, C., Mizuno, K., Uwanogho, D., Causevic, M., Asuni, A., To, A., Soriano, S., Giese, K. P., Lovestone, S., & Killick, R. (2015). The Notch intracellular domain represses CRE-dependent transcription. *Cellular Signalling*, *27*(3), 621–629. https://doi.org/10.1016/j.cellsig.2014.11.034

Hastings, N. B., & Gould, E. (1999). Rapid Extension of Axons Into the CA3 Region by Adult-Generated Granule Cells. In *J. Comp. Neurol* (Vol. 413).

Henze, D. A., & Buzsáki, G. (2007). Hilar mossy cells: functional identification and activity in vivo. In *Progress in Brain Research* (Vol. 163). Elsevier. https://doi.org/10.1016/S0079-6123(07)63012-X

Hitoshi S, Alexson T, Tropepe V, Donoviel D, Elia AJ, Nye JS, Conlon RA, Mak TW, Bernstein A, van der Kooy D. Notch pathway molecules are essential for the maintenance, but not the generation, of mammalian neural stem cells. Genes Dev. 2002 Apr 1;16(7):846-58. doi: 10.1101/gad.975202. PMID: 11937492; PMCID: PMC186324.

Hosp, J. A., Strüber, M., Yanagawa, Y., Obata, K., Vida, I., Jonas, P., & Bartos, M. (2014). Morpho-physiological criteria divide dentate gyrus interneurons into classes. *Hippocampus*, *24*(2), 189–203. https://doi.org/10.1002/hipo.22214

Hunt, R. F., Scheff, S. W., & Smith, B. N. (2011). Synaptic reorganization of inhibitory hilar interneuron circuitry after traumatic brain injury in mice. *The Journal of Neuroscience : The Official Journal of the Society for Neuroscience*, *31*(18), 6880–6890. https://doi.org/10.1523/JNEUROSCI.0032-11.2011

Ibrahim, S., Hu, W., Wang, X., Gao, X., He, C., & Chen, J. (2016). Traumatic Brain Injury Causes Aberrant Migration of Adult-Born Neurons in the Hippocampus. *Nature Publishing Group*, *November 2015*, 1–12. https://doi.org/10.1038/srep21793

Ikrar, T., Guo, N., He, K., Besnard, A., Levinson, S., Hill, A., Lee, H. K., Hen, R., Xu, X., & Sahay, A. (2013). Adult neurogenesis modifies excitability of the dentate gyrus. *Frontiers in Neural Circuits*, *7*(DEC). https://doi.org/10.3389/fncir.2013.00204

Imayoshi, I., Sakamoto, M., Yamaguchi, M., Mori, K., & Kageyama, R. (2010). Essential Roles of Notch Signaling in Maintenance of Neural Stem Cells in Developing and Adult Brains. *Journal of Neuroscience*, *30*(9), 3489–3498. https://doi.org/10.1523/JNEUROSCI.4987-09.2010

Jin K, Sun Y, Xie L, Peel A, Mao XO, Batteur S, Greenberg DA. Directed migration of neuronal precursors into the ischemic cerebral cortex and striatum. Mol Cell Neurosci. 2003 Sep;24(1):171-89. doi: 10.1016/s1044-7431(03)00159-3. PMID: 14550778.

Kageyama R, Ohtsuka T, Shimojo H, Imayoshi I. Dynamic regulation of Notch signaling in neural progenitor cells. Curr Opin Cell Biol. 2009 Dec;21(6):733-40. doi: 10.1016/j.ceb.2009.08.009. Epub 2009 Sep 23. PMID: 19783418.

Kee N, Teixeira CM, Wang AH, Frankland PW. Preferential incorporation of adult-generated granule cells into spatial memory networks in the dentate gyrus. Nat Neurosci. 2007 Mar;10(3):355-62. doi: 10.1038/nn1847. Epub 2007 Feb 4. PMID: 17277773.

Kempermann, G., Kuhn, H. G., & Gage, F. H. (1997). More hippocampal neurons in adult mice living in an enriched environment. *Nature*, *386*(6624), 493–495. https://doi.org/10.1038/386493a0

Kempermann G, Jessberger S, Steiner B, Kronenberg G. Milestones of neuronal development in the adult hippocampus. Trends Neurosci. 2004 Aug;27(8):447-52. doi: 10.1016/j.tins.2004.05.013. PMID: 15271491.

Kempermann, G., Song, H., & Gage, F. H. (2015). Neurogenesis in the adult hippocampus. *Cold Spring Harbor Perspectives in Medicine*, *5*(9). https://doi.org/10.1101/cshperspect.a018812

Kopan R, Ilagan MX. The canonical Notch signaling pathway: unfolding the activation mechanism. Cell. 2009 Apr 17;137(2):216-33. doi: 10.1016/j.cell.2009.03.045. PMID: 19379690; PMCID: PMC2827930.

Kosaka, T., Katsumaru, H., Hama, K., Wu, J.-Y., & Heizmann, C. W. (1987). GABAergic neurons containing the Ca2+-binding protein parvalbumin in the rat hippocampus and dentate gyrus. In *Brain Research* (Vol. 419).

Krzisch, M., Fülling, C., Jabinet, L., Armida, J., Gebara, E., Cassé, F., Habbas, S., Volterra, A., Hornung, J.-P., & Toni, N. (2016). Synaptic Adhesion Molecules Regulate the Integration of New Granule Neurons in the Postnatal Mouse Hippocampus and their Impact on Spatial Memory. *Cerebral Cortex*, 1–12. https://doi.org/10.1093/cercor/bhw217

Krzisch, M., Temprana, S. G., Mongiat, L. A., Armida, J., Schmutz, V., Virtanen, M. A., Kocher-Braissant, J., Kraftsik, R., Vutskits, L., Conzelmann, K. K., Bergami, M., Gage, F. H., Schinder, A. F., & Toni, N. (2015). Pre-existing astrocytes form functional perisynaptic processes on neurons generated in the adult hippocampus. *Brain Structure and Function*, *220*(4), 2027–2042. https://doi.org/10.1007/s00429-014-0768-y

Krzisch M, Temprana SG, Mongiat LA, Armida J, Schmutz V, Virtanen MA, Kocher-Braissant J, Kraftsik R, Vutskits L, Conzelmann KK, Bergami M, Gage FH, Schinder AF, Toni N. Pre-existing astrocytes form functional perisynaptic processes on neurons generated in the adult hippocampus. Brain Struct Funct. 2015 Jul;220(4):2027-42. doi: 10.1007/s00429-014-0768-y. Epub 2014 Apr 19. PMID: 24748560; PMCID: PMC4481333.

Kuhn HG, Toda T, Gage FH. Adult Hippocampal Neurogenesis: A Coming-of-Age Story. J Neurosci. 2018 Dec 5;38(49):10401-10410. doi: 10.1523/JNEUROSCI.2144-18.2018. Epub 2018 Oct 31. PMID: 30381404; PMCID: PMC6284110.

Li, Y., Stam, F. J., Aimone, J. B., Goulding, M., Callaway, E. M., & Gage, F. H. (2013). Molecular layer perforant path-associated cells contribute to feed-forward inhibition in the adult dentate gyrus. *Proceedings of the National Academy of Sciences of the United States of America*, *110*(22), 9106–9111. https://doi.org/10.1073/pnas.1306912110

Liu S, Wang Y, Worley PF, Mattson MP, Gaiano N. The canonical Notch pathway effector RBP-J regulates neuronal plasticity and expression of GABA transporters in hippocampal networks. Hippocampus. 2015 May;25(5):670-8. doi: 10.1002/hipo.22402. Epub 2015 Mar 27. PMID: 25515406; PMCID: PMC4412774.

Lowenstein, D. H., Thomas, M. J., Smith, D. H., & McIntosh, T. K. (1992). Selective vulnerability of dentate hilar neurons following traumatic brain injury: A potential mechanistic link between head trauma and disorders of the hippocampus. *Journal of Neuroscience*, *12*(12), 4846–4853. https://doi.org/10.1523/jneurosci.12-12-04846.1992

Lugert, S., Basak, O., Knuckles, P., Haussler, U., Fabel, K., Götz, M., Haas, C. A., Kempermann, G., Taylor, V., & Giachino, C. (2010). Quiescent and active hippocampal neural stem cells with distinct morphologies respond selectively to physiological and pathological stimuli and aging. *Cell Stem Cell*, *6*(5), 445–456. https://doi.org/10.1016/j.stem.2010.03.017

Marín-Burgin A, Mongiat LA, Pardi MB, Schinder AF. Unique processing during a period of high excitation/inhibition balance in adult-born neurons. Science. 2012 Mar 9;335(6073):1238-42. doi: 10.1126/science.1214956. Epub 2012 Jan 26. PMID: 22282476; PMCID: PMC3385415.

Markwardt, S. J., Wadiche, J. I., & Overstreet-Wadiche, L. S. (2009). Input-specific GABAergic signaling to newborn neurons in adult dentate gyrus. *Journal of*

Neuroscience, *29*(48), 15063–15072. https://doi.org/10.1523/JNEUROSCI.2727-09.2009

Mongiat LA, Espósito MS, Lombardi G, Schinder AF. Reliable activation of immature neurons in the adult hippocampus. PLoS One. 2009;4(4):e5320. doi: 10.1371/journal.pone.0005320. Epub 2009 Apr 28. PMID: 19399173; PMCID: PMC2670498.

Muroyama Y, Baba A, Kitagawa M, Saito T. Olfactory Sensory Neurons Control Dendritic Complexity of Mitral Cells via Notch Signaling. PLoS Genet. 2016 Dec 27;12(12):e1006514. doi: 10.1371/journal.pgen.1006514. PMID: 28027303; PMCID: PMC5189955.

Myers, C. E., & Scharfman, H. E. (2009). A Role for hilar cells in pattern separation in the dentate gyrus: A computational approach. *Hippocampus*, *19*(4), 321–337. https://doi.org/10.1002/hipo.20516

Nakashiba T, Cushman JD, Pelkey KA, Renaudineau S, Buhl DL, McHugh TJ, Rodriguez Barrera V, Chittajallu R, Iwamoto KS, McBain CJ, Fanselow MS, Tonegawa S. Young dentate granule cells mediate pattern separation, whereas old granule cells facilitate pattern completion. Cell. 2012 Mar 30;149(1):188-201. doi: 10.1016/j.cell.2012.01.046. Epub 2012 Feb 23. PMID: 22365813; PMCID: PMC3319279.

Nakayama M, Nakayama A, van Lessen M, Yamamoto H, Hoffmann S, Drexler HC, Itoh N, Hirose T, Breier G, Vestweber D, Cooper JA, Ohno S, Kaibuchi K, Adams RH. Spatial regulation of VEGF receptor endocytosis in angiogenesis. Nat Cell Biol. 2013 Mar;15(3):249-60. doi: 10.1038/ncb2679. Epub 2013 Jan 27. PMID: 23354168; PMCID: PMC3901019.

O'Neill, K. M., Akum, B. F., Dhawan, S. T., Kwon, M., Langhammer, C. G., & Firestein, B. L. (2015). Assessing effects on dendritic arborization using novel Sholl analyses. *Frontiers in Cellular Neuroscience*, *9*(July), 1–14. https://doi.org/10.3389/fncel.2015.00285

Paterno R, Folweiler KA, Cohen AS. Pathophysiology and Treatment of Memory Dysfunction After Traumatic Brain Injury. Curr Neurol Neurosci Rep. 2017 Jul;17(7):52. doi: 10.1007/s11910-017-0762-x. PMID: 28500417; PMCID: PMC5861722.

Petsophonsakul P, Richetin K, Andraini T, Roybon L, Rampon C. Memory formation orchestrates the wiring of adult-born hippocampal neurons into brain circuits. Brain Struct Funct. 2017 Aug;222(6):2585-2601. doi: 10.1007/s00429-016-1359-x. Epub 2017 Jan 6. PMID: 28062924.

Ponsford, J. L., Downing, M. G., Olver, J., Ponsford, M., Acher, R., Carty, M., & Spitz, G. (2014). Longitudinal follow-up of patients with traumatic brain injury: Outcome

at two, five, and ten years post-injury. *Journal of Neurotrauma*, *31*(1), 64–77. https://doi.org/10.1089/neu.2013.2997

Ran, Q., Yu, Y., Fu, X., & Wen, Y. (2015). Activation of the Notch signaling pathway promotes neurovascular repair after traumatic brain injury. *Neural Regeneration Research*, *10*(8), 1258. https://doi.org/10.4103/1673-5374.162758

Rangel LM, Alexander AS, Aimone JB, Wiles J, Gage FH, Chiba AA, Quinn LK. Temporally selective contextual encoding in the dentate gyrus of the hippocampus. Nat Commun. 2014;5:3181. doi: 10.1038/ncomms4181. PMID: 24518986; PMCID: PMC3929785.

Ratliff, W. A., Delic, V., Pick, C. G., & Citron, B. A. (2020). Dendritic arbor complexity and spine density changes after repetitive mild traumatic brain injury and neuroprotective treatments. *Brain Research*, *1746*(June). https://doi.org/10.1016/j.brainres.2020.147019

Redell, J. B., Maynard, M. E., Underwood, E. L., Vita, S. M., Dash, P. K., & Kobori, N. (2020). Traumatic brain injury and hippocampal neurogenesis: Functional implications. *Experimental Neurology*, *331*(October 2019), 113372. https://doi.org/10.1016/j.expneurol.2020.113372

Redmond, L., Oh, S. R., Hicks, C., Weinmaster, G., & Ghosh, a. (2000). Nuclear Notch1 signaling and the regulation of dendritic development. *Nature Neuroscience*, *3*(1), 30–40. https://doi.org/10.1038/71104

Reeves, T. M., Kao, C. Q., Phillips, L. L., Bullock, M. R., & Povlishock, J. T. (2000). Presynaptic excitability changes following traumatic brain injury in the rat. *Journal of Neuroscience Research*, *60*(3), 370–379. https://doi.org/10.1002/(SICI)1097-4547(20000501)60:3<370::AID-JNR12>3.0.CO;2-B

Restivo L, Niibori Y, Mercaldo V, Josselyn SA, Frankland PW. Development of Adult-Generated Cell Connectivity with Excitatory and Inhibitory Cell Populations in the Hippocampus. J Neurosci. 2015 Jul 22;35(29):10600-12. doi: 10.1523/JNEUROSCI.3238-14.2015. PMID: 26203153; PMCID: PMC6605118.

Ribak, C. E., & Shapiro, L. A. (2007). Ultrastructure and synaptic connectivity of cell types in the adult rat dentate gyrus. In *Progress in Brain Research* (Vol. 163, pp. 155–166). https://doi.org/10.1016/S0079-6123(07)63009-X

Rice, A. C., Khaldi, A., Harvey, H. B., Salman, N. J., White, F., Fillmore, H., & Bullock, M. R. (2003). Proliferation and neuronal differentiation of mitotically active cells following traumatic brain injury. *Experimental Neurology*, *183*(2), 406–417. https://doi.org/10.1016/S0014-4886(03)00241-3

Rolls, E. T. (2013). The mechanisms for pattern completion and pattern separation in the hippocampus. In *Frontiers in Systems Neuroscience* (Vol. 7, Issue OCT). https://doi.org/10.3389/fnsys.2013.00074

Rovira-Esteban, L., Hájos, N., Nagy, G. A., Crespo, C., Nacher, J., Varea, E., & Blasco-Ibáñez, J. M. (2020). Semilunar granule cells are the primary source of the

perisomatic excitatory innervation onto parvalbumin-expressing interneurons in the dentate gyrus. *ENeuro*, *7*(4), 1–17. https://doi.org/10.1523/ENEURO.0323-19.2020

Sahay, A., Scobie, K. N., Hill, A. S., O'Carroll, C. M., Kheirbek, M. A., Burghardt, N. S., Fenton, A. A., Dranovsky, A., & Hen, R. (2011). Increasing adult hippocampal neurogenesis is sufficient to improve pattern separation. *Nature*, *472*(7344), 466–470. https://doi.org/10.1038/nature09817

Salama-Cohen, P., Arévalo, M. Á., Grantyn, R., & Rodríguez-Tébar, A. (2006). Notch and NGF/p75NTR control dendrite morphology and the balance of excitatory/inhibitory synaptic input to hippocampal neurones through Neurogenin 3. *Journal of Neurochemistry*, *97*(5), 1269–1278. https://doi.org/10.1111/j.1471-4159.2006.03783.x

Salazar JL, Yang SA, Yamamoto S. Post-Developmental Roles of Notch Signaling in the Nervous System. Biomolecules. 2020 Jul 1;10(7):985. doi: 10.3390/biom10070985. PMID: 32630239; PMCID: PMC7408554.

Save, L., Baude, A., & Cossart, R. (2019). Temporal Embryonic Origin Critically Determines Cellular Physiology in the Dentate Gyrus. *Cerebral Cortex*, *29*(6), 2639–2652. https://doi.org/10.1093/cercor/bhy132

Saxe MD, Battaglia F, Wang JW, Malleret G, David DJ, Monckton JE, Garcia AD, Sofroniew MV, Kandel ER, Santarelli L, Hen R, Drew MR. Ablation of

hippocampal neurogenesis impairs contextual fear conditioning and synaptic plasticity in the dentate gyrus. Proc Natl Acad Sci U S A. 2006 Nov 14;103(46):17501-6. doi: 10.1073/pnas.0607207103. Epub 2006 Nov 6. PMID: 17088541; PMCID: PMC1859958.

Schmidt-Hieber, C., Jones, P., & Bischofberger, J. (2004). Enhanced synaptic plasticity in newly generated granule cells of the adult hippocampus. *Nature*, *429*(6988), 184–187. https://doi.org/10.1038/nature02553

Schretlen DJ, Shapiro AM. A quantitative review of the effects of traumatic brain injury on cognitive functioning. Int Rev Psychiatry. 2003 Nov;15(4):341-9. doi: 10.1080/09540260310001606728. PMID: 15276955.

Seress, L., & Ribak, C. E. (1984). Direct commissural connections to the basket cells of the hippocampal dentate gyrus: anatomical evidence for feed-forward inhibition. *Journal of Neurocytology*, *13*(2), 215–225. https://doi.org/10.1007/BF01148116

Sestan N, Artavanis-Tsakonas S, Rakic P. Contact-dependent inhibition of cortical neurite growth mediated by notch signaling. Science. 1999 Oct 22;286(5440):741-6. doi: 10.1126/science.286.5440.741. PMID: 10531053.

Shapiro, L. A. (2017). Altered hippocampal neurogenesis during the first 7 days after a fluid percussion traumatic brain injury. *Cell Transplantation*, *26*(7), 1314–1318. https://doi.org/10.1177/0963689717714099

Shapiro, L. A., Korn, M. J., Shan, Z., & Ribak, C. E. (2005). GFAP-expressing radial glia-like cell bodies are involved in a one-to-one relationship with doublecortin-immunolabeled newborn neurons in the adult dentate gyrus. *Brain Research*, *1040*(1–2), 81–91. https://doi.org/10.1016/j.brainres.2005.01.098

Sibbe M, Förster E, Basak O, Taylor V, Frotscher M. Reelin and Notch1 cooperate in the development of the dentate gyrus. J Neurosci. 2009 Jul 1;29(26):8578-85. doi: 10.1523/JNEUROSCI.0958-09.2009. PMID: 19571148; PMCID: PMC6665659.

Smith, D. H., Chen, X. H., Pierce, J. E., Wolf, J. A., Trojanowski, J. Q., Graham, D. I., & McIntosh, T. K. (1997). Progressive atrophy and neuron death for one year following brain trauma in the rat. *Journal of Neurotrauma*, *14*(10), 715–727. https://doi.org/10.1089/neu.1997.14.715

Soriano, E., & Frotscher, M. (1989). A GABAergic axo-axonic cell in the fascia dentata controls the main excitatory hippocampal pathway. In *Brain Research* (Vol. 503).

Spalding KL, Bergmann O, Alkass K, Bernard S, Salehpour M, Huttner HB, Boström E, Westerlund I, Vial C, Buchholz BA, Possnert G, Mash DC, Druid H, Frisén J. Dynamics of hippocampal neurogenesis in adult humans. Cell. 2013 Jun 6;153(6):1219-1227. doi: 10.1016/j.cell.2013.05.002. PMID: 23746839; PMCID: PMC4394608.

Steine, I. M., Zayats, T., Stansberg, C., Pallesen, S., Mrdalj, J., Havik, B., Soulé, J., Haavik, J., Milde, A. M., Skrede, S., Murison, R., Krystal, J., & Grønli, J. (2016).

Implication of NOTCH1 gene in susceptibility to anxiety and depression among sexual abuse victims. *Translational Psychiatry*, *6*(12). https://doi.org/10.1038/tp.2016.248

Sulhan, S., Lyon, K. A., Shapiro, L. A., & Huang, J. H. (2020). Neuroinflammation and blood–brain barrier disruption following traumatic brain injury: Pathophysiology and potential therapeutic targets. *Journal of Neuroscience Research*, *98*(1), 19–28. https://doi.org/10.1002/jnr.24331

Sun, D. (2005). Cell Proliferation and Neuronal Differentiation in the Dentate Gyrus in Juvenile and Adult Rats following Traumatic Brain Injury. *Journal of Neurotrauma*, *22*(1), 95–105.

Sun, D., Bullock, M. R., McGinn, M. J., Zhou, Z., Altememi, N., Hagood, S., Hamm, R., & Colello, R. J. (2009). Basic fibroblast growth factor-enhanced neurogenesis contributes to cognitive recovery in rats following traumatic brain injury. *Experimental Neurology*, *216*(1), 56–65. https://doi.org/10.1016/j.expneurol.2008.11.011

Sun, D., Daniels, T. E., Rolfe, A., Waters, M., & Hamm, R. (2015). Inhibition of injury-induced cell proliferation in the dentate gyrus of the hippocampus impairs spontaneous cognitive recovery after traumatic brain injury. *Journal of Neurotrauma*, *32*(7), 495–505. https://doi.org/10.1089/neu.2014.3545

Sun, D., McGinn, M. J., Zhou, Z., Harvey, H. ben, Bullock, M. R., & Colello, R. J. (2007). Anatomical integration of newly generated dentate granule neurons following traumatic brain injury in adult rats and its association to cognitive recovery. *Experimental Neurology*, *204*(1), 264–272. https://doi.org/10.1016/j.expneurol.2006.11.005

Sun, G. J., Sailor, K. A., Mahmood, Q. A., Chavali, N., Christian, K. M., Song, H., & Ming, G. L. (2013). Seamless reconstruction of intact adult-born neurons by serial end-block imaging reveals complex axonal guidance and development in the adult hippocampus. *Journal of Neuroscience*, *33*(28), 11400–11411. https://doi.org/10.1523/JNEUROSCI.1374-13.2013

Taqi MO, Saeed-Zidane M, Gebremedhn S, Salilew-Wondim D, Khdrawy O, Rings F, Neuhoff C, Hoelker M, Schellander K, Tesfaye D. Sexual dimorphic expression and release of transcription factors in bovine embryos exposed to oxidative stress. Mol Reprod Dev. 2019 Dec;86(12):2005-2019. doi: 10.1002/mrd.23272. Epub 2019 Sep 22. PMID: 31544319.

Teramoto T, Qiu J, Plumier JC, Moskowitz MA. EGF amplifies the replacement of parvalbumin-expressing striatal interneurons after ischemia. J Clin Invest. 2003 Apr;111(8):1125-32. doi: 10.1172/JCI17170. PMID: 12697732; PMCID: PMC152938.

Thurman, D. J., Alverson, C., Dunn, K. A., Guerrero, J., & Sniezek, J. E. (1999). Traumatic brain injury in the United States: A public health perspective. *Journal of*

Head Trauma Rehabilitation, *14*(6), 602–615. https://doi.org/10.1097/00001199-199912000-00009

Toni, N., Laplagne, D. A., Zhao, C., Lombardi, G., Ribak, C. E., Gage, F. H., & Schinder, A. F. (2008). Neurons born in the adult dentate gyrus form functional synapses with target cells. *Nature Neuroscience*, *11*(8), 901–907. https://doi.org/10.1038/nn.2156

Trinchero, M. F., Buttner, K. A., Sulkes Cuevas, J. N., Temprana, S. G., Fontanet, P. A., Monzón-Salinas, M. C., Ledda, F., Paratcha, G., & Schinder, A. F. (2017). High Plasticity of New Granule Cells in the Aging Hippocampus. *Cell Reports*, *21*(5), 1129–1139. https://doi.org/https://doi.org/10.1016/j.celrep.2017.09.064

Tronel S, Belnoue L, Grosjean N, Revest JM, Piazza PV, Koehl M, Abrous DN. Adult-born neurons are necessary for extended contextual discrimination. Hippocampus. 2012 Feb;22(2):292-8. doi: 10.1002/hipo.20895. Epub 2010 Nov 3. PMID: 21049483.

Tronel, S., Fabre, A., Charrier, V., Oliet, S. H. R., Gage, F. H., & Abrous, D. N. (2010). Spatial learning sculpts the dendritic arbor of adult-born hippocampal neurons. *Proceedings of the National Academy of Sciences of the United States of America*, *107*(17), 7963–7968. https://doi.org/10.1073/pnas.0914613107

Urrea, C., Castellanos, D. a, Sagen, J., Tsoulfas, P., Bramlett, H. M., & Dietrich, W. D. (2007). Widespread cellular proliferation and focal neurogenesis after traumatic

brain injury in the rat. *Restorative Neurology and Neuroscience*, *25*(1), 65–76. https://doi.org/17473396

Van Dussen KL, Carulli AJ, Keeley TM, Patel SR, Puthoff BJ, Magness ST, Tran IT, Maillard I, Siebel C, Kolterud Å, Grosse AS, Gumucio DL, Ernst SA, Tsai YH, Dempsey PJ, Samuelson LC. Notch signaling modulates proliferation and differentiation of intestinal crypt base columnar stem cells. Development. 2012 Feb;139(3):488-97. doi: 10.1242/dev.070763. Epub 2011 Dec 21. PMID: 22190634; PMCID: PMC3252352.

van Praag, H., Christie, B. R., Sejnowski, T. J., & Gage, F. H. (1999). *Running enhances neurogenesis, learning, and long-term potentiation in mice*. www.pnas.org

Vascak, M., Sun, J., Baer, M., Jacobs, K. M., & Povlishock, J. T. (2017). Mild Traumatic Brain Injury Evokes Pyramidal Neuron Axon Initial Segment Plasticity and Diffuse Presynaptic Inhibitory Terminal Loss. *Front Cell Neurosci*, *11*(June), 1–24. https://doi.org/10.3389/fncel.2017.00157

Villasana, L. E., Kim, K. N., Westbrook, G. L., & Schnell, E. (2015). Functional Integration of Adult-Born Hippocampal Neurons after Traumatic Brain Injury. *ENeuro*, *2*(5). https://doi.org/10.1523/ENEURO.0056-15.2015

Villasana, L. E., Westbrook, G. L., & Schnell, E. (2014). Neurologic impairment following closed head injury predicts post-traumatic neurogenesis. *Experimental Neurology*, *261*, 156–162. https://doi.org/10.1016/j.expneurol.2014.05.016

Vivar, C., Potter, M. C., Choi, J., Lee, J. Y., Stringer, T. P., Callaway, E. M., Gage, F. H., Suh, H., & van Praag, H. (2012). Monosynaptic inputs to new neurons in the dentate gyrus. *Nature Communications*, *3*. https://doi.org/10.1038/ncomms2101

Vivar, C., & van Praag, H. (2013). Functional circuits of new neurons in the dentate gyrus. In *Frontiers in Neural Circuits* (Issue JAN). https://doi.org/10.3389/fncir.2013.00015

Wang, K., Zhang, L., Rao, W., Su, N., Hui, H., Wang, L., Peng, C., Tu, Y., Zhang, S., & Fei, Z. (2015). Neuroscience Letters Neuroprotective effects of crocin against traumatic brain injury in mice : Involvement of notch signaling pathway. *Neuroscience Letters*, *591*, 53–58. https://doi.org/10.1016/j.neulet.2015.02.016

Wang, W. (2017). *Notch1 Signaling Activation Contributes to Adult Hippocampal Neurogenesis Following Traumatic Brain Injury*. 5480–5487. https://doi.org/10.12659/MSM.907160

Wang, X., Gao, X., Michalski, S., Zhao, S., & Chen, J. (2016). Traumatic Brain Injury Severity Affects Neurogenesis in Adult Mouse Hippocampus. *Journal of Neurotrauma*, *33*(8), 721–733. https://doi.org/10.1089/neu.2015.4097

Wang Y, Chan SL, Miele L, Yao PJ, Mackes J, Ingram DK, Mattson MP, Furukawa K. Involvement of Notch signaling in hippocampal synaptic plasticity. Proc Natl Acad Sci U S A. 2004 Jun 22;101(25):9458-62. doi: 10.1073/pnas.0308126101. Epub 2004 Jun 9. PMID: 15190179; PMCID: PMC438998.

Weston, N. M., Rolfe, A. T., Freelin, A. H., Reeves, T. M., & Sun, D. (2021). Traumatic brain injury modifies synaptic plasticity in newly-generated granule cells of the adult hippocampus. *Experimental Neurology*, *336*(September 2020), 113527. https://doi.org/10.1016/j.expneurol.2020.113527

Whitfield, J., Littlewood, T., & Soucek, L. (2015). Tamoxifen administration to mice. *Cold Spring Harbor Protocols*, *2015*(3), 269–271. https://doi.org/10.1101/pdb.prot077966

Wi S, Yu JH, Kim M, Cho SR. In Vivo Expression of Reprogramming Factors Increases Hippocampal Neurogenesis and Synaptic Plasticity in Chronic Hypoxic-Ischemic Brain Injury. Neural Plast. 2016;2016:2580837. doi: 10.1155/2016/2580837. Epub 2016 Nov 9. PMID: 27900211; PMCID: PMC5120183.

Wilhelmsson, U., Lebkuechner, I., Leke, R., Marasek, P., Yang, X., Antfolk, D., Chen, M., Mohseni, P., Lasič, E., Bobnar, S. T., Stenovec, M., Zorec, R., Nagy, A., Sahlgren, C., Pekna, M., & Pekny, M. (2019). Nestin Regulates Neurogenesis in Mice Through Notch Signaling From Astrocytes to Neural Stem Cells. *Cerebral Cortex*, 1–17. https://doi.org/10.1093/cercor/bhy284

Williams, P. A., Larimer, P., Gao, Y., & Strowbridge, B. W. (2007). Semilunar granule cells: Glutamatergic neurons in the rat dentate gyrus with axon collaterals in the inner molecular layer. *Journal of Neuroscience*, *27*(50), 13756–13761. https://doi.org/10.1523/JNEUROSCI.4053-07.2007

Witter, M. P. (2007). The perforant path: projections from the entorhinal cortex to the dentate gyrus. In *Progress in Brain Research* (Vol. 163, pp. 43–61). https://doi.org/10.1016/S0079-6123(07)63003-9

Woods, N. I., Vaaga, C. E., Chatzi, C., Adelson, J. D., Collie, M. F., Perederiy, J. v., Tovar, K. R., & Westbrook, G. L. (2018). Preferential targeting of lateral entorhinal inputs onto newly integrated granule cells. *Journal of Neuroscience*, *38*(26), 5843–5853. https://doi.org/10.1523/JNEUROSCI.1737-17.2018

Wu, C. C., Chawla, F., Games, D., Rydel, R. E., Freedman, S., Schenk, D., Young, W. G., Morrison, J. H., & Bloom, F. E. (2004). Selective vulnerability of dentate granule cells prior to amyloid deposition in PDAPP mice: Digital morphometric analyses. *Proceedings of the National Academy of Sciences of the United States of America*, *101*(18), 7141–7146. https://doi.org/10.1073/pnas.0402147101

Zaloshnja, E., Miller, T., Langlois, J. A., & Selassie, A. W. (2005). Prevalence of Long-Term Disability From Traumatic Brain Injury in the Civilian Population of the United States, 2005. In *J Head Trauma Rehabil* (Vol. 23, Issue 6). http://journals.lww.com/headtraumarehab

Zhang, Z., Gao, F., Kang, X., Li, J., Zhang, L., & Dong, W. (2015). Exploring the potential relationship between Notch pathway genes expression and their promoter methylation in mice hippocampal neurogenesis. *Brain Research Bulletin*, *113*, 8–16. https://doi.org/10.1016/j.brainresbull.2015.02.003

Zhang, Z., Yan, R., Zhang, Q., Li, J., Kang, X., Zhang, J., Ren, X., & Yang, X. (2014). Hes1 , a Notch signaling downstream target , regulates adult hippocampal neurogenesis following traumatic brain injury. *Brain Research*, *1583*, 65–78. https://doi.org/10.1016/j.brainres.2014.07.037

Zhao X, van Praag H. Steps towards standardized quantification of adult neurogenesis. Nat Commun. 2020 Aug 26;11(1):4275. doi: 10.1038/s41467-020-18046-y. PMID: 32848155; PMCID: PMC7450090.

Zhao, C., Teng, E. M., Summers, R. G., Ming, G. L., & Gage, F. H. (2006). Distinct morphological stages of dentate granule neuron maturation in the adult mouse hippocampus. *Journal of Neuroscience*, *26*(1), 3–11. https://doi.org/10.1523/JNEUROSCI.3648-05.2006

Zhao, M., Chen, S., Li, X., Wang, L., Chen, F., & Zhong, S. (2018). *Optical Depolarization of DCX-Expressing Cells Promoted Cognitive Recovery and Maturation of Newborn Neurons via the Wnt / ☙ -Catenin Pathway*. *63*, 303–318. https://doi.org/10.3233/JAD-180002

Zheng W, ZhuGe Q, Zhong M, Chen G, Shao B, Wang H, Mao X, Xie L, Jin K. Neurogenesis in adult human brain after traumatic brain injury. J Neurotrauma.

2013 Nov 15;30(22):1872-80. doi: 10.1089/neu.2010.1579. Epub 2013 Jul 24. PMID: 21275797; PMCID: PMC3815038.

Zipp, F., Nitsch, R., Soriano, E., & Frotscher, M. (1989). Entorhinal fibers form synaptic contacts on parvalbumin-immunoreactive neurons in the rat fascia dentata. In *Brain Research* (Vol. 495).